INSTITUT FÜR ZOOLOGIE DER RHEINISCHEN FRIEDRICH-WILHELMS-UNIVERSITÄT BONN,
MARINE ZOOLOGIE DER UNIVERSITÄT BREMEN

Size-dependent Community Structure and Ecology of Zooplankton in the Benguela Coastal Upwelling System off Namibia

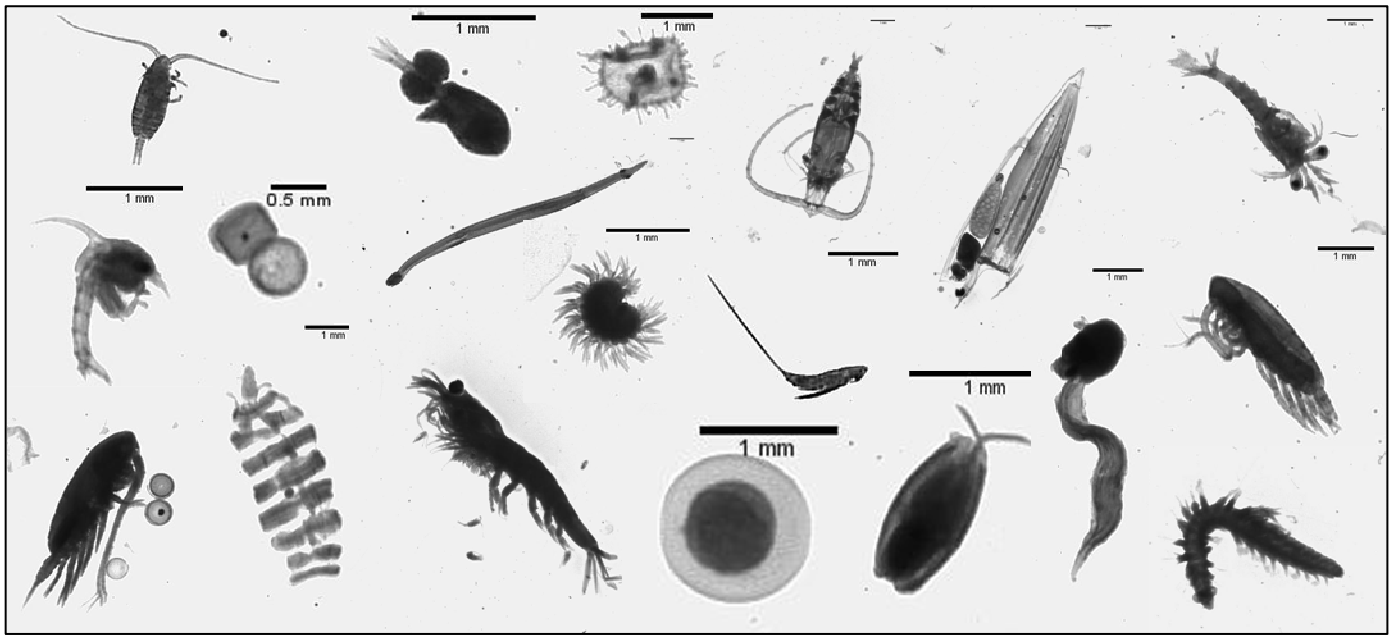

Diplomarbeit zur Erlangung des Grades
Diplom-Biologin
an der Mathematisch-Naturwissenschaftlichen Fakultät der
Rheinischen Friedrich-Wilhelms-Universität Bonn

vorgelegt von

Lena Teuber

Bonn, November 2009

Diplomarbeit

angefertigt an

der Universität Bremen,

Marine Zoologie,

Fachbereich 2 (Biologie/Chemie)

1. Referent:

PD Dr. Holger Auel
Marine Zoologie
Universität Bremen

2. Referent:

Prof. Dr. Gerhard von der Emde
Neuroethologie/
Sensorische Ökologie
Universität of Bonn

Contents

List of Abbreviations

ABF	Angola-Benguela Front
ECD	Equivalent circular diameter
OML	Oxygen minimum layer
SST	Sea surface temperature
C4	Copepodite stage C4
C5	Copepodite stage C5

Abstract

Zooplankton plays a central role in the transfer of energy along the food chain. The Benguela region is a highly variable ecosystem and the zooplankton community is therefore exposed to strong temporal and spatial variations. Due to occasional upwelling events and changing conditions, such as sea surface temperature and availability of food particles, the distribution of zooplankton organisms in this region is closely related to the hydrographic features of the environment. In this study, it is investigated if zooplankton body size, abundance and biomass are higher in the Benguela system compared to tropical regions. Moreover, it should be tested if zooplankton body size increases with increasing depth, while biomass and abundance decrease. Vertical as well as horizontal changes in the species composition of the zooplankton community are examined and trophic relations among organisms are illuminated.

Zooplankton samples were taken in the northern Benguela upwelling region during two cruises in austral fall of 2007 and 2008. Two transects were chosen for the analysis, a meridional transect across the Angola-Benguela Front (ABF) at 11°30E from 14°S to 18°S and a cross-shelf transect at 20°S. Stations were sampled from the surface to a maximum depth of 1000 m. Zooplankton samples were analysed by means of automated image analysis with the software ZooImage to reveal abundance and biomass patterns, size spectra distribution and species composition. The technique of stable carbon and nitrogen isotope analysis was used to study trophic relationships within the pelagic food web of the northern Benguela upwelling system.

Differences in the community structure of zooplankton were most significant in the vertical direction due to strongest changes in physical parameters such as temperature, oxygen concentration and light. Highest biomass and abundance were recorded in the surface layer of coastal stations and south of the ABF in 2008 where upwelling activity was evident and phytoplankton biomass high. In warm, nutrient-poor regions, offshore and north of the ABF, biomass and abundance were generally rather low. Below the thermocline, both parameters drastically decreased with increasing depth. This could be the consequence of an oxygen minimum layer (OML) in depths of 100-500 m, besides the general decrease in food availability with increasing depth.

Copepods dominated the zooplankton community by up to 90% of total abundance. Cyclopoid copepods dominated in neritic regions, whereas calanoids were predominantly found in offshore areas. *Calanoides carinatus*, *Metridia lucens* and *Pleuromamma* spp. were the most common calanoid copepods. Among the Cyclopoida, *Oithona* spp. and *Oncaea* spp. dominated. *C. carinatus* was abundant at the surface in coastal areas and at depths below 200 m in offshore regions and north of the ABF. These two centres of abundance can be related to the life cycle of

the species that conducts ontogenetic vertical migrations as an adaptation to changes in upwelling intensity. For *Metridia lucens* and *Pleuromamma* spp., diel vertical migration could be recorded. While herbivorous organisms were predominantly found at the surface, omnivorous species also resided at greater depth.

There was an increase of mean zooplankton body size with increasing depth. This could be related to the numerous occurrences of bigger species such as *C. carinatus*, *M. lucens*, *Eucalanus* spp., chaetognaths or euphausiids in deeper water layers. There was also a trend towards bigger body size in the coastal upwelling region, but differences were not significant.

Stable nitrogen isotope signatures ($\delta^{15}N$) ranged from 6.2‰ in the pteropod *Cymbulia* spp. to 14.2‰ in the storm petrel (Hydrobatidae). Stable carbon isotope ratios ($\delta^{13}C$) ranged from -24.2‰ in a tunicate to -16.0‰ in the anchovy *Engraulis capensis*. $\delta^{15}N$ ratios clearly reflected the feeding behaviour of the organisms in that carnivorous species displayed much higher $\delta^{15}N$ ratios than herbivorous species. The results also indicate that omnivory is a widespread feeding mode of zooplankton organisms in the Benguela region.

The analysis of the isotopic composition as well as the size spectra of zooplankton organisms provided insight into possible trophic relationships within the zooplankton community, since most predator-prey interactions are size-related. Revealing the trophodynamics of the system as well as the distribution patterns of zooplankton will contribute to a better understanding of the functioning of the entire ecosystem. Variations within the zooplankton community structure are strongly related to environmental conditions and reflect hydrographic characteristics of the Benguela upwelling region. The knowledge of these interrelations will allow predicting potential future scenarios affected by anthropogenic impacts and climatic changes such as increasing water temperatures.

Zusammenfassung

Zooplankton nimmt eine zentrale Rolle in der Energieübertragung entlang von Nahrungsketten ein. Das Benguela-Küstenauftriebsgebiet ist ein sehr variables Ökosystem, wodurch die Zooplanktongemeinschaft innerhalb dieses Systems starken zeitlichen und räumlichen Variationen ausgesetzt ist. Durch zeitlich begrenzte Auftriebsereignisse und sich verändernde Bedingungen, wie zum Beispiel Oberflächentemperaturen und Nahrungsverfügbarkeit, ist die Verbreitung von Zooplankton in dieser Region stark von den hydrographischen Gegebenheiten in diesem Gebiet abhängig. In dieser Studie wird untersucht, ob die Körpergröße, Verbreitung und Biomasse von Zooplankton im Benguela-Aufriebsgebiet größer ist als in den angrenzenden tropischen Regionen. Außerdem wird getestet, ob die Körpergröße des Zooplanktons mit steigender Tiefe zunimmt, während Biomasse und Abundanz mit der Tiefe abnehmen. Unterschiede in vertikaler wie auch horizontaler Verteilung verschiedener Zooplanktonarten werden untersucht und trophische Beziehungen zwischen Organismen beleuchtet.

Zooplanktonproben wurden während zwei Expeditionen im südlichen Herbst in 2007 und 2008 im nördlichen Benguela-Küstenauftriebsgebiet genommen. Zwei Transekte wurden für die Analysen ausgewählt: ein meridionaler Transekt durch die Angola-Benguela Front (ABF) bei 11°30E von 14°S bis 18°S und ein Ost-West Transekt bei 20°S. Die Stationen wurden von der Oberfläche bis in eine maximale Tiefe von 1000 m beprobt. Zooplanktonproben wurden mittels einer automatisierten Bildanalyse mit der Software ZooImage analysiert, um Abundanz- und Biomassemuster, Größenverteilungen und Artenzusammensetzungen zu bestimmen. Die Analyse von stabilen Isotopen des Stickstoffs und des Kohlenstoffs wurde verwendet um die Nahrungsbeziehungen im pelagischen Nahrungsnetz des nördlichen Benguela-Küstenauftriebsgebiet zu untersuchen.

Unterschiede in der Artenzusammensetzung des Zooplanktons waren in der vertikalen Verteilung am signifikantesten, weil dort die größten Veränderungen in physikalischen Parametern, wie Temperatur, Sauerstoffkonzentration und Lichtintensität, zu finden waren. Die größte Zooplankton-Biomasse und -Abundanz wurde in der Oberflächenschicht der Küstenstationen und südlich der ABF in 2008 gefunden, wo Küstenauftrieb vorhanden und auch die Phytoplankton-Biomasse am höchsten war. In warmen, nährstoffarmen Gebieten, küstenfern und nördlich der ABF, waren Biomasse und Abundanz des Zooplanktons generell kleiner. Unterhalb der Thermokline fielen beide Parameter mit zunehmender Tiefe drastisch ab. Dies könnte, neben der generellen Abnahme der Nahrungsverfügbarkeit mit zunehmender Tiefe, aus einer Sauerstoffminimumzone (OML) in einer Tiefe von 100-500 m resultieren.

Copepoden dominierten die Zooplanktongemeinschaft mit 90% der Gesamtabundanz des Zooplanktons. Cyclopoide Copepoden dominierten in neritischen Regionen, wogegen calanoide Copepoden überwiegend in küstenfernen Gebieten gefunden wurden. *Calanoides carinatus*, *Metridia lucens* und *Pleuromamma* spp. waren die häufigsten calanoiden Copepoden. Unter den Cyclopoida dominierten *Oithona* spp. und *Oncaea* spp. *C. carinatus* war zahlreich an der Oberfläche in Küstengebieten und in Tiefen ab 200 m in küstenfernen Gebieten und nördlich der ABF zu finden. Diese beiden Abundanzzentren sind auf den Lebenszyklus dieser Art zurückzuführen, welche ontogenetische Vertikalwanderungen als Anpassung an Veränderungen in der Auftriebsintensität durchführt. Für *Metridia lucens* und *Pleuromamma* spp. konnten tägliche Vertikalwanderungen nachgewiesen werden. Während herbivore Organismen weitestgehend in den Oberflächenschichten gefunden wurden, waren omnivore Arten auch in größeren Tiefen zu finden.

Es gab einen Anstieg in der durchschnittlichen Größe des Zooplanktons mit zunehmender Tiefe zu verzeichnen. Dies ist darauf zurückzuführen, dass viele große Arten oft in größerer Tiefe zu finden waren, wie zum Beispiel *C. carinatus*, *M. lucens*, *Eucalanus* spp., Chaetognathen oder Euphausiaceen. Es war außerdem ein Trend zu größeren Körperlängen in den Küstenauftriebsregionen zu finden, jedoch waren die Unterschiede nicht signifikant.

Stabile Isotopen Signaturen des Stickstoffs ($\delta^{15}N$) lagen zwischen 6.2‰ in dem Pteropoden *Cymbulia* spp. und 14.2‰ in der Sturmschwalbe. Stabile Isotopen Verhältnisse des Kohlenstoffs ($\delta^{13}C$) variierten zwischen -24.2‰ in einem Tunicaten bis hin zu -16.0‰ in der Sardelle *Engraulis capensis*. Die $\delta^{15}N$ Verhältnisse spiegelten deutlich die Ernährungsweisen der Organismen wider, indem karnivore Arten höhere $\delta^{15}N$ Verhältnisse aufwiesen als herbivore Arten. Die Ergebnisse deuten ebenfalls an, dass Omnivorie eine weit verbreitete Form der Ernährung von Zooplanktonorganismen des Benguela-Küstenauftriebsgebietes darstellt.

Die Analyse der Isotopenzusammensetzung, sowie das Größenspektrum des Zooplanktons bieten Einsicht in mögliche trophische Beziehungen innerhalb der Zooplanktongemeinschaft, denn die meisten Räuber-Beute-Verhältnisse sind größenabhängig. Der Einblick in die Trophodynamik des Systems, wie auch der Verbreitungsmuster des Zooplanktons tragen zu einem besseren Verständnis des gesamten Ökosystems bei. Variabilitäten in der Zooplanktonzusammensetzung sind stark an Umweltbedingungen gekoppelt und reflektieren dadurch die hydrographischen Charakteristika des Benguela-Küstenauftriebsgebietes. Das Wissen über diese Zusammenhänge macht es möglich, potenzielle Auswirkungen anthropogener Einflüsse und des Klimawandels, wie steigende Wassertemperaturen, auf Auftriebsgebiete vorherzusagen.

1 Introduction

Zooplankton plays a key role in the functioning of marine ecosystems, particularly for the transfer of energy along the food chain. Marine food webs are mainly based on the primary production by phytoplankton and zooplankton organisms link primary producers with higher trophic level consumers, such as fish (Fenchel 1988, Loick et al. 2005, Verheye et al. 2005). Zooplankton consists of a variety of pelagic species belonging to many different phyla and, as meroplankton, it also includes certain developmental stages of benthic animals and fish. Plankton is often classified by size, since size spectra determine the appropriate sampling methodology and, to a certain extent, correspond to taxonomic composition. Nanoplankton (2-20 µm) and microplankton (20-200 µm) mainly contain phytoplankton and protozoans, whereas invertebrate zooplankton, which is the main focus of this study, usually belongs to the mesoplankton (200 µm to 20 mm) and macroplankton (2-20 cm).

The distribution and abundance of plankton organisms is to a great extent influenced by the physical and chemical conditions of the sea. Therefore, plankton is very receptive to environmental variations such as increasing sea surface temperature and CO_2 concentrations, availability of nutrients and prey or anthropogenic impacts like pollution (Lenz 2000). Differences in zooplankton abundance and distribution patterns can therefore reflect changes in ecosystems due to climatic variations.

Upwelling systems are among the most productive regions in the oceans (Fenchel 1988). The four major eastern boundary upwelling systems (Benguela, California, Humboldt, Canary) comprise cool equatorward flowing currents. The upwelling of cool, nutrient-rich waters to the surface (Hardman-Mountford et al. 2003) provides optimal environmental conditions for phytoplankton growth which is the food source for a very abundant marine fauna. Zooplankton species in upwelling systems benefit from the temporarily high food availability, but have to be physically adapted to very variable environmental conditions (Jarre-Teichmann et al. 1998, Peterson 1998). Some species have developed characteristic life-cycle strategies and are well adapted in terms of reproduction and growth (Lenz 2000). These adaptations prevent them from being advected offshore and away from the productive upwelling region. A key species of coastal upwelling systems on both sides of the Atlantic Ocean and around the African continent is the herbivorous copepod *Calanoides carinatus*, which conducts ontogenetic vertical migrations to overcome periods of food shortage in a dormant stage at depth and successfully maintains its population within the coastal upwelling region (Peterson 1998).

The Benguela Current upwelling system is located in the South East Atlantic Ocean off the coast of South Africa and Namibia. It consists of two separate sub-systems, a northern and a southern part (Shannon & Nelson 1996). This study will focus on the northern sub-system. A variety of different zooplankton organisms contribute to the complexity of the northern Benguela upwelling ecosystem. The zooplankton community is dominated by copepods (Timonin 1990) such as *C. carinatus*, *Metridia lucens* and Eucalanidae (Peterson 1998, Loick et al. 2005, Auel & Verheye 2007). Furthermore, euphausiids, chaetognaths, appendicularians and salps belong to the most common zooplankton taxa (Timonin 1990, Timonin et al. 1992).

Short food chains (phytoplankton → zooplankton → fish) are characteristic for upwelling regions and allow a very efficient transfer of energy to higher trophic levels (Cushing 1989). Therefore they generally support high biomass of fish (Shannon & O'Toole 2003). The Benguela upwelling system is, together with the Humboldt system, the most productive of the four regions and reaches an average primary production of 1.25 kg C m^{-2} a^{-1}, which is around six times more than accomplished in the North Sea (Boyer & Hampton 2001, Shannon & O'Toole 2003). In spite of very high rates of primary and secondary production in the Benguela region, estimated biomass of fish does not reflect this (Hocutt & Verheye 2001). For Namibia's fishery the most important fish species are southern African sardine *Sardinops sagax,* Cape anchovy *Engraulis capensis,* Cape hake *Merluccius capensis* and *M. paradoxus* and Cape horse mackerel *Trachurus trachurus capensis* (Boyer & Hampton 2001). Many high level predators such as seabirds, seals and other marine mammals in the Benguela region prey on these fish species (Crawford et al. 1992). On the other hand, fish, especially in early life stages, are dependent on the availability of plankton as prey organisms, which abundance highly reflects the variability of physical conditions in the Benguela system. Since the 1970's the fish stocks in the Benguela upwelling region have been rapidly decreasing (Boyer & Hampton 2001) and in the 1990's, many populations of commercial interest reached critically low levels (Payne et al. 2001). It is believed that, besides overfishing, also environmental changes during the past decades have contributed to the collapse of living resources in the Benguela region (Ekau & Verheye 2005, Auel & Verheye 2007).

The structure of food webs is often closely related to the body size of consumers and their prey (Arim et al. 2007). Larger organisms usually feed on smaller ones and often select their prey according to size rather than to species (Arim et al. 2007). Some species also display large variations in body size during their life history and therefore may occupy different trophic positions during their ontogenetic development (Rodríguez 1994). Through the examination of trophic interactions between organisms in the northern Benguela upwelling region, important information can be gained on environmental processes that influence predator-prey relationships and what impacts can be expected on the ecosystem and on the fisheries.

The analysis of stable isotope signatures of food-web components has proven to be a valuable tool to characterise trophic flows in marine ecosystems (Michener & Schell 1994). For terrestrial and aquatic ecosystems, naturally occurring stable isotopes of carbon ($^{13}C/^{12}C$) and nitrogen ($^{15}N/^{14}N$) reveal trophic relations between different species and trace energy flows within food webs (Peterson & Fry 1987, Hobson & Welch 1992, Michener & Schell 1994). In a process, called isotopic fractionation, lighter isotopes are more quickly excreted, whereas heavier isotopes accumulate in the animal's body tissue (Vander Zanden & Rasmussen 1999, Bode & Alvarez-Ossorio 2004). The stable isotope composition of a consumer therefore reflects the isotopic composition of its prey, but it is further enriched in heavier isotopes (DeNiro & Epstein 1978, Minagawa & Wada 1984, Michener & Schell 1994). For marine food webs, the enrichment factor per trophic level is commonly quoted as 3.4‰±1.1 for nitrogen and around 0.8‰ for carbon (DeNiro & Epstein 1978, Minagawa & Wada 1984, Peterson & Fry 1987, Hobson & Welch 1992). For this reason, the stepwise enrichment of the stable isotope ratio of nitrogen ($\delta^{15}N$) along the food chain can be applied as an indicator of different trophic levels (Quillfeldt et al. 2005). In contrast, the stable carbon isotope ratio ($\delta^{13}C$) shows more pronounced differences in geographical aspects such as benthic versus pelagic food webs and thus can provide evidence of origins and sources of primary production. In this study, $\delta^{13}C$ and $\delta^{15}N$ are used to provide insight into predator-prey relationships and energy flows among organisms in the Benguela upwelling ecosystem.

The analysis of large series of plankton samples constitutes a methodical problem to planktologists for that it is very time-consuming and physically challenging to examine plankton under the dissecting microscope (Grosjean et al. 2004). Since the 1980's, various approaches have been made to develop alternative techniques for a more effective analysis of plankton samples (Rolke & Lenz 1984, Foote 2000, Bell & Hopcroft 2008). The silhouette photography, optical counting and video recording of plankton were among these newly developed techniques and were designed to capture and record zooplankton organisms on film or on video, both *in situ* and *ex situ* (Beaulieu et al. 1999, Foote 2000, Benfield et al. 2007). The optical plankton counter (OPC) initiated automatic size measurements of plankton organisms and supported the analysis of size spectra distribution and abundance of zooplankton (Beaulieu et al. 1999, Nogueira et al. 2004). The video plankton recorder (VPR) was one of the most advanced devices at that time and also permitted the automated classification of common zooplankton groups (Foote 2000). On this basis, computer-assisted counting and automatic identification techniques were introduced to the methodology of this field. Along with the technological progress of computers and other technical tools, these automated devices were further developed and today present a realistic alternative in the handling of zooplankton. Enumeration, length measurements and biomass estimations have successfully been obtained

by automatic techniques (Alcaraz et al. 2003). Furthermore, the automatic classification of plankton and the identification of individual species have become accessible.

Among the widely used automatic identification methods is the technique of image analysis. For this approach, a digital image of the plankton sample or of individual organisms is obtained (e.g. by camera, scanner) and analysed during automated processes by a computer. Devices, which apply this technique, are the ZOOSCAN and the software ZooImage (Grosjean et al. 2004, Warembourg et al. 2005, Grosjean & Denis 2007). Both methods were especially designed for the analysis of large series of preserved plankton samples (Grosjean et al. 2004, Grosjean & Denis 2007). The software ZooImage was chosen as image analysis device for this thesis, because it is a free software (http://www.sciviews.org/Zoo/PhytoImage). Furthermore, it has proven by many authors to be well applicable to zooplankton samples and provides a wide range of possible operations for individual adjustments (Bell & Hopcroft 2008, Fernandes et al. 2009). The software ZooImage processes digital images of zooplankton samples, identifies particles and conducts measurements. At last, it analyses the samples and extracts biological and ecological relevant parameters such as biomass, abundance and size spectra (Grosjean & Denis 2007). Nonetheless, taxonomic skills are not expendable and the computer has to be trained by an experienced planktologist in order to automatically identify plankton organisms. The computer is able to reach accuracies of 70-80% (Benfield et al. 2007) and the analysis of large series of zooplankton samples can be achieved in an adequate period of time (Bell & Hopcroft 2008).

One aim of this thesis is to establish this method of automatic image analysis of zooplankton and to apply it on zooplankton samples from the northern Benguela upwelling region for community and ecology studies. It should be demonstrated, that this method provides advantages towards traditional techniques and is suitable in detecting trends in zooplankton abundance and species composition.

The analysis of large series of zooplankton samples with focus on abundance, distribution and taxonomic composition, is necessary in order to find out about variations in community structure and species composition over a long period of time (Beaulieu et al. 1999). The study of zooplankton and their interactions with their abiotic environment (e. g. temperature, oxygen, currents) as well as their biotic relations (e.g. food supply, predator-prey relationships) provide meaningful information about the processes and current status of an ecosystem. Changes in species composition may lead to alternated feeding behaviour of fish and other planktivorous animals (Crawford 1987, Cury et al. 2000). Additionally, variations in physical parameters, such as climatic change, may have consequences on the entire ecosystem and populations of marine animals (Petchey et al. 1999). This might lead to changes in the community structure of

organisms at lower trophic levels and therefore food web structures and specific interactions of organisms may change as well (Manriquez et al. 2009).

Purpose of this study

The aim of this study is to examine the community structure and ecology of zooplankton in the northern Benguela upwelling system during austral fall in 2007 and 2008.

In order to analyse zooplankton communities, the distribution of biomass and size spectra, the abundance of major zooplankton groups, as well as the species composition are studied (Fock 2000). All of these aspects are influenced by environmental parameters, such as temperature, oxygen concentration and water depth, which lead to the development of certain distribution patterns of zooplankton that are characteristic of a geographic region (Lenz 2000). The main objective of this study is to detect patterns in zooplankton abundance, biomass, size spectra and composition along a cross-shelf gradient in the northern Benguela upwelling system and across the Angola-Benguela Front as well as potential changes between the two years of sampling. Besides regional trends, vertical changes from the surface to 1000 m depth will be studied.

With the novel technique of computer-based image analysis, special focus will be given to differences in size spectra of zooplankton organisms. The body size of a marine organism affects its position in the food web and reveals important information about possible predator-prey relationships because the majority of predators select their prey by size (Rodríguez 1994, Arim et al. 2007). In a complementary approach, trophic interactions in the Benguela region are illuminated by stable carbon and nitrogen isotope signatures. Based on these data, a model of potential trophic relations in the northern Benguela upwelling system is developed and discussed. In order to pursue these objectives, the following working hypotheses will be tested.

Hypothesis 1: Vertical trends

There are pronounced vertical changes in mesozooplankton abundance, biomass, size spectra and taxonomic composition at the offshore stations. Total mesozooplankton biomass and abundance decrease with increasing depth. In contrast, the individual body size of zooplankton organisms in general and specifically that of calanoid copepods increases with increasing depth.

Primary production is restricted to the sunlit surface layer of the ocean. Therefore, food availability for herbivorous zooplankton sharply declines below the euphotic zone. Total

zooplankton biomass and abundance follow this trend and exponentially decrease with increasing depth. Zooplankton composition will change accordingly, also affected by vertical profiles in physical parameters such as temperature and oxygen concentration. Since species of deep-sea zooplankton are often larger than related species at the surface, an increase in individual body size is expected with increasing depth.

Hypothesis 2: Cross-shelf gradients

Mesozooplankton abundance and biomass decrease with increasing distance from the shoreline. There are changes in zooplankton composition along the cross-shelf transect. Oceanic zooplankton is generally smaller than neritic specimens.

Coastal upwelling ecosystems are defined by a very high productivity compared to the open ocean. Based on the rich primary production, secondary production by zooplankton is expected to be higher in the active upwelling zone than further offshore. The changes in environmental conditions from the active upwelling at the coast to oligotrophic oceanic waters will affect zooplankton composition. Even within the same species, e.g. *C. carinatus*, changes in stage composition are expected with reproducing adults close to the coast and a sequence of ontogenetic stages associated with the offshore transport of the upwelling plume. Zooplankton organisms in warm and oligotrophic oceanic waters are often smaller than species of productive cold-water ecosystems. Therefore, it is proposed that zooplankton body size will decline along the cross-shelf transect with increasing distance from the active upwelling cell.

Hypothesis 3: Changes across the Angola-Benguela Front

Mesozooplankton abundance and biomass decrease towards the tropical Atlantic and are highest in the Benguela upwelling system. The composition of the zooplankton community changes across the Angola-Benguela Front. Zooplankton organisms are smaller in warm water regions of the Angola Basin than in the Benguela Current region.

The tropical region north of the Angola-Benguela Front is characterised by warm, nutrient-poor water compared to the cold, highly productive region of the Benguela upwelling system. Biomass and abundance of zooplankton organisms are therefore expected to be higher in regions, where phytoplankton production is high. Since the Angola-Benguela Front separates two ecosystems with different hydrographical conditions, it is assumed that the composition of the zooplankton community will reflect these characteristics. Zooplankton organisms are usually smaller in tropical environments compared to cold water regimes. Thus, it is expected that the

body size of zooplankton organisms declines towards areas north of the Angola-Benguela Front.

Topic 4: Trophic-interactions in the northern Benguela upwelling system

Based on stable isotope signatures of food web components and information on size classes of potential prey, a conceptual model of the pelagic food web of the northern Benguela upwelling system and the respective energy flows will be developed and discussed.

Upwelling systems are known for their usually short food chains that lead to a very efficient transfer of energy from primary production to fish and provide the basis for extensive commercial fishing.

2 Material and Methods

2.1 Study Area

The Benguela upwelling region is located in the South East Atlantic Ocean off the coast of South Africa and Namibia between 16°S and 34°S (Fig. 2.1). It comprises the cool Benguela Current which flows in a north to north-westward direction along the coast. The unique character of the Benguela upwelling system derives from the fact, that it is bounded in the North and South by warm water regimes. The northern boundary is the Angola Current which transports warm tropical water southwards along the Angolan coast. In the south, the Benguela system is bordered by the Agulhas Current retroflection area (Shannon & Nelson 1996). A mixture of water masses of different origins is prevalent in the Benguela upwelling region. Tropical and subtropical waters occur at the surface, whereas thermocline water masses primarily consist of South Atlantic and tropical Atlantic central water. Below the thermocline, Atlantic intermediate water is prevalent in average depths of 700-800 m (Nelson & Hutchings 1983, Shannon & Nelson 1996). A poleward flowing undercurrent on the shelf can be found in depths of 200 to 300 m and is described as a compensation current to the northward flowing Benguela Current (Nelson & Hutchings 1983).

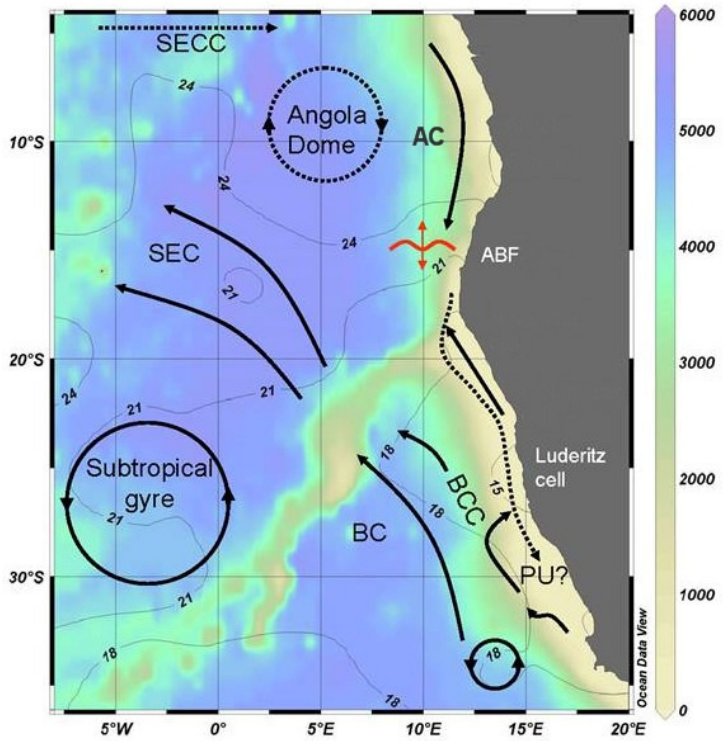

Fig. 2.1. The Benguela upwelling system with major oceanographic features. SECC: South Equatorial Counter Current, SEC: South Equatorial Current, AC: Angola Current, BC: Benguela Current, BCC: Benguela Coastal Current, PU: Poleward Undercurrent, ABF Angola-Benguela Front (modified after GENUS-proposal).

Coastal upwelling in the Benguela system is induced by strong south-easterly trade winds. These winds cause strong offshore Ekman transport of surface water masses so that cool and nutrient-rich South Atlantic central water from depths of around 300-400m wells up to the surface (Hardman-Mountford et al. 2003). Upwelling in the Benguela system occurs in separate patches (upwelling cells) along the coast and is described as sporadic (Nelson & Hutchings 1983, Shannon & Nelson 1996). Upwelling intensities fluctuate throughout the year in seven to ten-day cycles between active upwelling and relaxation. The only structure within the Benguela system, for which intense perennial upwelling is recorded, is the Lüderitz upwelling cell (Duncombe Rae 2005).

The Lüderitz upwelling cell is located at 27°S and presents a permanent structure within the Benguela system. It is known to be one of the most powerful upwelling cells of the world's ocean (Wasmund et al. 2005). The Lüderitz upwelling cell separates the Benguela upwelling system into a northern and a southern sub-system (Shannon & Nelson 1996, Hardman-Mountford et al. 2003). It may also prevent the transport of plankton organisms between the two sub-systems (Largier & Boyd 2001). North of the Lüderitz cell, in the northern Benguela upwelling region, a few other active upwelling cells have been identified. They are located at around 20°S and 23°S off the Namibian coast (Shannon & Nelson 1996, Hardman-Mountford et al. 2003). The northernmost upwelling cell that has been observed is situated at 18°S near Cape Frio (Nelson & Hutchings 1983). In the vicinity of Cape Frio, the shelf is very narrow with only 40 km in width (Nelson & Hutchings 1983). This aspect of the shelf topography is characteristic for major upwelling cells in the northern Benguela system (Nelson & Hutchings 1983, Hardman-Mountford et al. 2003). Off the coast of Namibia, maximal upwelling intensity is recorded for austral winter and spring (Branch et al. 1987). In the southern Benguela system, highest upwelling activity is prevalent during spring and summer (and autumn) (Shannon & Nelson 1996). These alternating periods of highest upwelling activity in the subsystems are due to changes in the atmospheric pressure system and resulting winds (Shannon & O'Toole 2003).

Another significant structure associated with the Benguela upwelling system is the Angola-Benguela Front (ABF). This convergence zone forms where the cool equatorward flowing Benguela Current meets the warm poleward flowing Angola Current (Shannon et al. 1987). The ABF is a permanent structure of the Benguela upwelling region sustained throughout the year between 14°S and 17°S (Nelson & Hutchings 1983, Meeuwis & Lutjeharms 1990, Shannon & Nelson 1996). Within this area, the location of the front fluctuates seasonally, depending on the strength of the two adjacent current systems. During austral winter and early spring, the ABF is located furthest north correlating with strongest upwelling in the northern Benguela system. In summer and autumn, the ABF is found furthest south during a period of weak coastal upwelling and greatest southward transport of tropical waters from the Angola Current (Nelson &

Hutchings 1983, Meeuwis & Lutjeharms 1990, Shannon & Nelson 1996, Hardman-Mountford et al. 2003). The ABF may expand to a depth of 200 m, but is significantly represented in the upper 50 m (Nelson & Hutchings 1983, Meeuwis & Lutjeharms 1990, Shannon & Nelson 1996). Distinct changes of temperature and salinity patterns can be observed throughout the front which characterise different water masses north and south of it. The ABF therefore represents a temporally and spatially very variable structure (Shannon & Nelson 1996).

Approximately every 10 years periodic warm events influence the northern Benguela system and are commonly described as 'Benguela Niños' (Shannon & Nelson 1996). In these years, an enhanced intrusion of warm water with high salinities originating in the Angola Basin can be observed. This goes along with a decrease in upwelling intensity in the northern Benguela region. These factors consequently result in a southward shift of the ABF (Shannon & Nelson 1996). The Benguela Niño phenomenon can to some extend be compared to the El Niño Southern Oscillation events that occur in the Pacific Ocean (Shannon & Nelson 1996). Benguela Niños were recorded for the years of 1934, 1949, 1963, 1972-1974, 1984 and 1995 (Shannon & Nelson 1996).

Occasionally there are also severe hypoxic events recorded in the Benguela upwelling region (Nelson & Hutchings 1983). These hypoxic, or even anoxic, conditions of the shelf water derive from intrusions of oxygen depleted water from the Angola Basin which is transported into the northern Benguela region by the poleward undercurrent (Nelson & Hutchings 1983). Moreover, the decomposition of organic matter after strong upwelling events can contribute to hypoxic conditions on the shelf (Shannon & O'Toole 2003). Anoxic events lead to high mortality rates of zooplankton organisms and fish and to altered abundance patterns (Shannon & O'Toole 2003).

2.2 Sampling Strategy

Sample collection and preservation

The zooplankton samples, which were analysed for this thesis, originate from the northern Benguela upwelling system off the coast of Namibia between 14°S and 20°S.

Samples were collected during two different cruises in the years 2007 and 2008. The cruise on the research vessel Dr Fridtjof Nansen took place from February 7th 2007 to February 23rd 2007 and the Maria S. Merian cruise was conducted from March 9th 2008 to April 4th 2008. The Maria S. Merian cruise was split into two different legs, the first leg (2b), started on March 9th 2008 and ended on the 20th of March 2008 and the second leg (3), took place from March 22nd to April 4th 2008.

For the purpose of this study, a cross-shelf transect at 20°S and a meridional transect at 11°30'E along the Namibian and Angolan coast, ranging from 14°S to 18°S in the area of the Angola-Benguela Front were chosen. The cross-shelf transect (T-7) was only sampled in 2008, while the meridional transect (T-3) was sampled during both cruises and different stations were chosen for analysis (Fig. 2.2 and Tab. 2.1).

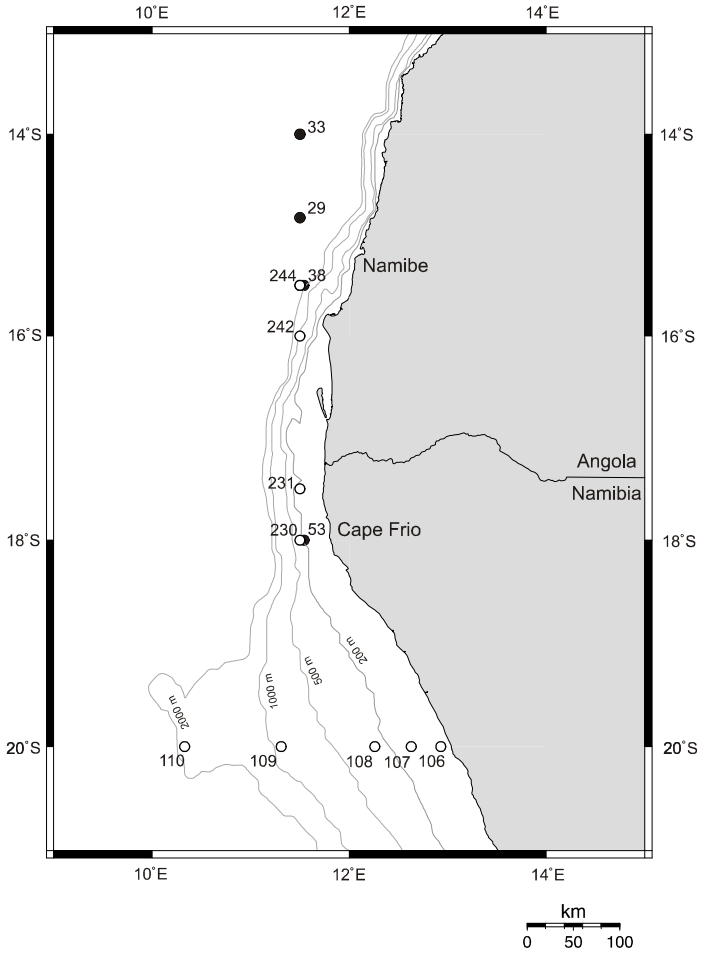

Fig. 2.2. Study area and position of stations. Black dots indicate stations from the Dr Fridtjof Nansen cruise in 2007 and white dots indicate stations from the Maria S. Merian cruise in 2008.

Mesozooplankton samples derived from stratified vertical hauls using a multiple opening/closing net system (Hydrobios Multinet Midi) with a 0.25 m^2 mouth area and with five nets of 150 µm mesh size (Maria S. Merian) and 180 µm mesh size (Dr Fridtjof Nansen). Maximum sampling depth was 1000 m. The net was heaved vertically at a sampling speed of 0.5 m s^{-1}. Samples were hauled at different times of the day (Tab. 2.1). At each station, water temperature, oxygen concentration and salinity were measured by a Conductivity-Temperature-Depth profiler (CTD) and appropriate depth intervals for sampling were determined according to these data. Samples from stratified vertical hauls were preserved in 4% buffered formaldehyde in seawater solution. Some individuals of the most common species were selected and separately deep-frozen at

-80°C. Samples were stored either at the Department of Marine Zoology at the University of Bremen or at the Center for Tropical Marine Ecology in Bremen.

Table 2.1. Positions of stations.

Cruise	Station	Date	Time	Latitude [°S]	Longitude [°E]	Bottom depth [m]	Max. sampling depth [m]
Dr Fridtjof Nansen							
	33	15.02.2007	night	14.00	11.30	3300	200
	29	16.02.2007	night	14.50	11.30	2577	600
	38	18.02.2007	day	15.30	11.30	1739	200
	53	20.02.2007	day	18.00	11.30	242	200
Maria S. Merian 2b							
	106	12.03.2008	night	19.59	12.56	59	60
	107	13.03.2008	night	19.59	12.38	129	120
	108	13.03.2008	day	19.59	12.16	238	230
	109	13.03.2008	night	19.59	11.19	967	950
	110	14.03.2008	day	19.58	10.20	1387	1000
Maria S. Merian 3							
	230	31.03.2008	day	18.00	11.30	240	220
	231	31.03.2008	day	17.30	11.30	165	155
	242	03.04.2008	day	16.00	11.30	1239	600
	244	03.04.2008	day	15.30	11.30	1709	600

Sample preparation

Each zooplankton sample, representing a defined depth layer, was rinsed with water through a sieve of 100 µm mesh size. The sample was then re-suspended in fresh water and transferred into a Folsom plankton splitter. The Folsom splitter provided suitable aliquots of the original samples by dividing them into two equal portions. In this way, a series of aliquots was acquired which contained defined fractions (1/2, 1/4, 1/8, 1/16…) of the original volume of the sample. Depending on the concentration of particles in each sample, the process was repeated as many times as necessary. In the end, the volume of the aliquot was appropriate for the following scanning procedure as it fitted into a square Petri dish of the size of 10 x 10 cm but still contained enough individuals of each taxon (around 50) to be representative (Grosjean et al. 2004). Some species were too rare to fulfil this prerequisite.

The suitable subsample was poured into a square Petri dish with the minimum amount of water possible (10-20 ml), to prevent the particles from floating during the scanning process. To acquire a digital image of the subsample, it was scanned with an EPSON Perfection V 750 Pro flatbed scanner by placing the plastic dish with the subsample onto the scanner window. The particles in the dish were manually separated from each other to make sure that they neither

touched one another nor the sides of the dish. This procedure is essential because overlapping particles would be misidentified as one during image analysis. Particles with contact to the edges of the dish will be ignored and thus will not be taken into account for the following analysis. Larger organisms such as pteropods and their pseudoconches, large krill and jellyfish as well as other large particles such as marine snow, were removed prior to the scanning process. All previously removed organisms were recorded and added later to the abundance data. In case of the removal of marine snow or other discard particles, it is important to confirm that no smaller zooplankton organisms are tangled up within. The scanner was operated in transparent mode in order to obtain a light background and contrasting dark silhouettes of the particles. A frame of the size of 97.8 mm x 97.8 mm (equivalent to 9234 x 9234 pixels at a resolution of 2400 dots per inch (dpi)) was adjusted to the area of the plastic dish that was scanned. At a resolution of 2400 dpi, the corresponding pixel size is thus 0.0106 mm which results in an image size of 9234x9234 pixels.

Two scans per sample were made. The first scan was made in 24-bits colour with a low resolution of 600 dpi and saved in jpeg format. The second scan was made in 16-bits grey scale with a higher resolution of 2400 dpi and saved in tiff format. The first picture could immediately be inspected; the latter one was used for the image analysis by ZooImage. A resolution of 2400 dpi is appropriate for the study of mesozooplankton and for the recognition of essential details (Grosjean et al. 2004, Warembourg et al. 2005). Sample preparation, including scanning, took around 45 min depending on the concentration of particles in the sample and the dilution steps required.

The computer aided optical analysis of the zooplankton samples prevented the use of some samples of stations 106, 230 and 231 because of too high phytoplankton abundance, which affects image analysis.

2.3 Image Analysis with ZooImage

All computer based analyses were conducted using a 2.0 GHz Acer Aspire X3200 desktop computer with an AMD Athlon™ 64 X2 Dual-Core Processor and 4 GB of RAM. For the automated image analysis of the zooplankton samples, the newest version (1.2-1) of the software Zoo/PhytoImage was used. Zoo/PhytoImage is opensource software for the analysis of digital plankton images and is available for download at the Zoo/PhytoImage web site http://www.sciviews.org/Zoo/PhytoImage. It has been designed by Philippe Grosjean and Kevin Denis in 2001. ZooImage operates in R language and provides ImageJ and XnView as additional software.

The process of image analysis with ZooImage is divided into three parts. The first part deals with the management and storage of images, the second part includes the training of the automatic particle recognition procedure and the third part is focused on the analysis of complete series of zooplankton samples in terms of abundance, biomass and size spectra (Grosjean & Denis 2007). The different steps of the analysis are represented by the symbols on the toolbar of the ZooImage assistant (Fig. 2.3).

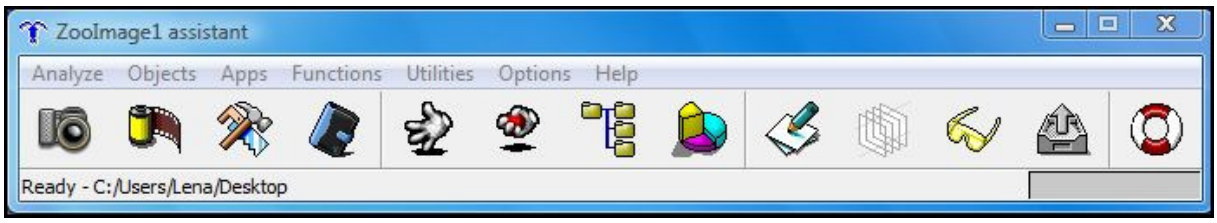

Fig. 2.3. The ZooImage toolbar with 12 different symbols representing the different steps of image analysis.

Image processing

For each image, a metadata file needs to be provided, containing information on image type, volume of the subsample, volume of seawater filtered, pixel size, pixel unit and minimum and maximum size of particles to be measured. All these information are essential for the calculation of abundances, biomasses or size spectra. The pixel size (mm) has automatically been determined by the scanner and is 0.0106 mm. The minimum size of 0.2 mm and the maximum size of 20 mm for the particles that will be taken into account for length measurements were chosen according to the size range of mesozooplankton. The whole process takes around 7 to 10 min per image, depending on the size of the image and the number of particles in the sample. During the analysis, the software extracts vignettes (small images of each identified object in the sample) and makes length measurements of each (Fig. 2.4).

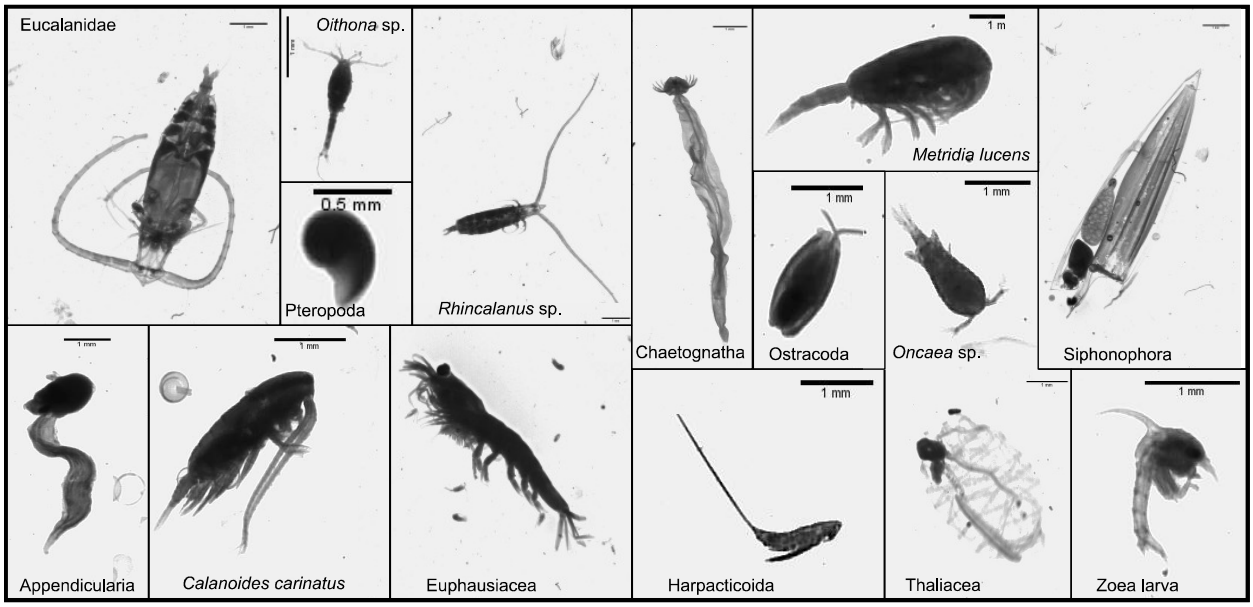

Fig. 2.4. Example of individual vignettes of zooplankton organisms.

Creation of the training set

The second part of ZooImage focuses on training the automated particle recognition procedure. 'A training set is a manual classification of representative particles in different groups' (Grosjean & Denis 2007) which is created with the free software XnView (http://www.xnview.com) supplied by ZooImage. Depending on the accuracy and the taxonomic level of classification desired by the user, a hierarchy of directories and subdirectories can be established.

In order to create the training set, a number of different samples must be chosen that represent the entirety of samples to be analysed. It is recommended to select at least 10 samples from the whole geographic region, various depths and different seasons to cover the variety of zooplankton organisms within the study area and to achieve the largest diversity in the training set as possible. Subdirectories correspond to subgroups of a taxon, e.g. 'Calanoida' and 'Cyclopoida' are subdirectories within the group of 'Copepoda'. Besides categories for each organism group, it is also important to include discard categories for example 'marine snow', 'fibre', 'debris', 'dirt', 'bubble' or 'scratch'. Discard particles often occur in high abundance and must be identified properly so that they can be excluded from further analyses (Bell & Hopcroft 2008). In addition, groups like 'unknown' or 'bad image' can be added to the training set. Furthermore, directories such as 'Copepoda multiple' have to be included in case of multiple organisms in one image, as well as categories for organisms that are not of primary interest but are existent in the samples, e.g. phytoplankton.

For the creation of the training set for this thesis, 12 samples of the Maria S. Merian cruise were chosen and particles were sorted into 38 different groups. Number and identity of groups were chosen in accordance with the abundance of common zooplankton organisms in the Benguela

upwelling region as well as with recommendation by ZooImage. Within the software XnView, the vignettes of each scanned sample chosen for the training set, were manually classified by dragging each vignette into its corresponding directory. It is important to note, that each directory should contain at least 15 to 50 vignettes to provide a variety of different aspects of the organisms to the identification routine. Once each category contains enough vignettes, the preliminary training set is loaded into ZooImage. In the next step, the ability of the computer to correctly classify objects, i.e. the quality of the training set, can be verified. Therefore, a machine learning algorithm has to be chosen. According to the manual classification of objects, the algorithm generates an adequate recognition tool (Grosjean & Denis 2007). This means that it applies certain parameters to predict the category of unknown particles on the basis of all the different measurements made on them in the first section (Grosjean et al. 2004). There are six different machine learning algorithms available within ZooImage that all use different techniques for the classification of particles and show varying accuracy in performance (Table 2.2).

Table 2.2. Performance of different machine learning algorithms provided by ZooImage.

Algorithm/Classifier	Mismatch in classification [%]	*k*-fold cross-validation error [%]
Linear discriminant analysis	41	44
Recursive partitioning tree	45	53
k-nearest neighbour	42	57
Learning vector quantization	49	59
Neural network	35	45
Random forest	0	38

The performance of the machine learning algorithms is measured by a method called '*k*-fold cross-validation'. In particular, ZooImage applies '10-fold cross-validation'. This technique is usually used in order to choose a suitable classification method (Stone 1974, Schaffer 1993) and to establish an estimation of error rate of a predictive model (Grosjean & Denis 2007, Fernandes et al. 2009). For this purpose, the dataset (here: the training set) is randomly divided into 10 different parts (folds) (Bell & Hopcroft 2008). A classification algorithm is then trained and validated 10 times. In every round, a different fold is used as validation data for testing the model and the remaining folds are used for training (Stone 1974, Fernandes et al. 2009). In this way, each particle/vignette in the training set is used in the validation step and in the training step, but never at the same time (Grosjean & Denis 2007). To obtain a single evaluation of the accuracy of the algorithm, the mean value of the validation results in the 10 test folds is estimated (Fernandes et al. 2009). In contrast to two or five fold cross-validation, the estimates for 10 folds are satisfactory and nearly unbiased (Efron & Gong 1983, Kohavi 1995). For the

purpose of choosing the best classifier (algorithm), all of the six machine learning algorithms are applied on the originally established training set and the accuracy of their performance is verified. A list of the different algorithms and their tested performance in the classification of objects is shown in Table 2.2.

According to the results of the performance test, random forest was selected as the classification algorithm for the present training set. It produced the lowest *k*-fold cross validation error (38%) and was the only algorithm with 0% of mismatch in classification. The method of classification by the random forest algorithm is based on classification trees. It creates numerous decisional random trees where every decision node discriminates between two variables (Grosjean & Denis 2007, Bell & Hopcroft 2008). Some of the advantages of the random forest algorithm are a very high accuracy in classification, an efficient handling of large data sets, the estimation of significance of variables for classification and its efficient method for the estimation of missing data (Cutler et al. 2007). Moreover, random forest is widely recommended as a classification algorithm for zooplankton and is supposed to be among the most efficient methods in accuracy of classification (Grosjean et al. 2004, Grosjean & Denis 2007, Bell & Hopcroft 2008). Although the random forest algorithm produced the lowest *k*-fold cross validation-error of all six algorithms, 38% of error in classification is still too high to be accepted for accurate analysis of zooplankton samples. Therefore the training set has been modified according to the following procedure intending to reduce the error value.

In order to analyse the performance of the chosen classifier and to measure the precision of automatic classification (Hu & Davis 2006), a 10-fold cross-validated confusion matrix is calculated (Fig. 2.5). A confusion matrix is a contingency table which matches up all categories of the manual classification (rows) with the categories of the automated recognition (columns) (Grosjean & Denis 2007) and displays the error. Therefore, it shows the efficiency of the recognition tool. The red diagonal line from the top left to the bottom right corner represents the correct classification and corresponds to agreement between manual and automatic classification (Hu & Davis 2006). The red squares apart from the diagonal, stand for confusion between two different categories where human and machine classifications are not the same; the darker the colour, the higher the degree of confusion between these groups.

The confusion matrix can therefore be used to improve the training set. By modifying the training set, e.g. adding additional groups or combining them, it is possible to reduce confusion between manual and automated classification and to optimise the performance of the recognition tool. In Figure 2.5, a confusion matrix of the final training set, classified by the random forest algorithm, is shown. As cited above, the original training set had been modified several times on the basis of the results of intermediate confusion matrices. The original number of 38 categories was reduced to only 26 categories by combining several classes or

rejecting others with a too inaccurate character. The training set, as well as the random forest classifier were saved for further use in section three of the software package.

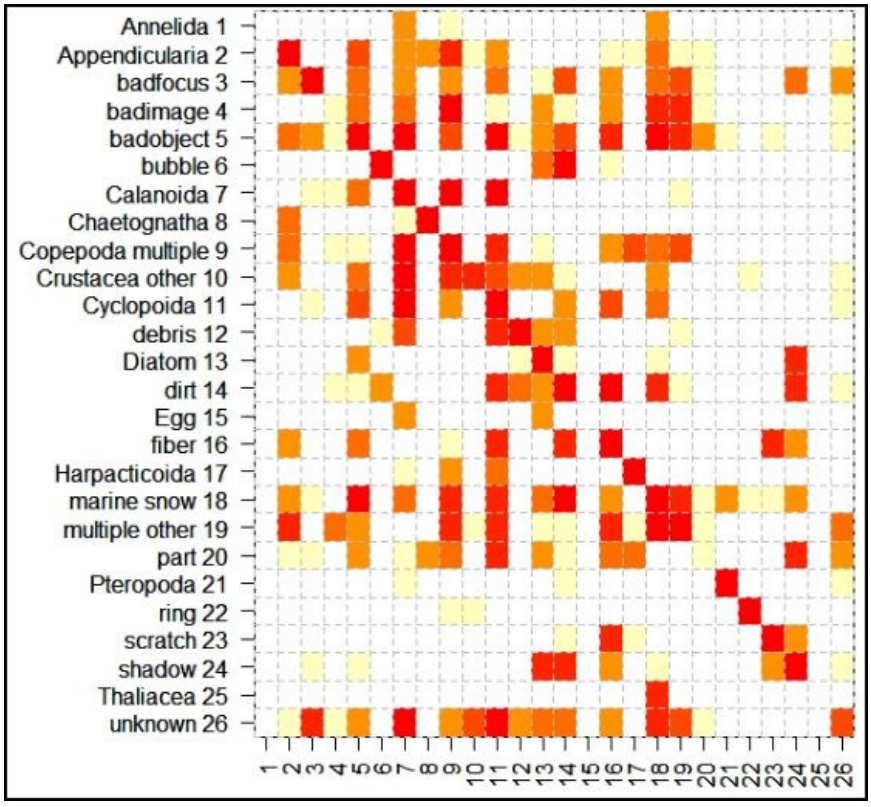

Fig. 2.5. Confusion matrix of the final training set with 26 different categories using the random forest algorithm.

Figure 2.5 clearly shows that there still exists a high degree of confusion between manual and automated classification. This derives from the fact that categories such as ‘Copepoda multiple’ or ‘multiple other’, ‘marine snow’, ‘dirt’ or ‘debris’ and even ‘Crustacea other’ contain particles of very diverse shapes and sizes. This makes it difficult for the computer to clearly distinguish between these objects and sort them into specific groups. However, these categories must remain in the training set. Confusion also occurs between distinct groups with similar body shape such as ‘Appendicularia’ and ‘Chaetognatha’ or between the subgroups of the category ‘Copepoda’, i.e. ‘Calanoida’ and ‘Cyclopoida’. Apparently, the differences between these groups do not appear as remarkable to the computer as they might be to a human taxonomist. The categories where there is no or little confusion are ‘Pteropoda’ and ‘ring’ due to their characteristic silhouettes. The category ‘ring’ derives from a ring-shaped artefact in the plastic dish which holds the sample during the scanning process. There are also categories, where there is no red square within the diagonal line, meaning that there is no correlation between manual and automatic classification at all. This is true for groups such as ‘Annelida’, ‘badimage’, ‘Egg’, ‘part’ or ‘Thaliacea’. Presumably this is because these categories do not contain enough vignettes for the computer to successfully recognise as such. For the groups of ‘Annelida’, ‘Egg’

and ‘Thaliacea’ this is because they were not very abundant in the samples and thus not many vignettes could be added to the respective folders.

Finally, the reduction of the *k*-fold cross-validation error after numerous modifications of the training set is not very great with 36%. However, if all discard categories were neglected and only organism groups considered, the *k*-fold cross-validation error would reach an substantially lower value of 19%. A further strong reduction of the error rate can be accomplished by excluding the catagory ‘Copepoda multiple’. The error value then decreases to 13% which is acceptable and lies in the range of the classification error by a human taxonomist (Bell & Hopcroft 2008).

In conclusion, the most important issue is to find a compromise between the number of meaningful categories and the accuracy that can be obtained by automatic classification through the computer (Bell & Hopcroft 2008, Fernandes et al. 2009). Because of this difficulty, the creation of the training set is the most essential part of the process of image analysis as well as the most time consuming aspect of ZooImage (Bell & Hopcroft 2008).

Sample analysis

Once the second part of the process is completed, the computer is able to recognise particles (with a known error value) and to automatically sort them into their corresponding groups. The last section of image analysis is the part where the samples are being analysed in means of biological and ecological information such as biomass, abundance and size spectra (Grosjean & Denis 2007). This section is especially designed for spatial and temporal analyses of large series of samples. Results are calculated in cubic meter of seawater by taking into account all the details indicated in the metadata file (Grosjean & Denis 2007). For each single particle a series of measurements such as width, height, equivalent circular diameter (ECD), etc., will be made and stored in a corresponding text file. This file also contains the identification of each particle based on the parameters. The extraction of ecological parameters of each sample is accomplished in only a few seconds.

Validation of species identification

Each species’ identification obtained from ZooImage was manually checked against the respective vignette. If automatic classification did not match the actual identity of a particle or organism, computer-based classifications were corrected.

One advantage of the manual crosscheck was that a much higher taxonomic resolution could be achieved than by ZooImage alone. In contrast to the rather rough classification of

zooplankton groups by the computer, it was possible to distinguish between different genera or even species within the order of Calanoida and Cyclopoida and to identify different developmental stages of Crustacea, e.g. copepod nauplii, decapod larvae, adult krill, etc. In this way, the two most common cyclopoid genera *Oncaea* and *Oithona* and several common calanoid genera and species such as *Calanoides carinatus*, *Metridia lucens*, *Pleuromamma* spp., *Eucalanus* spp. and *Rhincalanus* spp. could be identified. This higher taxonomic resolution provided additional information on the distribution of important copepod species in the Benguela upwelling system.

Critical discussion of ZooImage as an analysis method for zooplankton samples

The application of the software ZooImage for the analysis of zooplankton samples has several advantages. Compared to classical methods for the treatment of plankton samples, automatic plankton analysis processes can save a lot of time once the software is trained. Especially the automatic size, biomass and abundance measurements that are conducted during the process are very efficient. Manual sorting of the sample as well as size measurements and biomass estimations are very time-consuming. Nevertheless, the creation of the training set is certainly a time-consuming process of ZooImage, but it is also the most essential step (Bell & Hopcroft 2008). Moreover, it is essential to bear in mind, that computer-based image analysis can only be as good as the quality of the training set (Bell & Hopcroft 2008). Therefore taxonomic knowledge and experience in the identification of zooplankton species is irreplaceable. Even though, the creation of the training set and the classification of particles that were conducted for this study had been done to the best of my knowledge and checked and discussed with an experienced zooplanktologist, there might still remain a source of error.

If the training set is well established, ZooImage can reach accuracies of up to 70-80% (Benfield et al. 2007). Bell and Hopcroft (2008) obtained an error rate of only 13% which is comparable to accuracies a human taxonomist is able to achieve. The higher error rate of 36% in the present study is less promising. However, it may be explained by the more diverse zooplankton communities of tropical and subtropical waters providing a harder challenge for classification and species identification. The manual crosscheck significantly reduced the error rate of the automatic classification by ZooImage. In the majority of cases, particles that were incorrectly classified were ‘badobject’, ‘debris’, ‘marine snow’, ‘unknown’ and ‘dirt’. This is because particles of these groups comprise very diverse silhouettes that do not fit a common, easily detectable outline. Classes that were often confused with each other were ‘Calanoida’ and ‘Cyclopoida’, ‘Chaetognatha’ and ‘Appendicularia’, ‘Pteropoda’ and ‘debris’, and ‘Chaetognatha’ and ‘fiber’. These examples demonstrate that differences that seem obvious to a human eye are not always significant to the algorithm.

In order to test the capacities of ZooImage in comparison to the manual identification by humans, a test has been conducted where the same aliquot (1/16) of a North Sea zooplankton sample was analysed by four groups of students and at the same time in by ZooImage. The automatic classification was manually verified. Table 2.3 shows that manual and automatic classifications come to nearly the same results in the case of this example with a sample of rather low biodiversity.

Table 2.3. Comparison between manual and automatic classification of a zooplankton sample from the North Sea. Sub-samples were analysed by four groups of students (A-D) and by ZooImage (E). The copepod-categories *Centropages* spp., *Pseudocalanus* spp. and *Calanus* spp. were combined to the class 'Calanoida' for automated analysis.

Taxa	A	B	C	D	E
Temora longicornis	80	43	74	61	93
Acartia spp.		3		2	2
Centropages spp.		1	2	3	
Pseudocalanus spp.		3		3	**10**
Calanus spp.	1	7	2	9	
Oithona spp.		5		1	
Decapoda larvae	53	39	49	36	53
Cladocera	2	2	4	2	1
Polychaeta larvae	109	86	108	87	106
Fish eggs & fish larvae	17	23	24	18	21

A difficulty which comes along with the creation of the training set is to determine the right number of classes (Fernandes et al. 2009). This has to be decided regarding the taxonomic resolution that should be achieved and the ability of the computer to distinguish between categories. This study shows that with this method, it is difficult to receive adequate results if categories are very detailed and that the software is not able to successfully identify organisms on the species level. Better results can be obtained if categories describe higher taxa like Chaetognatha, Calanoida, Thaliacea or even 'Crustacea other'. Bell and Hopcroft (2008) advise that instead of high taxonomic level, size might be a better feature to accomplish a higher grade of accuracy, since size seems to be a predominant aspect in classification algorithms of ZooImage.

In conclusion, ZooImage is a useful tool for the automatic analysis of zooplankton samples, especially if data on particle sizes are required. Nevertheless, it becomes clear that ZooImage can only perform well if the training set is chosen carefully and contains sufficient vignettes (Bell & Hopcroft 2008). Keeping in mind that also a human taxonomist can not achieve accuracies of 100% (Culverhouse et al. 2003), the performance of ZooImage can reach acceptable levels. A combination of automatic classification and manual control, as conducted in this study, seems to obtain the best results, although it requires additional time. This method is also appropriate

for the analysis of diverse plankton samples from subtropical regions. The application of an automatic method for the analysis of zooplankton is especially effective for large series of samples that otherwise could not be treated in an adequate period of time.

2.4 Data Analysis

Abundance of zooplankton groups

For the following eight dominant zooplankton groups, abundance data were calculated according to the given equation: Calanoida, Cyclopoida, Harpacticoida, other Crustacea, Pteropoda, Chaetognatha, Appendicularia and Thaliacea.

$$\text{Abundance per } m^3 = \frac{\text{No. of Individuals} \cdot \text{dilution factor}}{\text{volume filtered}}$$

Zooplankton size spectra

Size frequency analyses were conducted for calanoid copepods and for total zooplankton in general for each sample, based on the equivalent circular diameter (ECD) of each particle provided by ZooImage. The ECD value corresponds to the diameter of a circle, which encompasses the same spatial area as the body shape of the animal. Appendages of plankton organisms like long antennae or rami are also taken into account and contribute to the overall dimension of the resulting circular area of the individual. The ECD does therefore not depict the actual length of an organism and can not be directly compared to total body or prosome length measurements available from published sources. Nevertheless, the ECD value as an indicator of body size is commonly used in size spectra analysis (Sheldon et al. 1972, Isla et al. 2004, Martin et al. 2006). Furthermore, the ECD of organisms underlies little changes relative to actual body length and is a useful measure to compare organisms of different shapes.

Spatial changes in size-frequency distribution of calanoid copepods and of total zooplankton are presented for the surface layers of the three transects and for vertical profiles from the surface to the deep sea at two stations north of the Angola-Benguela Front (stns. 244 and 29) and at the two offshore stations 109 and 110 of the cross-shelf transect. Mean size and standard deviation were calculated from original ECD values of all individuals of the Calanoida and total zooplankton of every sample. Due to a large sample size and high numbers of individuals, this procedure is very robust and, thus, legitimate, although the size-frequency data often did not follow a normal Gaussian distribution (De'ath, personal communication).

2.5 Estimation of Biomass

The biovolume of each sample was measured by volumetric analysis as a proxy for total mesoplankton biomass. For most of the samples, a measuring cylinder of 25 ml volume was used. If sample volume was very small, a 10 ml cylinder was used. Every sample was rinsed with freshwater into a sieve of 100 µm mesh size. The sample was subsequently transferred with some water into the cylinder. After 20-30 min when the content of the sample had settled at the bottom of the cylinder, its volume in ml was recorded. In some samples, the content had not settled completely after 30 min. This was for the most part due to gelatinous components or crustaceans exuviae, which floated at the surface. This proportion of the sample was added to the settled volume and in most of the samples it was below 10% of total sample volume. If the volume of the floating material exceeded 10% of total sample volume, it is indicated in the results section. Some samples of station 106 (30-60 m), station 230 (25-40 m and 40-70 m) and station 231 (10-25 m and 25-50 m) had to be treated differently due to the dominance of phytoplankton. Biomass of these five samples was estimated in their original preservative using a 100 ml measuring cylinder. The final biomass value was recorded after 45 min because of longer settling times of smaller particles in fluids with higher densities. Results are given as biovolume per volume of filtered water, applying the following formula:

$$\text{Biovolume (ml m}^{-3}) = \frac{\text{biovolume}}{\text{volume filtered}}$$

2.6 Stable Isotope Analysis

For the analysis of stable carbon ($\delta^{13}C$) and nitrogen ($\delta^{15}N$) isotope ratios of different zooplankton and other species such as fish and seabirds, deep-frozen samples of the Maria S. Merian cruise in 2008 and of the Dr Fridtjof Nansen cruise in 2007 were used. Samples of a variety of different species were selected with the objective to achieve a high taxonomic diversity of consumers that live in the northern Benguela system. For some of the species different developmental stages, i.e. adults and copepodite stages C4-C5 were analysed.

Frozen samples of selected species were lyophilised for about 48 h in a freeze-dryer (Christ®, Alpha 1-4 LD plus). Dry mass of each sample was determined on a micro-balance (Sartorius R200D, precision ± 10 µg). The samples were then transferred into little tin capsules. The final weight of each sample had to be between 0.8 mg and 9 mg in order to be properly analysed. Eventually, only a subpart of an individual was used and individuals of small species were

combined in order to achieve an adequate dry mass for the analysis. Stable isotope ratios of carbon and nitrogen were determined by Agroisolab GmbH in Jülich with a mass spectrometer (Carlo Erba Instruments, EA NA1500 Series 2) using PeeDee Belemnite (PDB) limestone as a standard for carbon and atmospheric nitrogen (N_2) as a reference for nitrogen. Isotopic ratios of $\delta^{13}C$ and $\delta^{15}N$ are given in the unit ‰. For the calculation of isotope ratios, the following formula was used:

$$\delta X = [(R_{sample}/R_{standard}) - 1] \times 1000$$

where X is ^{13}C or ^{15}N, R is the corresponding ratio ^{13}C:^{12}C or ^{15}N:^{14}N, $R_{standard}$ for ^{13}C and ^{15}N is PDB and atmospheric air (N_2), respectively (Hodum & Hobson 2000).

$\delta^{15}N$ values of different developmental stages were treated separately and also different sizes of individuals, i.e. body dry mass, were taken into consideration. In contrast to some publications (Hobson et al. 2002, Smyntek et al. 2007, Mintenbeck et al. 2008), lipids were not extracted from the samples before analysis because foremost attention was given to stable nitrogen isotope ratios.

Stable nitrogen isotope signatures were used to reveal trophic relations among organisms in the Benguela food web. The calculation of explicit trophic levels, however, requires a given baseline (e.g. phytoplankton or particulate organic matter) as reference value to which the trophic position of consumers can be related to (Vander Zanden & Rasmussen 1999). Since these baseline data were not available for the two expeditions, the results of this study can only be used for relative comparisons of trophic levels among different consumers within the food web

3 Results

3.1 Hydrographical Parameters

Sea Surface Temperature

Figure 3.1 shows the distribution of sea surface temperature (SST) in the northern Benguela upwelling system during the Dr Fridtjof Nansen cruise in 2007 and during the Maria S. Merian cruise in 2008.

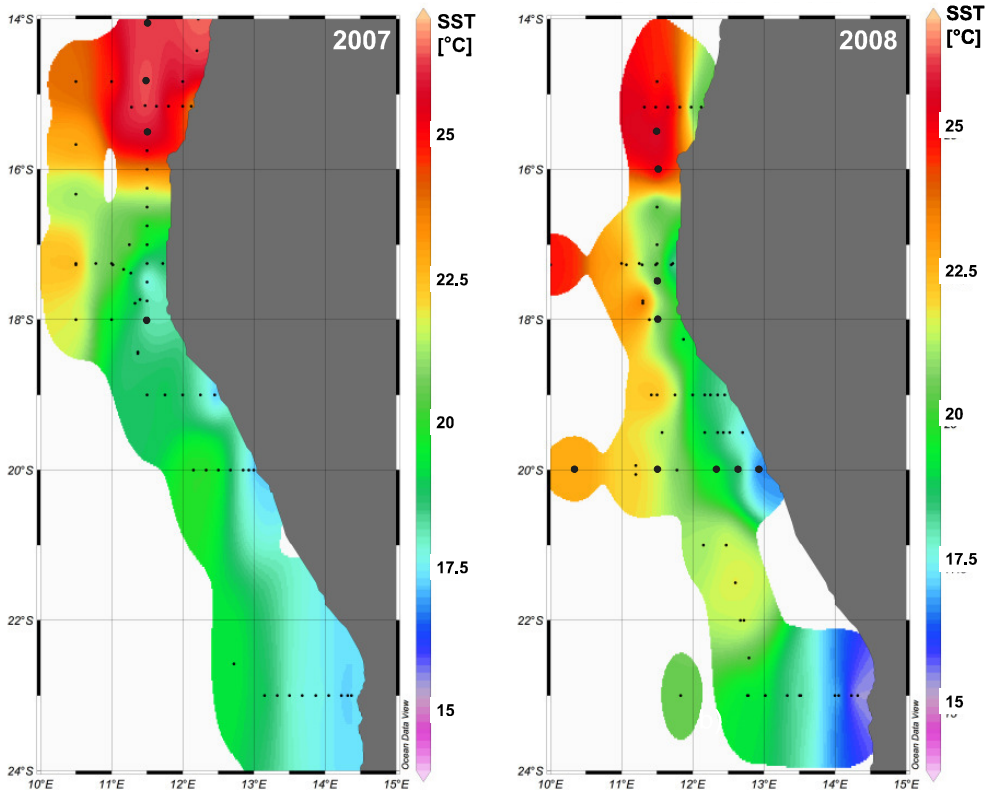

Fig. 3.1. Distribution of sea surface temperature in the northern Benguela upwelling system in 2007 and 2008. Small black spots represent all stations and big black spots specify selected stations for this study. White patches indicate areas where no data is available (modified after Auel & Ekau 2009).

In 2007, the Angola-Benguela Front (ABF) was located at 16°S (Fig. 3.1). The Angola Current water in the north of the front had a SST of 25°C or more and the warmest temperatures were measured close to the coast. Further offshore, the water still had temperatures of around 22.5°C and reached as far south as 18°S. The coastal waters in the south of the ABF displayed SST of less than 20°C. Areas of active upwelling could be observed close to the Namibian coast which were characterised by temperatures of around 17.5°C. These distinct upwelling spots occurred from 17.5°S to 18.5°S and at around 19°S. Between 20°S and 24°S, constant SST of 17.5°C were measured along this part of the Namibian coast. Water masses of around 20°C bordered the upwelling areas off the Namibian coast to the west.

The distribution of SST in 2008 was quite different from the situation in 2007 (Auel & Ekau 2009). An extensive southward intrusion of warm water of 22.5°C could be observed which reached as far south as 20°S in offshore regions. SST reached maximum values of more than 25°C in the north of the ABF which was also located at 16°S during this period. The Benguela Current region was characterised by a narrow area of 20°C warm water close to the coast in the north and regions of extensive upwelling south of 20°S with temperatures below 17.5°C. Upwelling was more intense in 2008 than in 2007 and occurred in the area at 20°S and south of 22°S with absolute minimum values of 15.5°C at 23°S. Through the southward intrusion of warm water from the north, the area affected by upwelling was limited close to the Namibian coast (Auel & Ekau 2009).

Vertical Profiles of Temperature and Oxygen

Meridional Transect T-3 of the Dr Fritdjof Nansen Cruise 2007

Along this transect, temperature (°C) and oxygen concentrations (ml l^{-1}) displayed nearly constant values in the upper, well mixed 20 m of the water column (Fig. 3.2). SST was above 25°C at the three stations north of the ABF (33, 29 and 38) with highest values at station 29 (26.3°C). The lowest SST was observed at station 53 (19°C) which is located south of the ABF. The stations north of the ABF displayed a strong stratification of the water column and a pronounced thermocline could be observed between 20 and 50 m. At station 29, the gradient was strongest; temperature dropped from 26°C to 16°C. Below the thermocline, temperatures continuously decreased at all three northern stations and reached a minimum of 3.3°C at a depth of 1000 m at station 29. At the southernmost station 53, temperature did not decrease as drastically with depth as observed at the other stations. Only a small temperature gradient existed at this station but no distinct thermocline developed. Temperature dropped merely by 4°C throughout a depth of 200 m.

Oxygen concentrations along this transect showed a similar vertical profile in the upper 500 m and generally decreased with increasing depth. They were highest at the surface of the southernmost station 53 (4.7 ml l^{-1}) and were around 4.3 ml l^{-1} at the northern stations. A subsurface maximum could be observed at the three northern stations in the water layer where the thermocline was located. Below the thermocline, oxygen concentrations decreased to 1.3 ml l^{-1} at around 60 m at stations 29 and 38, while at station 33, the amount of dissolved oxygen in the water column fluctuated stronger until it reached a minimum of 0.8 ml l^{-1} at around 80 m. At stations 38 and 33, the oxygen concentration below 80 m stayed relatively constant at around 1 ml l^{-1} down to a depth of 300 m. Below 300 m, an oxygen minimum layer (OML) developed with

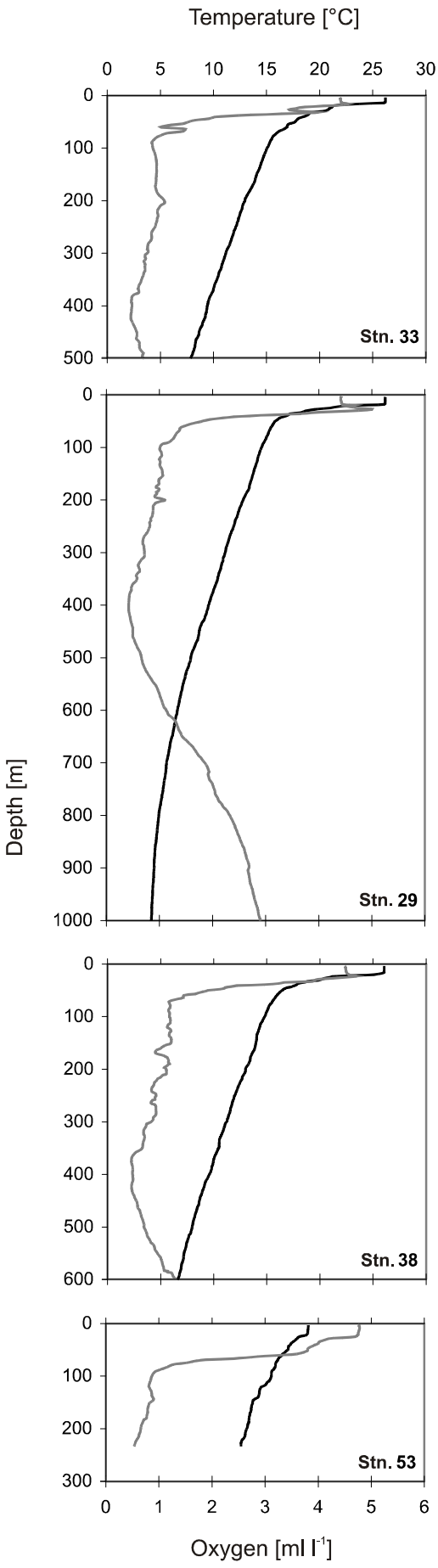

Fig. 3.2. Vertical profiles of temperature (black line) and oxygen (grey line) of the meridional transect T-3 at 11°30'E in 2007. Stns. 33, 29 and 38 are located north of the ABF, stn. 53 is located south of the ABF.

values beneath 1 ml l^{-1}. This oxygen depleted layer reached down to 500 m at station 38 where values began to increase again. At station 29, the oxygen content was below 1 ml l^{-1} between 160 and 570 m, with a small exception at 200 m, and reached an overall minimum of 0.4 ml l^{-1}. Below 600 m, oxygen concentration increased again until values of almost 3 ml l^{-1} were obtained in depths of 1000 m. At the southernmost station, oxygen concentrations did as well display a drastic decline in the upper 100 m of the water column. A minimum concentration of less than 1 ml l^{-1} was reached below 90 m and stayed below 1 ml l^{-1} down to the seafloor.

Salinity in the surface layers of the northern stations had maximum values of 36 psu. The variation in salinity in depths of 1000 m was only around 1.5 psu and overall minimum values of 34.5 psu were recorded in greater depths. At the southernmost station 53, salinity dropped by only 0.4 psu from the surface to 200 m.

Meridional Transect T-3 of the Maria S. Merian Cruise 2008

At all of the four stations of this transect, the surface layer from 0 to around 20 m was well mixed (Fig. 3.3). SST was highest at stations 242 and 244 north of the ABF reaching a maximum of 25.7°C. At stations 230 and 231, which are located south of the ABF, the SST was 19.4°C and 20.3°C, respectively. The two northern stations showed a pronounced stratification of the water column and a well developed thermocline at around 40 m depth. Below the thermocline, temperature decreased constantly to a minimum of 4°C at 1000 m depth at both northern stations. The stratification of the water column at the two southern stations 230 and 231 was not as pronounced as in the north and the temperature profile showed a gradually decrease down to minimum values of 12.4°C at station 230 and 13.6°C at station 231.

Oxygen concentrations decreased steadily with increasing depth at the southern stations 230 and 231. The surface water of these two stations contained maximum oxygen concentrations of 4.2 ml l^{-1} and in deeper layers below 66 m at station 230 and 53 m at station 231, an OML was observed with minimum concentrations of less than 1 ml l^{-1}. Oxygen concentrations at the northern stations 242 and 244 had a maximum in subsurface waters with values of 5.3 ml l^{-1} in 30 m depth and 4.9 ml l^{-1} in 20 m depth, respectively. These maximum subsurface concentrations correlate with maximum chlorophyll a values (1.8 mg m^{-3} at station 242 and 1.4 mg m^{-3} at station 244) in the corresponding depth and therefore indicate a high rate of primary production. In the layer where the thermocline was located, oxygen concentrations dropped below 1 ml l^{-1} in a depth of 76 m at both stations. At station 242, oxygen concentrations ranged around 1 ml l^{-1} with increasing depth and an evident OML was expressed in depths between 150 and 400 m with absolute minimum values of 0.3 ml l^{-1}. Oxygen concentrations at the

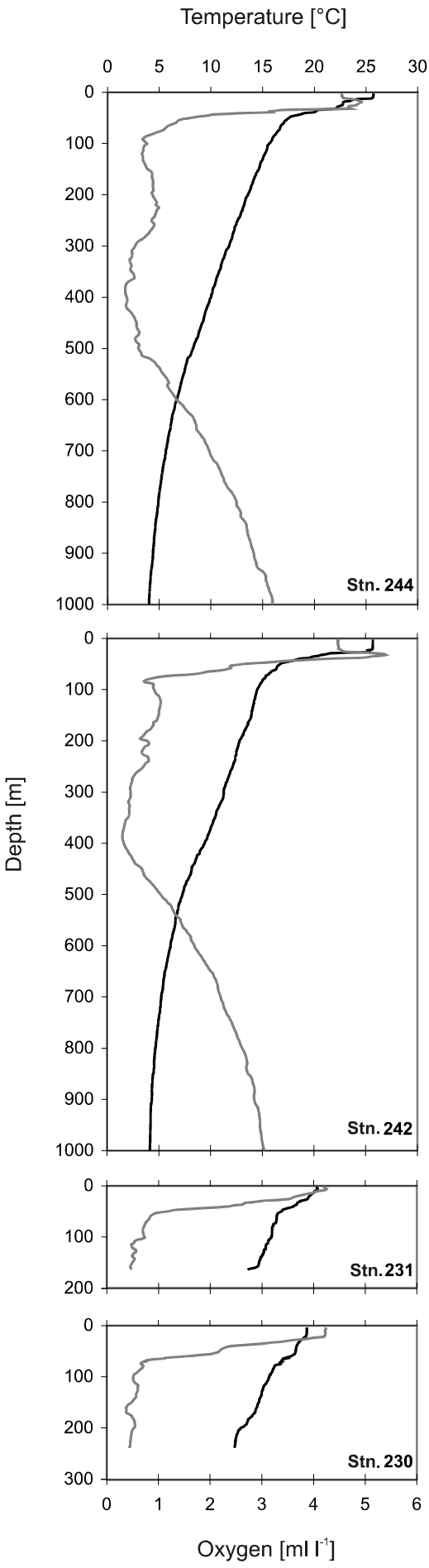

Fig. 3.3. Vertical profiles of temperature (black line) and oxygen (grey line) of the meridional transect T-3 at 11°30'E in 2008. Stns. 244 and 242 are located north of the ABF, stns. 231 and 230 are located south of the ABF.

northern station 244 stayed below 1 ml l^{-1} until a depth of 500 m and minimum values of 0.3 ml l^{1} were measured between 370 m and 420 m. Below 400 m at station 242 and below 500 m at station 244, oxygen concentrations began to increase again and reached concentrations of around 3 ml l^{-1} at maximum depths of 1000 m. The water below 500 m apparently represented a distinct water body of cool and oxygen enriched deep water.

At the southern stations 230 and 231, salinity values ranged from 35.8 psu at the surface to 35.2 psu at maximum sampling depth. At the northern stations, salinity at the surface was maximal 36.2 psu and decreased down to 34.5 psu at 1000 m depth.

Cross-shelf Transect T-7 of the Maria S. Merian Cruise 2008

At stations 106, 107, 109 and 110, the upper 20 m of the water column were well mixed (Fig. 3.4). This was not the case for station 108, where temperature and oxygen concentrations increased by around 1°C and 1 ml l^{-1} in the subsurface layer. SST was lowest at the coastal station 106 (16.8°C) indicating cool upwelled water. Highest SST were measured offshore at station 110 (22.8°C) where warm water from the South Atlantic subtropical gyre prevailed. The existence of a thermocline could be observed for all stations except for station 106. However, the stratification of the water column was less pronounced in neritic waters compared to the pelagic realm. At stations 107 and 108 a local thermocline was prevalent and only a small temperature gradient of around 5°C at station 107 and 4°C at station 108 could be observed. Temperatures hardly decreased below 13°C in subsurface waters at both stations. The pelagic stations 109 and 110 showed a very pronounced stratification and a distinct temperature gradient in the upper 200 m. In this depth range, temperature decreased by approximately 11°C.

In contrast to the general decrease in temperature with increasing depth, oxygen concentration rather fluctuated throughout the water column. These fluctuations were especially remarkable at the pelagic stations 109 and 110. At the inshore station 106, oxygen values in the surface layer were the lowest with 3.2 ml l^{-1}. All the other stations displayed higher surface concentrations of around 5 ml l^{-1}. At stations 106, 107 and 108, the decrease in oxygen below 20 m was significantly strong and constantly continued until concentrations reached the lowest values of less than 0.5 ml l^{-1} close to the seafloor. The oxygen gradient was most pronounced in the upper 100 m of stations 107 and 108 where concentrations dropped down to less than 1 ml l^{-1} below 80 m at station 107 and below 40 m at station 108. Station 108 displayed the broadest oxygen depleted layer which nearly covered 200 m of the water column with a small increase of oxygen values between 140 and 170 m. This might relate to a different water body prevalent at this depth. This irregular increase of oxygen concentration in intermediate depth could also be

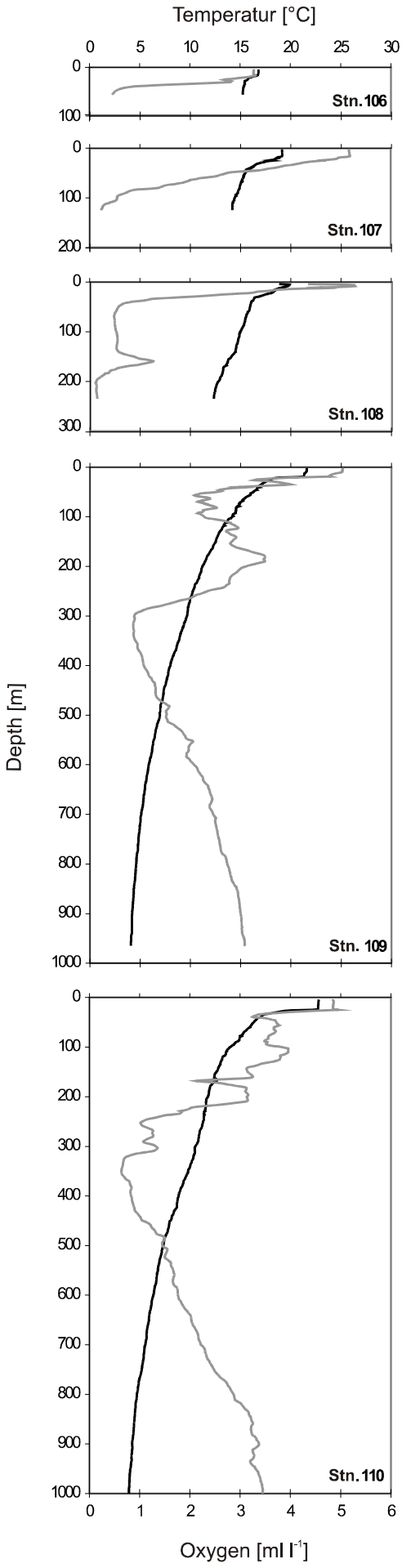

Fig. 3.4. Vertical profiles of temperature (black line) and oxygen (grey line) of the meridional transect T-3 at 20°S in 2008. Stn. 106 is located closest to the coast, stn. 110 is located furthest offshore.

observed at station 109 between 100 and 200 m where oxygen increased again to more than 3 ml l^{-1}. Station 110 expressed an opposite progression of the oxygen profile in this depth layer, which indicates that this water body did not extend further offshore. In general, stations 109 and 110 displayed strong fluctuations in the amount of dissolved oxygen in the upper 200 m. Below 200 m, oxygen concentrations began to decrease until they reached minimum values of less than 1 ml l^{-1} in intermediate depths from around 300 m to 400 m. This is where the OML was located. Below this zone, oxygen concentrations began to increase continuously until they reached values of more than 3 ml l^{-1} at the bottom depth of these two stations.

Salinity was at a constant range from 35 to 35.5 psu in the surface layer of all of the five stations along this transect and dropped down to 34.5 psu in depths of 1000 m at the offshore stations 109 and 110.

3.2 Abundance and Taxonomic Composition of Zooplankton

Meridional Transect T-3 of the Dr Fridtjof Nansen Cruise 2007

Mesozooplankton abundance patterns along transect T-3 in 2007 are shown in Figure 3.5. The southernmost station 53 was located south of the Angola-Benguela Front (ABF), whereas stations 38, 29 and 33 were located north of the ABF.

Along this transect, overall mesozooplankton abundance was rather low compared to the two transects of the Maria S. Merian cruise. Abundance was highest in the surface layers (0-30 m) at stations north of the ABF with maximum values at the northernmost station 33 with about 3000 ind. per m^{-3}. (Fig. 3.5). Subsurface layers from 30-60 m did also exhibit quite high zooplankton abundances and exceeded values from the surface layer at station 38. Below the surface layer at the northern stations, abundance decreased remarkably to 500 ind. per m^{-3} or less. Zooplankton abundance continuously declined with increasing depth at station 33, while at stations 29 and 38 an absolute minimum could be observed in intermediate depth intervals from 100 to 140 m. South of the ABF, mesozooplankton abundance was remarkably low. Station 53 showed the lowest abundance of all stations with only 25 ind. per m^{-3} in the surface layer and mesozooplankton abundance increased with depth to around 200 ind. per m^{-3} at 200 m.

At stations 29, 33 and 38 in the north of the ABF average diversity of existent zooplankton groups was very high, but copepods dominated the mesozooplankton community with up to 97% of all individuals (Fig. 3.5). The predominance of copepods in the samples decreased relatively towards the surface where other zooplankton taxa were present in higher numbers. Nonetheless, copepods made out at least 69% in all samples. Among the Copepoda, three orders could be recorded. The Harpacticoida composed only a minor proportion, whereas

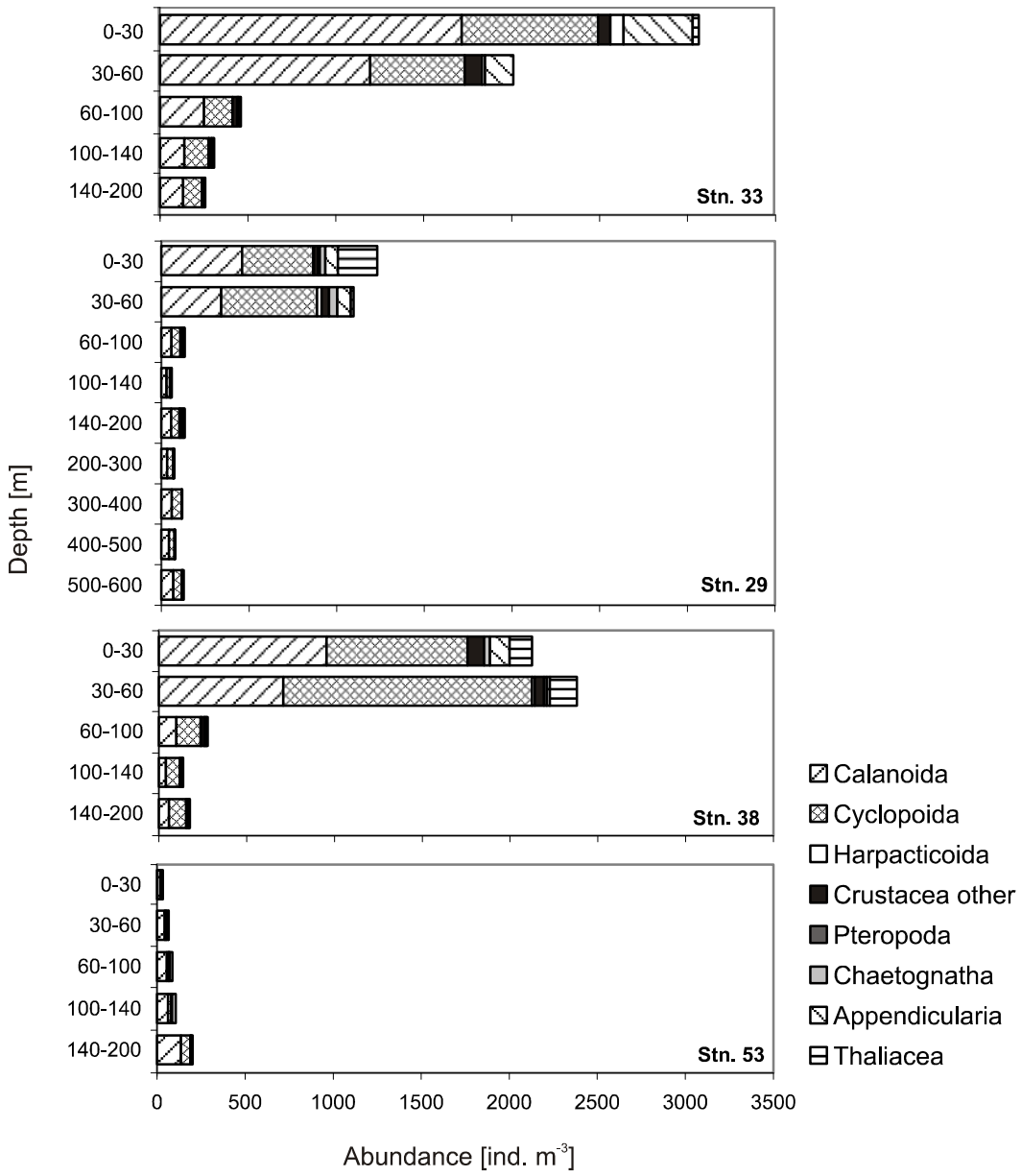

Fig. 3.5. Vertical distribution of zooplankton abundance along transect T-3 at 11°30'E in 2007 indicated as individuals per m^3. Stns. 33, 29 and 38 are located north of the ABF, stn. 53 is located south of the ABF.

Cyclopoida and Calanoida constituted the major fraction of the copepods in all samples. The distribution of these two orders seemed to be highly dependent on the location of each station and the depth layer. The Calanoida were generally the most abundant taxon along this transect and their predominance was especially significant in the upper 60 m of the northernmost station. Cyclopoids were most abundant in subsurface layers of stations 29 and 38 and occasionally outnumbered calanoid copepods in deeper water layers. At the southernmost station 53, cyclopoids constituted only a very small proportion of the zooplankton community. Other crustaceans were present in all samples of each of the four stations along this transect. They were considerably more abundant in the upper water layers from 0 to 60 m but also occurred in greater depth. Mainly euphausiids and copepod nauplii, which were also counted to this group,

dominated among the crustaceans. Ostracods were also frequently abundant at all stations throughout the water column. Euphausiids were predominantly recorded at the southernmost station 53. Some decapod larvae could also be found occasionally independent of water depth. Appendicularians were predominantly abundant in the epipelagial from 0 to 60 m at the northern stations while none were recorded at station 53 south of the ABF. Chaetognaths occurred in every sample in moderate numbers. Thaliaceans occurred predominantly at the surface, especially at station 29 where they strongly contributed to total zooplankton abundance. At station 38, thaliaceans were present throughout the water column and also at the northern stations 33 and 29 they occurred sporadically in greater depths. Only at station 53 they were very rarely present in the subsurface layer from 30 to 60 m. Pteropods of the genus *Limacina* were hardly present along this transect. Their shells irregularly occurred at stations 29, 38 and 53. Cnidaria, in particular Siphonophora, appeared in moderate numbers at all stations.

Species composition of the copepod community

The genus *Oithona* spp. was the dominant cyclopoid species at station 53 south of the ABF. North of the ABF, *Oncaea* spp. dominated at the surface (0-30 m) as well as in deeper waters of the mesopelagial and in water layers from 30 to 200 m, *Oithona* spp. was more abundant. Among the identified calanoid species, the most abundant were *Calanoides carinatus*, *Metridia lucens* and *Pleuromamma* spp. *M. lucens* and *Pleuromamma* spp. were predominantly abundant below 200 m at station 29 but did also sporadically occur in the epipelagial. At station 53, in the south of the ABF, they were present throughout the water column in higher numbers, but were especially concentrated between 140 and 200 m. At stations 33 and 38 these two species were hardly recorded at all. *C. carinatus* was abundant at each of the four stations, but displayed very different abundance patterns. At stations 33, 38 and 53 *C. carinatus* occurred throughout the epipelagic but was only present in very few individuals. A remarkable high abundance of *C. carinatus* was observed at station 29 in the mesopelagic water. In depths greater than 300 m this copepod was present in very high numbers compared to the epipelagial of station 29 where it was only sporadically observed. Eucalanidae were frequently present throughout the water column at all stations, but were remarkable high abundant at station 29 from 300 to 400 m. Other calanoid species that could be identified and sporadically occurred along this transect were *Megacalanus princeps* and *Gaetanus* spp. at station 53, *Euchaeta marina* at station 38 and 29, *Paraeuchaeta* spp. at station 29 and 33, *Rhincalanus* spp. and *Centropages* spp. as well as a few individuals of the family Augaptilidae at station 29.

Meridional Transect T-3 of the Maria S. Merian Cruise 2008

Figure 3.6 shows the overall abundance of mesozooplankton along transect T-3 in 2008. According to the position of the ABF in 2008, stations 230 and 231 were located south of the ABF, whereas stations 242 and 244 were located north of the ABF.

Average mesozooplankton abundance along this transect in 2008 was higher than along the same transect in 2007. Abundances were highest in the surface layers of stations 230 (0-25 m), 231 (0-10 m) and 244 (0-40 m) and ranged between 5000 and 6400 ind. per m^{-3} (Fig. 3.6). The highest overall abundance was recorded at the southern most station 230. At station 242 north of the ABF, surface abundance reached only about 2500 ind. per m^{-3}, which represented the lowest abundance of the stations along this transect. At the northern stations, zooplankton abundance drastically decreased below the surface layer to less than 1000 ind. per m^{-3} with minimum values between 50-200 m. In subsurface layers south of the ABF, phytoplankton abundance was very high and mesozooplankton abundance was above 1000 ind. m^{-3} down to a depth of 150 m.

Mesozooplankton diversity was highest in surface layers of all four stations (Fig. 3.6). Copepods dominated the zooplankton community with up to 85% at the surface and with more than 90% in deeper water layers. Harpacticoid copepods were only sporadically observed along this transect. Cyclopoids were often outnumbered by the Calanoida, especially in the surface layers. In greater depths below 80 m, cyclopoids often presented the most abundant taxon. The dominance of calanoids in the surface layers was most pronounced at stations 231 and 244 whereas at the southernmost station, the cyclopoids reached very high abundances. Other Crustacea were present at all stations throughout the water column, but abundances were rather low at stations north of the ABF compared to south of the ABF. Abundance of crustacean larvae (nauplii or decapod larvae) was highest at the surface. Euphausiids were absent in all samples. Appendicularians were widely distributed throughout epipelagic waters of all stations, but predominantly occurred at the surface. Chaetognaths and thaliaceans were rarely distributed across the ABF. While chaetognaths were present in the epipelagic of all stations, except at station 230, thaliaceans predominantly appeared in the surface layer south of the ABF. Pteropods were not very abundant in the samples of this transect. Although shells of *Limacina* spp. were present in the surface samples of each station, their total distribution was very low. In addition to these eight most common zooplankton groups, some cnidarians were also prevalent at the northernmost station from 200 to 600 m.

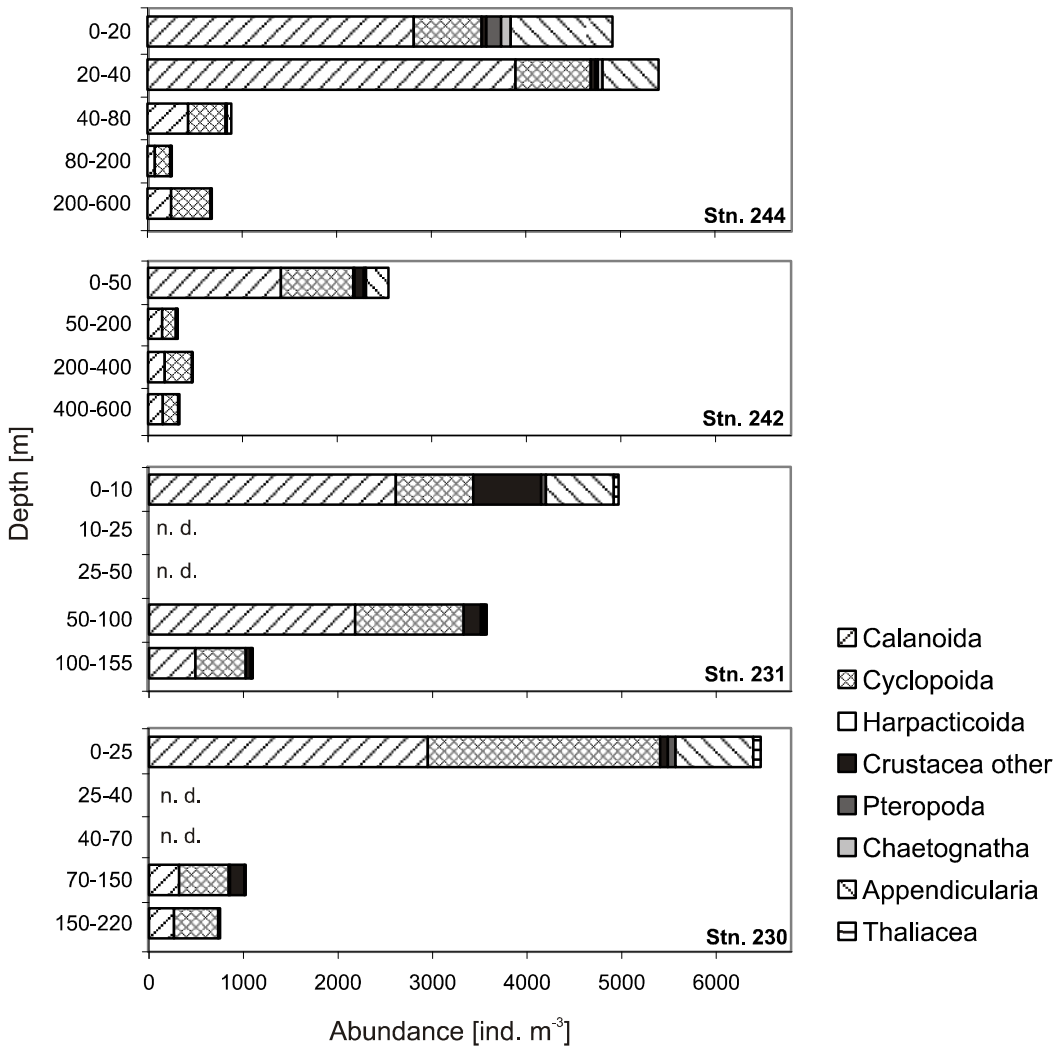

Fig. 3.6. Vertical distribution of zooplankton abundance along transect T-3 at 11°30'E in 2008 indicated as individuals per m^3. n. d. signifies no data. Stns. 244 and 242 are located north of the ABF, stns. 231 and 230 are located south of the ABF.

Species composition of the copepod community

The cyclopoid copepod *Oithona* spp. generally dominated in the upper 100 m of the water column (except at station 244), while *Oncaea* spp. was most abundant in the mesopelagial. In intermediate layers from 100 to 200 m, the two species displayed similar abundances. The distribution of calanoid copepods along this transect in 2008 was similar to their distribution in 2007. *Calanoides carinatus* was prevalent at all stations, but most abundant south of the ABF. At the southern stations, its abundance was twice as high at station 231 compared to station 230 and *C. carinatus* occurred almost exclusively in the surface layers. North of the ABF, *C. carinatus* was most abundant in greater depths below 200 m. *Metridia lucens* and *Pleuromamma* spp. were also among the most common calanoid copepods and primarily occurred in greater depths below 200 m at the northern stations. South of the ABF, they were sporadically observed also in the epipelagial. *Eucalanus* sp., as well as some individuals of *Rhincalanus* spp. and *Paraeuchaeta* spp., was mainly found in the mesopelagial north of the

ABF, whereas *Centropages* spp. and *Aetideopsis carinata* rarely occurred in the epipelagic south of the ABF.

Cross-shelf Transect T-7 of the Maria S. Merian Cruise 2008

Mesozooplankton abundance along the cross-shelf transect in 2007 is displayed in Figure 3.7. Station 106 is located closest to the coast while station 110 is the furthest offshore station.

Total mesozooplankton abundance was highest at the coastal station 106, reaching almost 9000 ind. per m^{-3} (Fig. 3.7). Abundance decreased with distance to the coast to not even 2000 ind. per m^{-3} at the offshore station 110. In general, mesozooplankton abundance was highest in the surface layer and decreased with increasing depth. This was not the case at the shallow station 107, where abundance was very low at the surface (around 1000 ind. per m^{-3}) and increased below 60 m. At stations 108, an abundance minimum could be observed in intermediate depth layers from 50 to 170 m. These zooplankton depleted layers were also prevalent at the offshore station 109 between 30 and 200 m and below 500 m and at station 110 from 100 to 200 m and below 600 m.

The diversity of mesozooplankton was highest in the upper 30 meters of the water column (Fig. 3.7). Copepods dominated the zooplankton community along the entire transect with up to 90% (Fig. 3.7). Calanoids and cyclopoids constituted the main proportion of copepods in all depths (70-90%), whereas Harpacticoida where only found in minor quantities in intermediate and lower depths. Cylopoids exhibited the highest general abundance of total mesozooplankton throughout the water column and considerably dominated the zooplankton community in coastal areas. Calanoids were the second most abundant taxon along this transect. Their abundance in the surface layer increased towards the open ocean and at the two pelagic stations 109 and 110 they presented the predominant taxon. Among other crustaceans, mostly decapod larvae, adult euphausiids and copepod nauplii were present. Although their abundance was generally low, they were present in small numbers throughout the water column. Highest abundances of mainly copepod nauplii and decapod larvae were found in the surface layers of stations 106, 109 and 110. Euphausiids were exclusively distributed in the epipelagic of stations 107, 108 and 109. Chaetognaths were only rarely observed in all water layers at stations 107 and 109 and at station 110, they occurred in the surface layer and in greater depths. Appendicularians appeared frequently in the upper 30 m of the water column and were especially numerous at stations 106, 109 and 110, while other tunicates, i.e. thaliaceans, were not widely distributed along this transect. Thaliacea predominantly occurred in the surface layer of the offshore station 110 and some individuals were also observed at station 109 between 300 and 500 m. Pteropods of the genus *Limacina* and *Cymbulia* were abundant at every station. Shells of

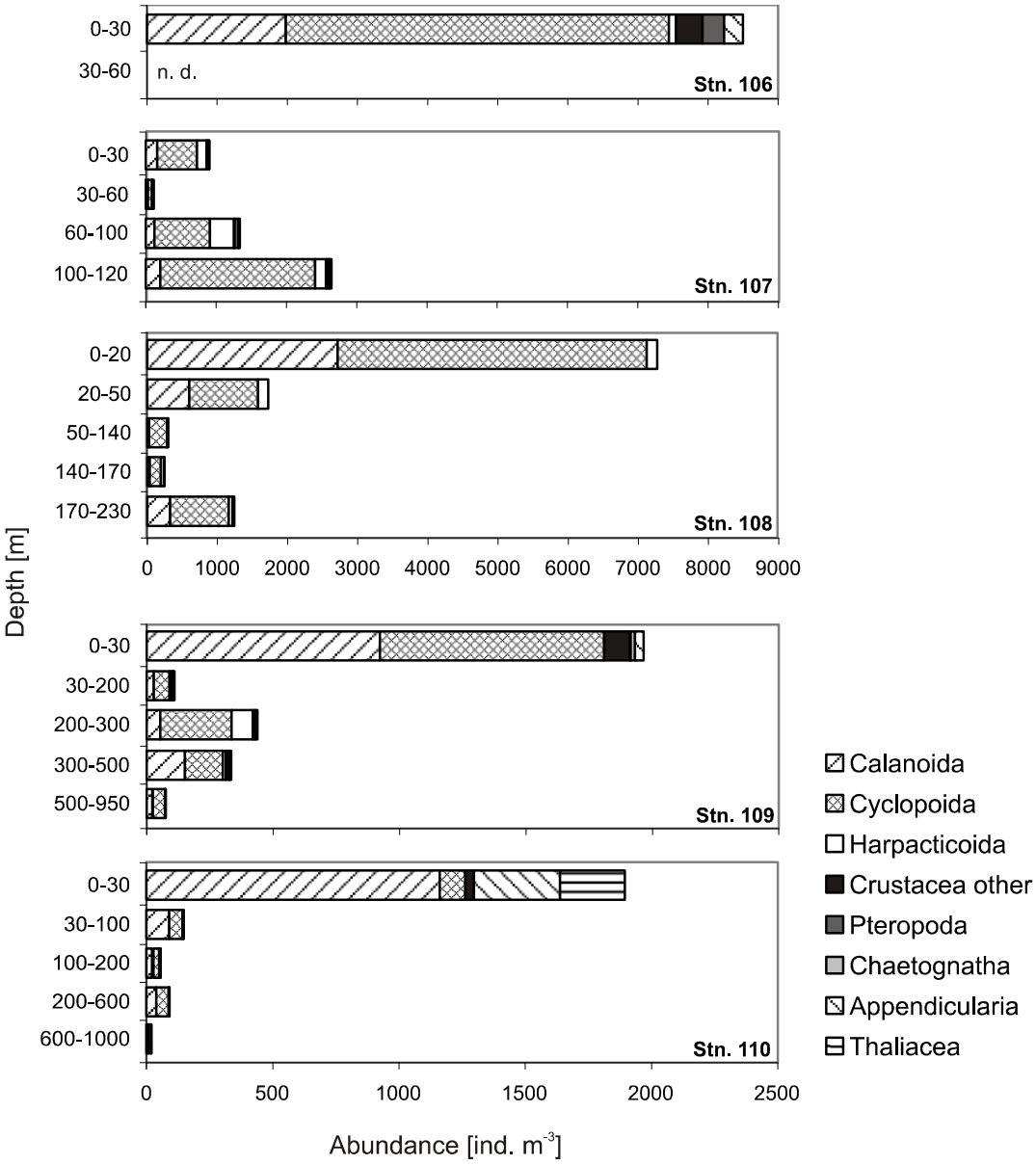

Fig. 3.7. Vertical distribution of zooplankton abundance along transect T-7 at 20°S in 2008 indicated as individuals per m^3. n. d. signifies no data. Stn. 106 is located closest to the coast, stn. 110 is located furthest offshore.

Limacina spp. were predominantly present at the surface in coastal areas and in deeper water layers at stations 107 and 110. Individuals of *Cymbulia* spp. and their pseudoconches occurred only in the upper layers of station 107, 108 and 109.

Species composition of the copepod community

Oithona spp. dominated at most stations in the epipelagic layer, whereas *Oncaea* spp. prevailed in the mesopelagial. Individuals of the calanoid copepods *Metridia lucens* and *Pleuromamma* spp. were most abundant in deeper water layers of the mesopelagial at the offshore stations 109 and 110. At station 109, several individuals were also prevalent at the surface. *Eucalanus* sp. also occurred predominantly in deeper waters at the offshore stations but was also scarcely

distributed between 100 and 200 m at station 110. *Calanoides carinatus* showed very low abundances along this transect. Some individuals occurred offshore at station 110 from 200 to 600 m and at the shallow station 107 between 30 and 100 m.

3.3 Size Spectra

Horizontal distribution of mesozooplankton size spectra

Size spectra distribution was analysed of the copepod order Calanoida and of total mesozooplankton in the surface layer of all stations of the three transects (Fig. 3.8). At the meridional transect T-3 in 2007, the surface layer of all of the four stations ranged from 0 to 30 m, whereas the surface layer of the stations along T-3 in 2008 ranged between 0 to 10 m and 0 to 50 m. The surface layer of stations of the cross-shelf transect T-7 was sampled from 0 to 30 m at all stations except at station 108 (12°16'E) where the surface layer was from 0 to 20 m. Values indicate mean size (mm) of the equivalent circular diameter (ECD) of each measured organism and corresponding standard deviation. In general, results do not demonstrate significant values because of a rather high variance in individual sizes resulting in high standard deviations of most of the mean sizes. These high variations, especially for mean sizes of total mesozooplankton, derive in most cases from single individuals of chaetognaths, euphausiids or tunicates that had very large ECD values compared to the average body size of the majority of individuals in the samples.

Calanoid copepods demonstrated only minor changes in mean size along the meridional transect as well as along the cross-shelf transect (Fig. 3.8 A, C, E). Although no significant results could be obtained, a trend towards increasing body sizes of calanoid copepods in regions of the Benguela upwelling system could be observed. This trend was more apparent along the meridional transect in 2008 than in 2007, where calanoids were larger south of the ABF (≥0.6 mm) compared to north of the ABF (≤0.5 mm). The smallest individuals with a mean size of 0.47 mm were found at the northernmost station in 2008. Changes in mean size of total zooplankton along the meridional transect were most apparent in 2007. Mean size remarkably increased towards the south exhibiting a maximum size of 1.35 mm at the southernmost station (Fig. 3.8 B). The strong increase was mainly due to larger euphausiids at this station south of the ABF.

Along the cross-shelf transect, mean size of calanoid copepods decreased from 0.53 mm at the coast, to 0.43 mm at the offshore station (Fig. 3.8 E). The decrease of body size towards the open ocean was not continuous and a slight increase of mean body size was observed between 11 and 12°E. Smallest variances in individual size of calanoid copepods were recorded at the furthest offshore station. Differences in body size of total zooplankton along the cross-shelf

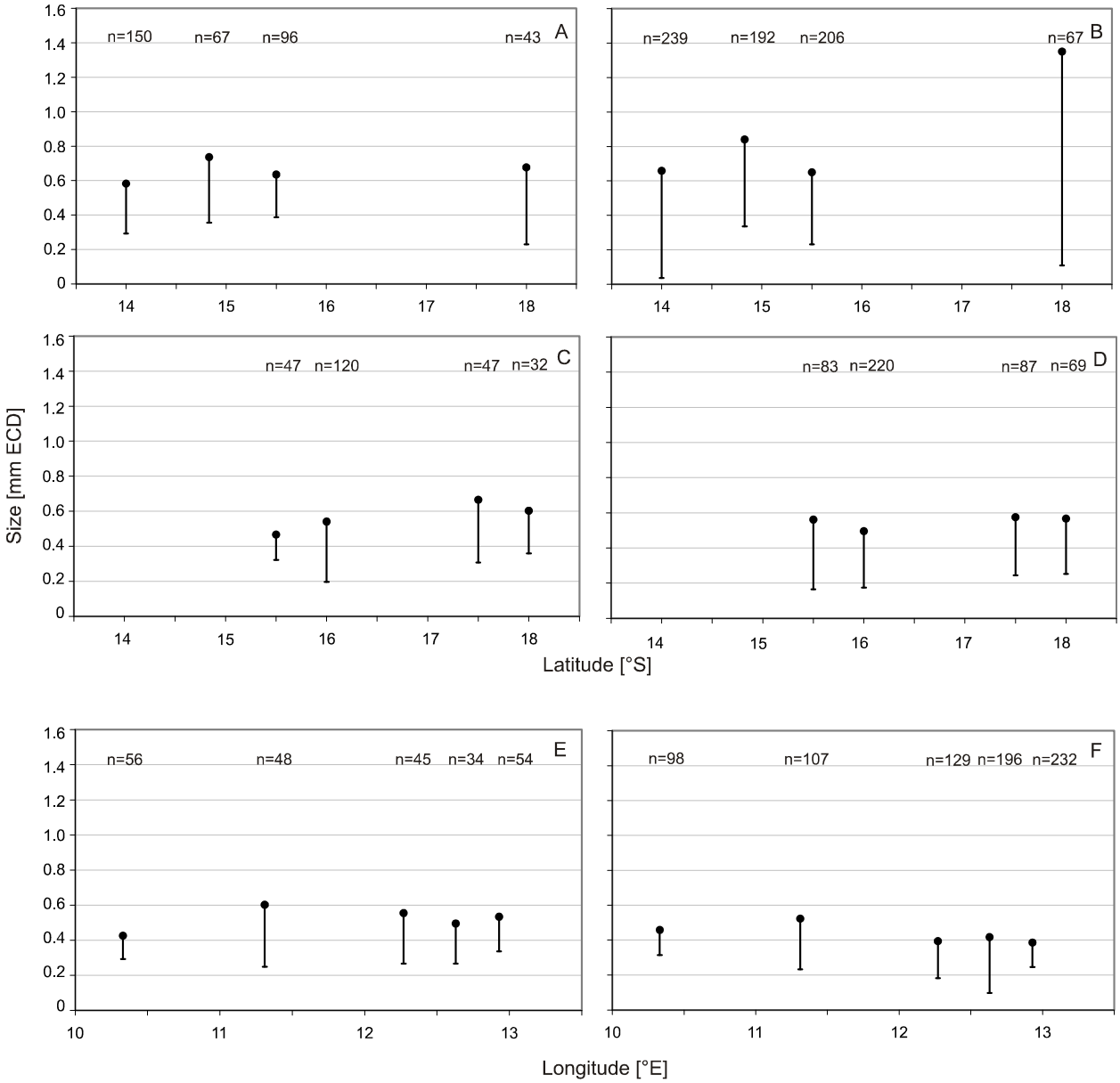

Fig. 3.8. Horizontal distribution of zooplankton size spectra in the surface layer. Mean body size is indicated as equivalent circular diameter (ECD). n indicates the number of measured individuals. A: Calanoida along transect T-3 at 11°30'E in 2007 B: Total zooplankton along transect T-3 in 2007 C: Calanoida along transect T-3 at 11°30'E in 2008 D: Total zooplankton along transect T-3 in 2008 E: Calanoida along transect T-7 at 20°S in 2008 F: Total zooplankton along transect T-7 in 2008.

transect were not remarkable and an increase towards the open ocean from 0.39 mm to 0.52 mm was observed between 11 and 12°E (Fig. 3.8 F). At the furthest offshore station however, mean body size decreased to 0.46 mm.

Vertical distribution of mesozooplankton size spectra

The vertical distribution of mean sizes of calanoid copepods and of total mesozooplankton at four stations is demonstrated in Figure 3.9 and 3.10. Two stations north of the ABF (29 and 244) with a maximum sampling depth of 600 m (Fig. 3.9) and the two offshore stations of the

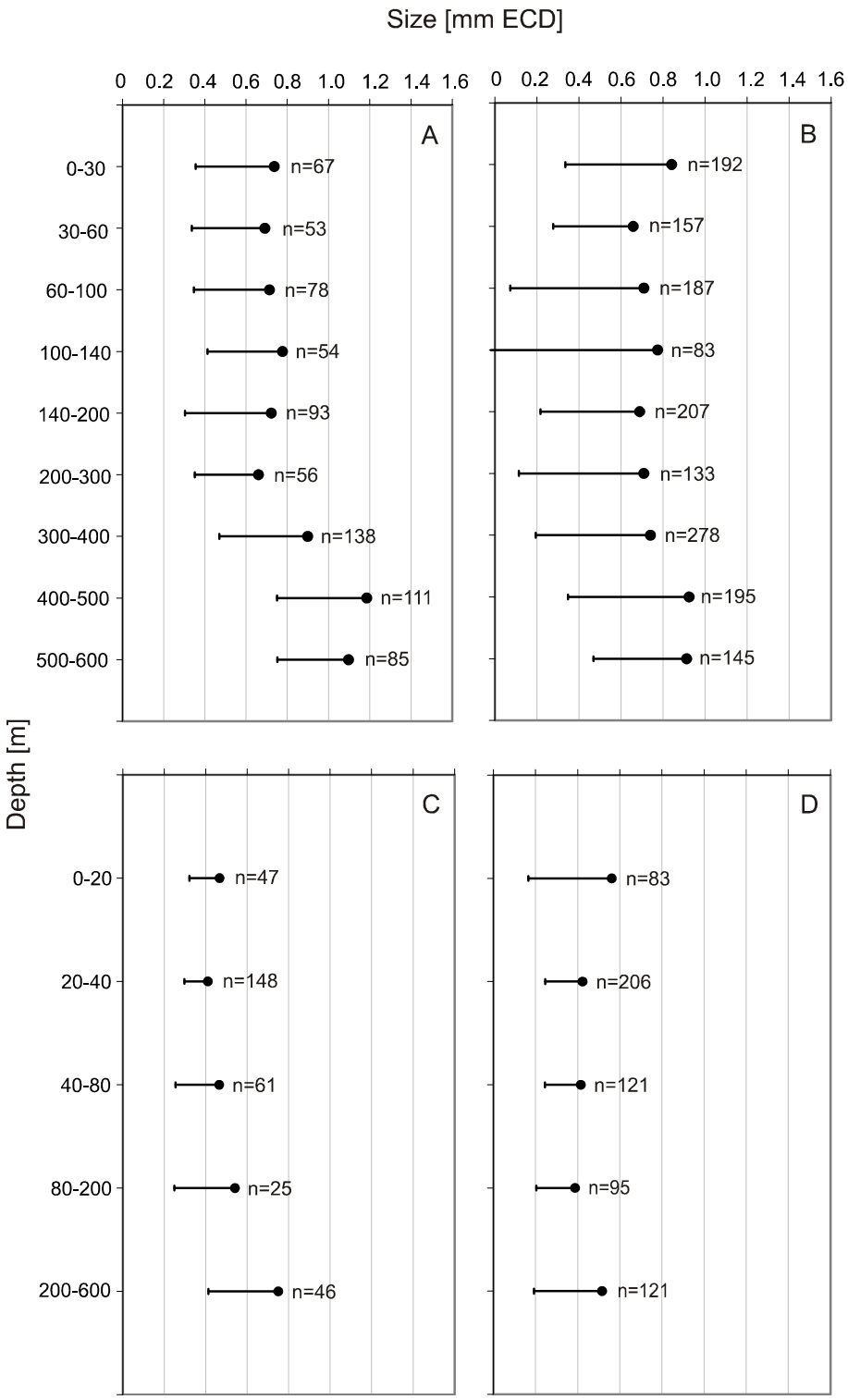

Fig. 3.9. Vertical distribution of zooplankton size spectra at two stations north of the ABF of transect T-3 at 11°30'E. Mean body size is indicated as equivalent circular diameter (ECD). n indicates the number of measured individuals. A: Calanoida at station 29 in 2007 B: Total zooplankton at station 29 in 2007 C: Calanoida at station 244 in 2008 D: Total zooplankton at station 244 in 2008.

cross-shelf transect (109 and 110) with a maximum sampling depth of 1000 m (Fig. 3.10) were selected. Vertical changes in mean calanoid and total mesozooplankton body size were not significant, and mean sizes often exhibited high variations (Fig. 3.9 and 3.10). Nevertheless, a

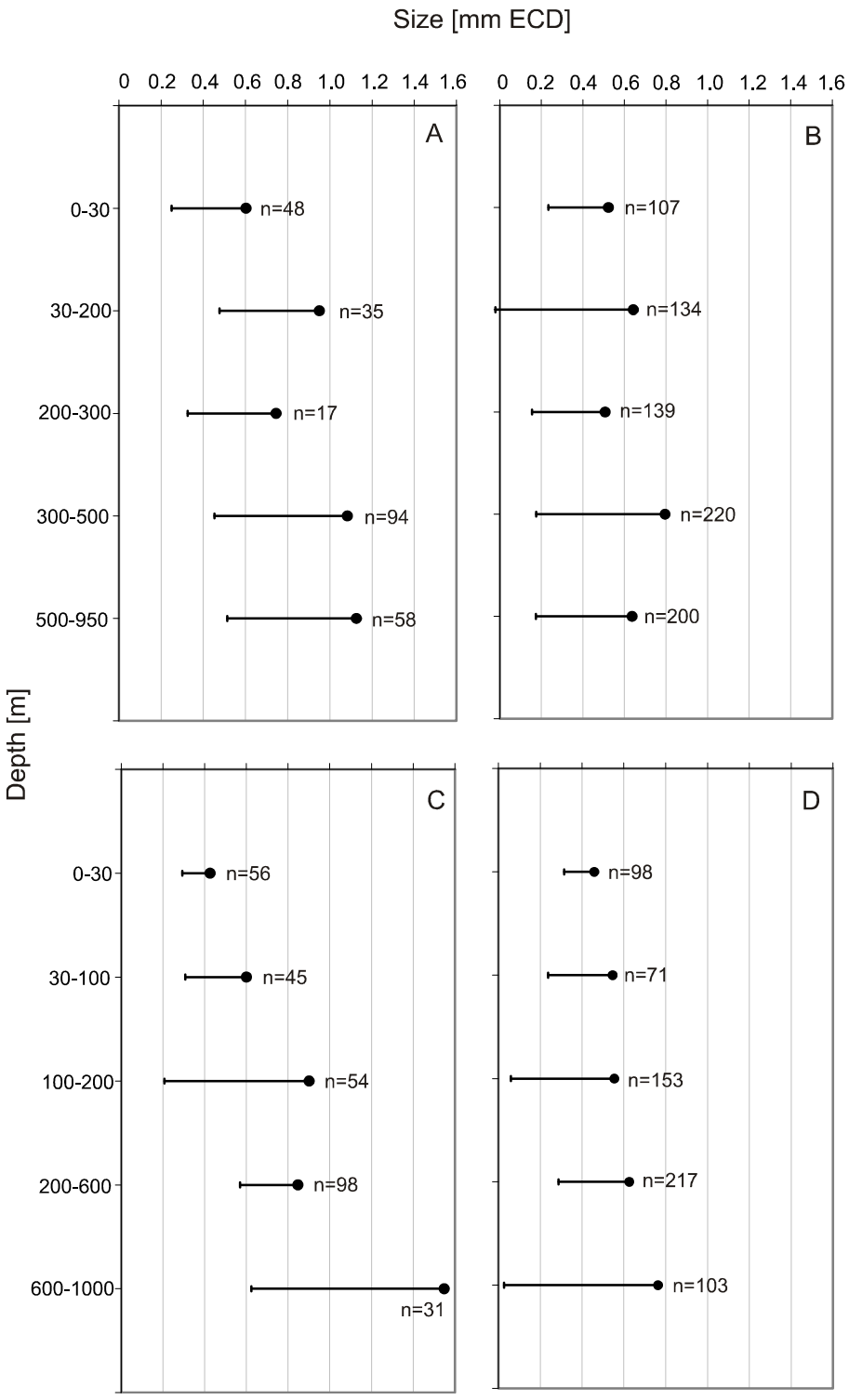

Fig. 3.10. Vertical distribution of zooplankton size spectra at two offshore stations of transect T-7 at 20°S. Mean body size is indicated as equivalent circular diameter (ECD). n indicates the number of measured individuals. A: Calanoida at station 109 in 2008 B: Total zooplankton at station 109 in 2008 C: Calanoida at station 110 in 2008 D: Total zooplankton at station 110 in 2008.

trend towards increasing body sizes with increasing depth could be observed. This was especially apparent at the offshore stations 109 and 110 (Fig. 3.10), where body sizes already increased below the surface. Mean body size of calanoids increased from 0.6 mm at the surface to 1.1 mm in the deepest layer at station 109 (Fig. 3.10 A) and from 0.43 mm to almost 1.55 mm

at station 110 (Fig. 3.10 C). Mean body size of total mesozooplankton increased from 0.52 mm at the surface to 0.64 mm in deeper layers at station 109 (Fig. 3.10 B) and from 0.46 mm to 0.76 mm at station 110 (Fig. 3.10 D). At the two stations north of the ABF (Fig. 3.9), an increase of calanoid and total mesozooplankton body size with increasing depth could also be observed, but the increase was only apparent below 300 m at station 29 (Fig. 3.9 A, B) and below 80 m at station 244 (Fig. 3.9 C). Mesozooplankton body size at station 244 (Fig. 3.9 D) stayed relatively the same throughout the water column. Mean size of calanoid copepods and of total mesozooplankton were generally higher in the upper water layers of stations 29 and 109 (Fig. 3.9 A, B and Fig. 3.10 A, B) that were sampled at night compared to those of stations 244 and 110 (Fig. 3.9 C, D and Fig. 3.10 C, D) which were sampled during the day.

3.4 Biomass

Meridional Transect T-3 of the Dr Fridtjof Nansen Cruise 2007

Along this transect in 2007, mesoplankton biomass was highest north of the Angola-Benguela Front (ABF) at stations 33, 29 and 38 (Fig. 3.11). Overall maximum biomass values of around 3 ml m^{-3} were recorded from 0 to 30 m at the two northernmost stations 33 and 29. High abundance of salps in the surface layer of station 29 might have accounted for the increased estimate. Mesoplankton biomass north of the ABF was highest in the upper 60 m and then rapidly decreased to values of less than 1ml m^{-3}. Station 53 south of the ABF displayed remarkably low mesoplankton abundances with a maximum amount of 1 ml m^{-3} from 30 to 60 m. An absolute minimum was observed from 100 to 140 m at all stations, where biomass ranged from 0.1 to 0.3 ml m^{-3}.

Meridional Transect T-3 of the Maria S. Merian Cruise 2008

Mesoplankton biomass of transect T-3 in 2008 was highest at stations 230 and 231 south of the ABF (Fig. 3.12). At these stations, biomass in the upper 50 m ranged between 2.6 and 8.8 ml m^{-3}. High phytoplankton abundance in subsurface layers at these stations, accounted for the remarkable high mesoplankton biomass with highest overall biomass of 14 ml m^{-3} at the southernmost station 230. North of the ABF, at stations 242 and 244, biomass did not exceed 2 ml m^{-3} and was very low in deeper layers. From 200 to 600 m at station 244, a high occurrence of gelatinous organisms resulted most likely in a higher overall biomass. At station 242 from 50 to 200 m, gelatinous components floated at the surface of the measuring cylinder and therefore might have increased the estimated value.

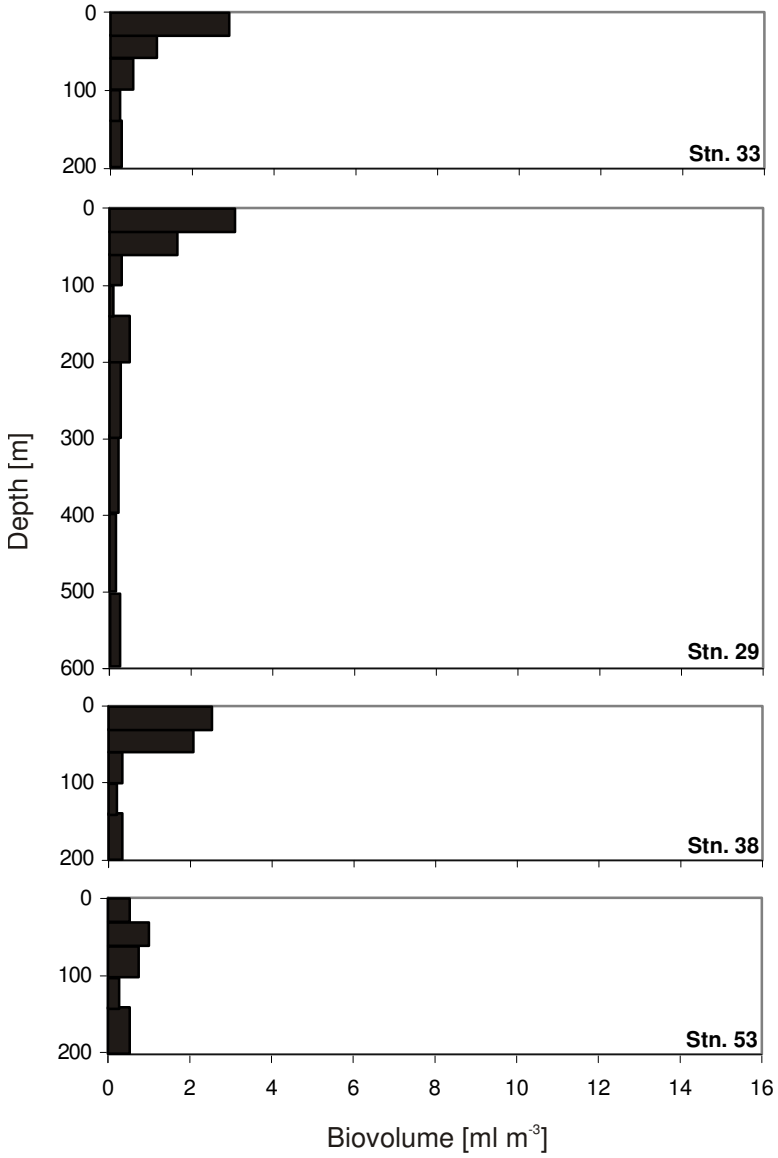

Fig. 3.11. Vertical distribution of total mesoplankton biovolume as measure for plankton biomass along transect T-3 at 11°30'E in 2007. Stns. 33, 29 and 38 are located north of the ABF, stn. 53 is located south of the ABF.

Cross-Shelf Transect T-7 of the Maria S. Merian Cruise 2008

Mesoplankton biomass along the cross-shelf transect in 2008 was generally low and did not exceed 6 ml m^{-3} (Fig. 3.13). Highest biomass was recorded in subsurface waters of the coastal station 106 (4.7 ml m^{-3}), due to high phytoplankton abundance and in the surface layer of the offshore station 109 (5.07 ml m^{-3}). Pteropods of the species *Cymbulia* spp. and their pseudoconches contributed to the increased biomass values at the surface of station 109. At the offshore stations, biomass was highest in the surface layers and decreased with increasing depth. Station 108 exhibited a biomass minimum from 50 to 170 m and biomass increased again below 170 m, due to the presence of gelatinous organisms. At the shallow station 107, mesoplankton biomass was generally low, but increased in the deepest water layer.

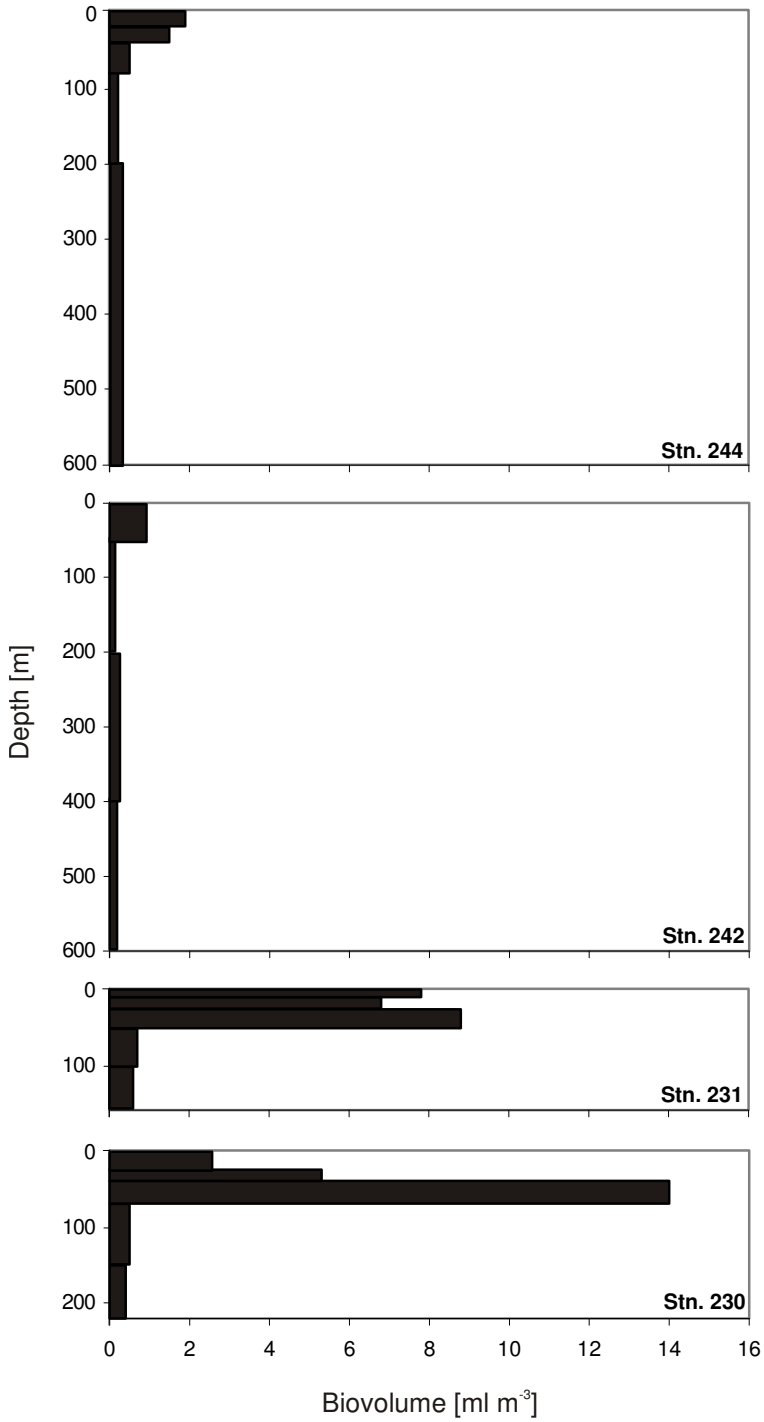

Fig. 3.12. Vertical distribution of total mesoplankton biovolume as measure for plankton biomass along transect T-3 at 11°30'E in 2008. Stns. 244 and 242 are located north of the ABF, stns. 231 and 230 are located south of the ABF.

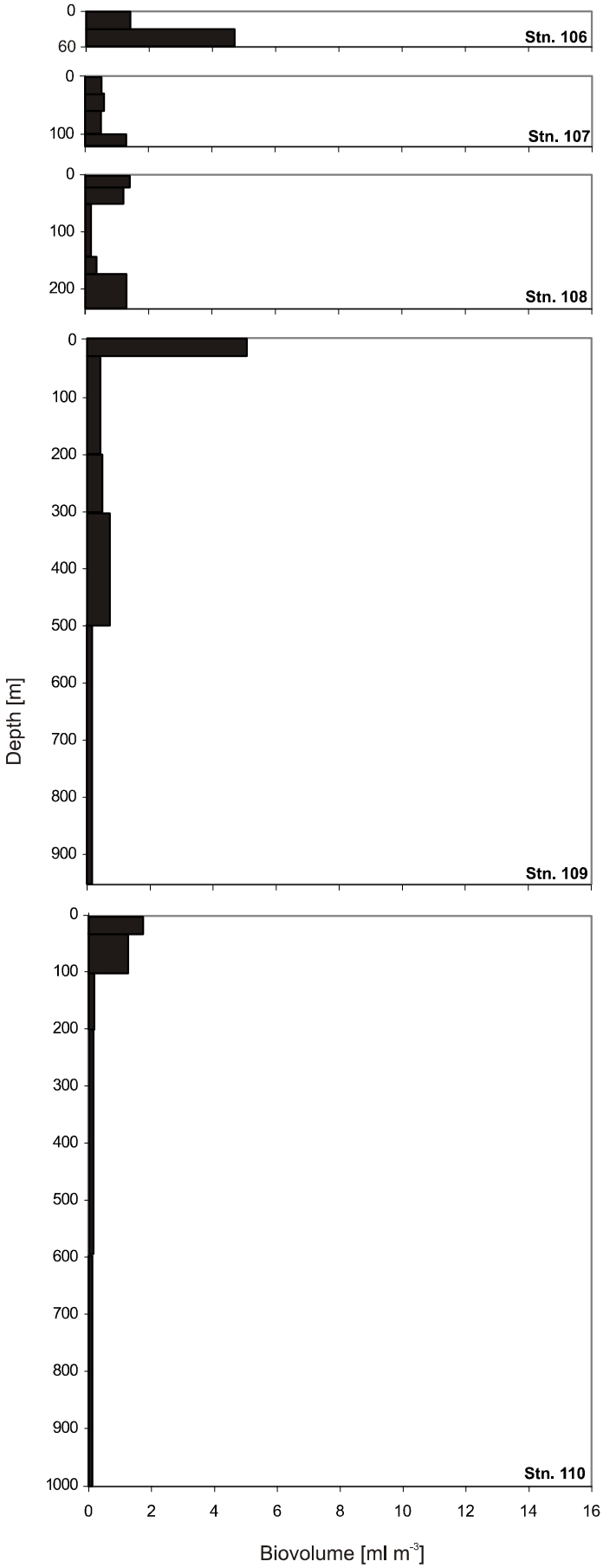

Fig. 3.13. Vertical distribution of total mesoplankton biovolume as measure for plankton biomass along transect T-7 at 20°S in 2008. Stn. 106 is located closest to the coast, stn. 110 is located furthest offshore.

3.5 Stable Isotope Signatures

Stable carbon ($\delta^{13}C$) and nitrogen ($\delta^{15}N$) isotope signatures of different species analysed for this food web study displayed a wide range of values (Fig. 3.14). Stable carbon isotope ratios ranged from -24.2‰ in salps to -16.0‰ in anchovy *Engraulis capensis*. Stable nitrogen isotope ratios varied from 6.1‰ in the pseudoconch of the pteropod *Cymbulia* sp. to 14.2‰ in the storm petrel of the family Hydrobatidae. To some extent, stable carbon and nitrogen signatures varied among individuals of the same species, possibly due to different developmental stages of one species or individuals with different dry mass.

Pteropods of the species *Cymbulia* sp. (pseudoconches as well as animals) had very low $\delta^{15}N$ ratios. The pseudochonches additionally displayed rather low $\delta^{13}C$ values whereas the animals of *Cymbulia* sp. were slightly enriched in ^{13}C compared to their pseudochonches. The copepod *Calanoides carinatus* had the lowest $\delta^{15}N$ values of all copepods. Both analysed individuals displayed similar $\delta^{15}N$ values as well as $\delta^{13}C$ values, which were also rather low. Among the species with low $\delta^{15}N$ ratios was also one individual of the copepod *Gaetanus* sp., the anchovy *Engraulis capensis* and the tunicate *Pyrosoma* sp. While *Pyrosoma* sp. had a very low $\delta^{13}C$ ratio, *Engraulis capensis* displayed the highest overall $\delta^{13}C$ value.

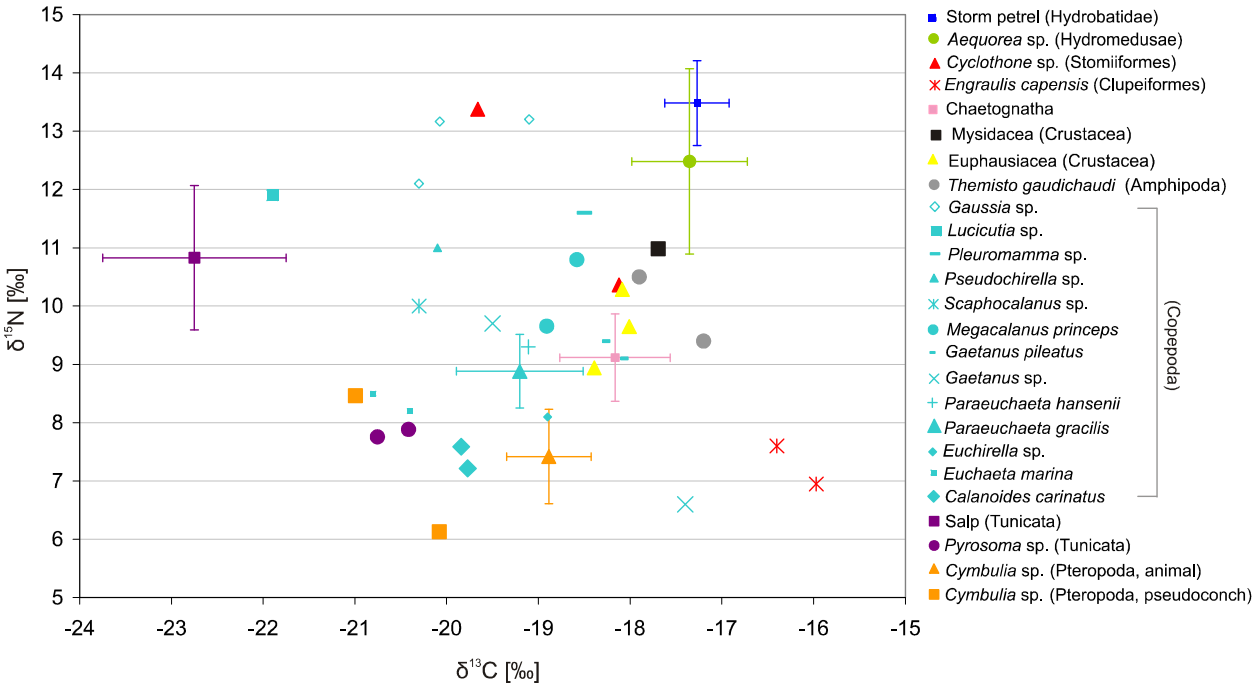

Fig. 3.14. Relationship between stable nitrogen ($\delta^{15}N$) and stable carbon ($\delta^{13}C$) isotopic signatures of different species of the northern Benguela upwelling system. If only one or two individuals were measured, single symbols are used. If more than two measurements were made, mean value and standard deviation are shown.

Euchaeta marina, *Euchirella* sp. and *Paraeuchaeta gracilis* displayed slightly enriched $\delta^{15}N$ ratios between 8‰ and 9.6‰. *Euchaeta marina* had a very low $\delta^{13}C$ ratio, while *Euchirella* sp. and *Paraeuchaeta gracilis* had intermediate $\delta^{13}C$ values. Intermediate stable nitrogen isotope values above 9‰ and below 12‰ were exhibited by the majority of the analysed individuals. Among them was the main proportion of different copepod species, like *Paraeuchaeta hansenii*, *Scaphocalanus* sp., *Pseudocalanus* sp., *Pleuromamma* sp., *Lucicutia* sp., *Gaetanus pileatus* and another individual of *Gaetanus* sp. For *Megacalanus princeps*, two copepodite stages (C4 and C5) were plotted. They displayed a difference of 1‰ in $\delta^{15}N$ with the lowest value belonging to the copepodite stage C4. All of the named copepods displayed intermediate $\delta^{13}C$ ratios, except *Lucicutia* sp. which had the lowest value of all copepods. On the other hand, *Lucicutia* sp., together with *Pleuromamma* sp., displayed the highest $\delta^{15}N$ ratios of all copepods.

Chaetognaths exhibited intermediate $\delta^{15}N$ as well as $\delta^{13}C$ ratios. The mysid showed a $\delta^{15}N$ value of 11‰ and was rather enriched in ^{13}C compared to the majority of analysed species. The $\delta^{15}N$ values of the two individuals of the amphipod *Themisto gaudichaudi* slightly varied between 9‰ and 11‰ and also the $\delta^{13}C$ ratios expressed a difference of nearly 1‰. The three plotted $\delta^{15}N$ ratios of the Euphausiacea also showed a variation between 8.9‰ and 10.3‰, while the $\delta^{13}C$ ratio was relatively constant around -18‰. The variation in $\delta^{15}N$ ratios correlated with the individual dry weight of the animals where the highest $\delta^{15}N$ value corresponded to the lightest individuals. Salps exhibited the lowest overall $\delta^{13}C$ ratios with -22.7‰±1 but where remarkably enriched in stable nitrogen isotopes compared to the other tunicate species *Pyrosoma* spp.

Species that displayed $\delta^{15}N$ ratios above 12‰ were not very numerous. Among them was the copepod species *Gaussia* sp. Three different individuals (male, female and C5) were analysed and displayed slightly different $\delta^{15}N$ and $\delta^{13}C$ signatures. Values varied from 12.1‰ (female) to 13.2‰ (male and C5) in $\delta^{15}N$ and from -20.3‰ (female) to -19.1‰ (male) in $\delta^{13}C$. The two analysed individuals of the fish *Cyclothone* sp. displayed very diverse $\delta^{15}N$ signatures; one had a value of 10.4‰ and the other of 13.4‰. Individuals of the jelly fish *Aequorea* sp. displayed also rather high $\delta^{15}N$ values with a mean of 12.5‰ and a very high variance of 1.59‰. Overall highest $\delta^{15}N$ signatures of all analysed animals were exhibited by individuals of the storm petrel (Hydrobatidae), reaching 13.5‰±0.73. The storm petrel and *Aequorea* sp. also displayed second highest $\delta^{13}C$ ratios after *Engraulis capensis* of average -17.6‰±0.35 and -17.4±0.63, respectively.

4 Discussion

Vertical trends

Vertical trends in zooplankton community structure are discussed for two offshore stations of the cross-shelf transect (stns. 109 and 110) and for two stations north of the Anogla-Benguela Front (ABF) (stns. 29 and 244). During the present study, mesozooplankton abundance decreased from 5000 ind. m^{-3} (stn. 244) at the surface to 20 ind. m^{-3} below 600 m depth (stn. 110). Zooplankton biomass did also reflect this pattern and dropped from 6 ml m^{-3} (stn. 109) to 0.1 ml m^{-3} (stn. 110). In contrast to this general trend, both parameters varied with depth at station 109 and 244. The general decline of abundance and biomass agrees with previous studies in the northern Benguela system (Olivar & Barangé 1990). Similar results have been obtained in the Humboldt upwelling system (Manriquez et al. 2009).

Individual body size of calanoid copepods and mesozooplankton in general increased with depth. This trend was most pronounced at station 110, where body size of calanoids increased from 0.43 mm at the surface to 1.55 mm below 600 m. Mesozooplankton body size increased as well from 0.46 mm to 0.76 mm. The observed trend was not as remarkable at station 244. At station 29, a pronounced increase in body size of zooplankton organisms was only apparent in greater depth. A general increase of body size with increasing depth is in agreement with results of Maucheline (1992).

The observed vertical trends at the offshore stations can be explained by drastic changes in abiotic and biotic factors with increasing depth. Primary production is restricted to the sunlit surface layer of the ocean and food availability for herbivorous zooplankton sharply declines below the euphotic layer. Typical species of the surface layer were salps and appendicularians, pteropods (*Cymbulia* spp. and *Limacina* spp.) and crustaceans, predominantly copepods. Through primary production and mixing processes, the surface layers are enriched with dissolved oxygen and concentrations of 2-8 ml l^{-1} may be reached (Nelson & Hutchings 1983). A permanent thermocline at around 50 m depth separated the surface layer from the underlying thermocline water mass and temperature as well as oxygen concentrations drastically decreased. Pronounced stratification at offshore stations, due to intense solar radiation, might contribute to the accumulation of zooplankton in the surface layer, as it was observed by Olivar and Barangé (1990).

Another aspect which may lead to a decrease in zooplankton abundance and biomass is the existence of an oxygen minimum layer (OML). The OML is characterised by oxygen concentrations of less than 1 ml l^{-1} (Nelson & Hutchings 1983, Mohrholz et al. 2001) and is

described as a nearly permanent feature in the northern Benguela upwelling region (Auel & Verheye 2007). The present data indicates that it predominantly occurred between 200 and 500 m, which agrees with findings of other authors (Lass et al. 2000, Loick et al. 2005, Verheye et al. 2005). A minimum of mesozooplankton abundance was often recorded in water layers of the OML. This suggests that the existence of an OML in intermediate depths might restrict the vertical distribution range of animals (Auel & Verheye 2007). The existence of an OML closely beneath the surface layer has also been recorded for the Humboldt upwelling system (Escribano & Schneider 2007), where zooplankton organisms accumulated above it (Manriquez et al. 2009). North of the ABF, the OML already developed below 100 m and in coastal areas, it was evident already below 80 m. High rates of oxygen consumption by consumers during decomposition processes of organic material and the general anoxic character of upwelling water along the Namibian coast contribute to the hypoxic character (Copenhagen 1953, Nelson & Hutchings 1983).

At the offshore station 109, the OML was not as pronounced as at other offshore stations and oxygen concentrations strongly fluctuated. These fluctuations in oxygen contents in the upper 200 m were also found by Von Bodungen et al. (2008) in the same area and might be caused by intrusions of South Atlantic central water. It can be assumed that this water mass may support higher abundances of zooplankton, due to more favourable conditions, but significant increases could not be observed. The core of the OML did not correlate with the minimum in zooplankton abundance at station 109 as well at station 244, but instead, an increase in zooplankton abundance could be observed in depths of 200 to 500 m and 200 to 600 m, respectively. This agrees with findings of Timonin et al. (1992), who also registered a second peak in abundance in these water depths in the region of the shelf break and the continental slope. This pattern is also visible in the distribution of biomass at both stations.

Within the OML, the zooplankton community was mainly composed of cyclopoid copepods. These observations are in accordance with those of Auel and Verheye (2007), who found out that the number of calanoid copepods was drastically limited within the OML. In spite of that, *Metridia lucens* and *Pleuromamma* spp. were frequently observed in depths below 200 m in this study. The predominant occurrence of *Pleuromamma robusta* within the OML has also been recorded (Auel & Verheye 2007). This suggests that some calanoid species are able to tolerate low oxygen levels, which has especially been recorded for species of the calanoid family Metridinidae (Loick et al. 2005).

The OML might as well negatively influence the diel vertical migration behaviour of some species (Auel & Verheye 2007). Diel vertical migration is a strategy of marine organisms to remain within highly productive areas (Verheye et al. 1991, Verheye & Field 1992, Peterson 1998). This behaviour is known for *M. lucens* as well as for *Pleuromamma* spp. (Timonin 1997,

Loick et al. 2005, Postel et al. 2007) which explains that these two species were also present in surface layers of stations that were sampled at night. The OML therefore did not seem to prevent the ascent of *M. lucens* and *Pleuromamma* spp. to the surface. Postel et al. (2007) did not find any indication that even oxygen levels below 0.2 ml l^{-1} prevented the vertical migration of organisms. On the other hand, the only station of the meridional transect that was sampled during the night (stn. 33) did not show any evidence of *M. lucens* and *Pleuromamma* spp. at the surface. This suggests that the OML in the northern study area, which was very pronounced and extended over several hundred meters, may have had an effect on the vertical distribution of these two species.

Calanoides carinatus, a key species of upwelling systems (Peterson 1998), was frequently found in depths below 200 m north of the ABF, at the surface in coastal areas and south of the ABF. This distribution pattern agrees with findings of other studies in the Benguela region (Timonin 1997, Auel et al. 2005, Auel & Verheye 2007). According to Hansen et al. (2005), *C. carinatus* prefers water bodies with temperatures of ≤13°C, but in this study *C. carinatus* was also observed at the surface with temperatures above 13°C. The vertical distribution patterns of *C. carinatus* can be related to its ontogenetic vertical migration, which is an adaptation to the seasonally changing availability of food particles in upwelling systems (Timonin 1997, Peterson 1998, Verheye et al. 2005). At the surface, females of *C. carinatus* profit from rich food supplies in coastal areas during active upwelling and reproduce (Verheye et al. 2005). In seasons of reduced upwelling, C5 copepodites migrate into greater depths below 400 m where they enter a resting phase to endure periods of small food supply (Timonin 1997, Auel et al. 2005, Verheye et al. 2005). During diapause, metabolism of copepodites is minimised by 96% compared to individuals at the surface (Auel et al. 2005) and lipid reserves are used for energy supply (Arashkevich et al. 1996, Auel et al. 2005, Verheye et al. 2005). Although different developmental stages of *C. carinatus* could not be identified with the employed method of image analysis, it can be assumed that the distribution patterns correlate with its life cycle and individuals that were found below 200 m in the northern study area were most likely in a diapausing state.

Numerous studies of the migration behaviour of *C. carinatus* stress, that it may also present a strategy to avoid the OML in intermediate depths (Auel et al. 2005, Verheye et al. 2005, Auel & Verheye 2007). Individuals of *C. carinatus* survive at oxygen concentrations as low as 1 ml l^{-1}, but mortality increased if concentrations dropped below this value (Auel & Verheye 2007). In this study, the detected distribution of *C. carinatus* in deeper layers below 200 m correlates with the depth layer where the OML was most pronounced. The assumption that *C. carinatus* avoids the OML can not be confirmed with the present distribution data for this copepod. However, based upon respiratory experiments conducted by Auel et al. (2005), copepodites consume

very low amounts of oxygen during diapause and are therefore probably able to survive low oxygen levels (Verheye et al. 1991, Loick et al. 2005).

A calanoid species that was frequently found below 600 m, associated with the cold Atlantic intermediate water, was *Eucalanus* spp. In this water body, *Eucalanus* spp. seemed to be the dominant calanoid copepod. Its occurrence in greater depths contributed to the increase of zooplankton body size with increasing depth. The abundance of other larger calanoid copepods in deeper layers, such as *Calanoides carinatus*, *Metridia lucens* and *Pleuromamma* spp. adds to the observed increase in body size. While body sizes of *C. carinatus*, *M. lucens* and *Pleuromamma* spp. ranged from 0.8 mm to 1.4 mm (ECD), *Eucalanus* spp. reached sizes of around 2.1 mm. Large chaetognaths or euphausiids accounted for the increase in body size of total mesozooplankton. All stations, with maximum sampling depth of 600 to 1000 m were located in offshore areas or north of the ABF, where sea surface temperatures were high. It could be assumed that zooplankton at the surface of these stations is smaller because warm water regimes rather support smaller organisms (Richardson & Verheye 1999, Martin et al. 2006). This is partly determined by differences in the size spectra of their food, since phytoplankton organisms in warm nutrient-poor waters are proposed to be smaller (e.g. nanoflagellates) compared to diatoms that occur in cool and nutrient-rich areas (Fenchel 1988, Barlow et al. 2001). Larger organisms predominantly consume larger particles because of more effective energy supply (Viitasalo et al. 1995). Thus, the body size of zooplankton may increase with depth, because food sources other than phytoplankton become more important and organisms are most likely omnivorous.

Based on these results, the hypotheses on vertical trends in zooplankton community structure can be accepted. Even though, vertical changes in discussed parameters were not as pronounced at some stations, general vertical trends in parameters that describe the zooplankton community were revealed and taxonomic differences were discussed.

Cross-shelf gradients

Along the cross-shelf transect at 20°S, mesozooplankton abundance in the surface layer decreased from 8500 ind. m^{-3} at the coast to less than 2000 ind. m^{-3} in offshore areas. Mesoplankton biomass did also show an evident decline with increasing distance to the coast and dropped from 5 ml m^{-3} to 1.7 ml m^{-3}. In contrast to these general trends, mesozooplankton showed very low biomass and abundances at the shallow station 107. Moreover, biomass at the surface of the offshore station 109 was remarkable high. A general decline in mesozooplankton biomass towards the subtropical Atlantic gyre was also observed by Piontkovski et al. (2003).

The present results are in contradiction with the observations of Timonin (1990, 1991) and Verheye et al. (2001) for the northern Benguela region.

Changes in mesozooplankton body size along the cross-shelf transect were not significant. Nevertheless, a trend of decreasing body size with increasing distance to the shore could be observed for calanoid copepods, while individual body size of zooplankton in general showed a slight increase towards offshore areas of the tropical Atlantic. A minor increase in body size was observed at the offshore station 109 for calanoids and total zooplankton. The general decrease of zooplankton body size from cold-water regimes towards the warm central Atlantic gyre was confirmed in several other studies (Piontkovski et al. 2003, Martin et al. 2006). Similar results were obtained in the Canary coastal upwelling system (Isla et al. 2004) and in the Humboldt system off Peru (Manriquez et al. 2009).

The observed cross-shelf changes in zooplankton community structure can be related to different conditions in the Benguela upwelling region compared to tropical areas of the Atlantic. Coastal regions are influenced by sporadic upwelling events, which supply high amounts of nutrients and support high productivity (Fenchel 1988, Shannon & O'Toole 2003). Primary production rates in the euphotic zone of inshore areas have been indicated as 4145 mg C m^{-2} day^{-1} compared to 1629±329 mg C m^{-2} day^{-1} in offshore areas (Wasmund et al. 2005). High phytoplankton abundance was recorded in samples of the coastal station, which supported high numbers of herbivorous zooplankton. Since samples were taken in austral fall during minimum upwelling in the northern Benguela region (Branch et al. 1987), mesozooplankton abundance and biomass are generally lower compared to periods of active upwelling (Timonin et al. 1992). Nevertheless, at 20°S, one of the most active upwelling cells off the Namibian coast is located (Shannon & Nelson 1996, Hardman-Mountford et al. 2003) and sea surface temperatures of around 16°C indicated the presence of upwelled water. In general, highest phytoplankton biomass is found downstream or offshore from upwelling patches (Hardman-Mountford et al. 2003). Peaks in zooplankton abundance and biomass generally follow highest phytoplankton densities with some distance (Olivar & Barangé 1990, Auel & Verheye 2007). In this study, highest phytoplankton abundance was found close to the coast, which has been recorded for seasons of moderate upwelling intensity (Barlow et al. 2001). Nevertheless, it can be assumed that the phytoplankton bloom did not derive from the upwelling cell at 20°S, but was transported downstream and possibly originated at the upwelling cell at 23°S, which would correlate with the findings of Hardman-Mountford et al. (2003). The observed inshore maximum of mesozooplankton abundance is in disagreement with observations of Timonin (1990, 1991), who found highest zooplankton abundance offshore, above or beyond the shelf edge in austral fall. According to this author, active upwelling was completely absent during that time and low food supply in coastal regions did not support high numbers of zooplankton. Similar

observations across the shelf at 20°S were made during winter when upwelling activity is high (Verheye et al. 2001). Enhanced wind stress and active coastal upwelling during winter (Branch et al. 1987), result in strong offshore transport of water masses and thus, highest zooplankton abundances are recorded offshore. This shows that the distribution of main zooplankton biomass and abundance is highly dependent on the upwelling intensity along the Namibian coast.

With increasing distance to the shore the influence of upwelling events on the zooplankton community decreases. Nevertheless, mesozooplankton biomass and zooplankton abundance did not continually decline towards the open ocean. The shallow station 107 exhibited remarkable low quantities of both parameters. In contrast to other stations along this transect, zooplankton abundance was extremely low in the surface layer of station 107 and slightly increased with depth. This phenomenon cannot be supported by neither temperature nor oxygen anomalies at this location. Zooplankton biomass and abundances were still high at station 108, which is located in the area of the shelf break. The waters associated with the continental slope exhibit rather stable conditions (Mitchell-Innes et al. 2001) and might therefore support higher zooplankton abundances and biomass. High occurrences of zooplankton above the shelf edge were also observed by Timonin (1991), Timonin et al. (1992) and Olivar and Barangé (1990). Similar cross-shelf distribution patterns of zooplankton abundance were observed in the Bay of Biscay (Albaina & Irigoien 2004). Zooplankton abundance displayed maximum values in coastal and shelf-break areas and minimum values in mid-shelf and offshore regions. In general, cross-shelf gradients in zooplankton abundance in the northern Benguela region are not as pronounced as in the southern Benguela region, due to a less distinct formation of the upwelling front, which separates coastal upwelling waters from oceanic regions (Olivar & Barangé 1990).

Changes in the zooplankton community structure across the shelf were most obvious in the distribution of copepods, which dominated the zooplankton community with 70-90% of total abundance. This agrees with studies from the northern Benguela region (Olivar & Barangé 1990, Hansen et al. 2005). The dominance of copepods has also been recorded in the coastal upwelling area off North West Spain (Bode et al. 1998) as well as in the Humboldt system off Peru (Manriquez et al. 2009). Cyclopoid copepods dominated in inshore areas, whereas calanoid copepods were predominantly observed in the surface layer of the offshore station. Since the abundance of small copepods has been underestimated in the past due to unsuitable sampling strategies and a focus on larger copepods (Paffenhöfer 1993, Gallienne & Robins 2001, Turner 2004), studies of the distribution of small cyclopoid copepods such as O*ithona* spp. and *Oncaea* spp. in the Benguela region are very scarce. *Oncaea* spp. and *Oithona similis* were also predominantly recorded in neritic areas in the Bay of Biscay (Albaina & Irigoien 2004).

Cyclopoid copepods are generally distributed throughout the world's oceans (Paffenhöfer 1993), but there is no clear explanation why their abundance is rather scarce in offshore areas compared to that of calanoid copepods.

Changes in the horizontal distribution of calanoid copepod species were not as significant as vertical variations. *Metridia lucens* and *Pleuromamma* spp. occurred predominantly in deeper waters off the shelf edge, which agrees with results of other studies of this region (Timonin 1990, Timonin 1991, Hansen et al. 2005). Nevertheless, individuals of these two species were also found at the surface of the offshore station 109 and at neritic stations 106 and 107, which were sampled at night. This might be related to their vertical migration behaviour as discussed in the previous section (Timonin 1997, Loick et al. 2005, Postel et al. 2007). Migrating individuals of these larger species accounted most likely for the observed increase in mean body size of calanoid copepods in the surface layer of the oceanic station 109.

Calanoides carinatus was not very abundant along this transect and occurred in small numbers on the shelf (stn. 107) and offshore in greater depths (stn. 110). This is noteworthy, because this species could be expected to numerously appear in coastal areas, where active upwelling was evident and food supply high. Nevertheless, the extremely low abundances correlate with findings of Hansen et al. (2005), who discovered, that *C. carinatus* was less abundant during months from February to September. Accordingly, *C. carinatus* reaches maximum abundance in December, when upwelling is high and it is found close to the coast (Timonin 1990, Hansen et al. 2005).

Increasing abundance towards offshore regions was recorded for pteropods and salps. Pteropods of the species *Cymbulia* spp. and their gelatinous pseudoconches accounted for the irregular high biomass in surface layers of station 109 and are characteristic for pelagic waters (Gibbons et al. 1992). In other studies, salps were also predominantly observed in pelagic waters (Acuña 2001, Verheye et al. 2001). Pelagic tunicates are generally very tolerant to low nutrient levels and are able to exploit food particles such as dinoflagellates or bacteria that are too small to be consumed by other planktonic organisms (Alldredge & Madin 1982, Acuña 2001).

Changes in zooplankton community structure and individual body size across the shelf can be related to different nutrient regimes and composition of the phytoplankton community. Primary production and phytoplankton cell size differ between inshore and offshore areas due to different amounts of provided nutrients (Dortch & Packard 1989). In nutrient-rich coastal waters, larger diatoms are predominantly found, whereas warm, nutrient-depleted offshore waters are colonised by smaller nanoflagellates (Fenchel 1988, Barlow et al. 2001). Since marine organisms in tropical environments have shorter generation times and higher metabolism rates,

their body size is smaller due to more efficient use of energy (Richardson & Verheye 1999). In highly productive ecosystems like the Benguela region, species can support bigger body sizes due to sufficient supply of larger food particles (Fenchel 1988, Viitasalo et al. 1995, Richardson et al. 2001). The observed trend of decreasing calanoid copepod body size towards offshore regions agrees with general trends in the distribution of zooplankton size spectra (Piontkovski et al. 2003). The high abundance of larger organisms such as salps in offshore samples, led to an increase in average body size of total mesozooplankton. Nevertheless, during reduced upwelling season, dinoflagellates may dominate over diatoms even in coastal waters (Sakko 1998). Thus, differences in food particle size may not be as pronounced as during active upwelling season and changes in zooplankton body size are therefore not very distinct between inshore and offshore regions.

The proposed hypotheses on cross-shelf changes in the zooplankton community structure can be accepted. Although zooplankton body size did not show significant differences and biomass and abundance irregularities occurred at single stations, there are evident cross-shelf trends in parameters that characterise the zooplankton community in coastal and oceanic regions.

Changes across the Angola-Benguela Front

Mesozooplankton abundance increased from 25 ind. m^{-3} in surface layers south of the Angola-Benguela Front (ABF) to maximum values of 3100 ind. m^{-3} north of the ABF in 2007. In 2008, abundance decreased towards the tropical Atlantic from 6400 ind. m^{-3} to 5400 ind. m^{-3} at the surface. Mesozooplankton biomass exhibited similar patterns in corresponding years and increased from 0.5 ml m^{-3} to maximum values of 3 ml m^{-3} towards northern regions in 2007 and decreased from 7.8 ml m^{-3} south of the ABF to maximum values of 2 ml m^{-3} north of the ABF. The observation of low zooplankton biomass in the tropical Atlantic in 2008 is in accordance with findings of Martin et al. (2006) and high mesozooplankton biomass was similarly found in the Canary Current region off North West Africa.

Individual body size of total mesozooplankton increased from 0.7 mm to 1.4 mm towards regions south of the ABF in 2007, whereas it stayed relatively constant across the ABF in 2008. Body size of calanoid copepods in particular, did not vary much across the ABF in 2007, whereas individuals were smaller in warm water regions north of the ABF (0.5 mm) compared to southern regions (0.7 mm) in 2008. General trends of decreasing body size towards tropical regions are in accordance with other studies of the Atlantic Ocean (Martin et al. 2006).

The observed changes in mesozooplankton abundance, biomass and size spectra across the ABF can be explained by changing conditions from the cool Benguela Current towards northern

regions of the tropical Atlantic. Sea surface temperatures (SST) increased by 6 to 10°C and nutrient availability is assumed to decrease towards regions north of the ABF. Therefore, mesozooplankton abundance and biomass were generally low in regions north of the ABF. In both years of study, the ABF was located at 16°S. This location corresponds to enhanced southward flow of warm Angolan water due to less intense upwelling in the northern Benguela region in austral fall (Meeuwis & Lutjeharms 1990, Mohrholz et al. 2001). During this season, the ABF is generally broadest and distinctly defined (Meeuwis & Lutjeharms 1990). The results of this study show that changes across the AFB are most evident in the upper 60 m where the front is most pronounced (Meeuwis & Lutjeharms 1990, Shannon & Nelson 1996). According to measured SST of 17.5°C south of the ABF in 2007, upwelling activity was evident. Although upwelling is at its minimum in austral fall, the Cape Frio upwelling cell at 18°S demonstrates a bimodal character of high upwelling activity in spring and in fall (Mouton et al. 2001, Hardman-Mountford et al. 2003). A primary production rate at the Cape Frio cell of 4145 mg C m^{-2} day^{-1}, compared to considerably lower rates of 1665±509 mg C m^{-2} day^{-1} in nearshore regions within the ABF were measured (Wasmund et al. 2005). Although upwelling was evident in 2007 south of the ABF, biomass and abundance of mesozooplankton did not reflect this and were remarkable low. Temperature and oxygen profiles did not show any anomalies at this station that explain these remarkable low values. However, it could be assumed that highest phyto- and zooplankton biomass were advected offshore so that waters at station 53 were rather depleted (Hardman-Mountford et al. 2003, Auel & Verheye 2007). The situation in 2008 was completely different and high phytoplankton as well as zooplankton biomass and abundances were found at southern stations, even though SST did not indicate coastal upwelling at the Cape Frio cell. Since upwelling was evident at 20°S in 2008, it may be assumed that phytoplankton patches were transported downstream with the Benguela Current, as it was proposed by Hardman-Mountford et al. (2003). Frontal regions are known to accumulate biological material (Verheye et al. 2001) and thus, phytoplankton as well as zooplankton abundances were enhanced in areas south of the ABF.

The ABF may also present a physical barrier between the two ecosystems and might prevent the distribution of marine organisms across the front (John et al. 2004). However, differences in taxonomic composition of mesozooplankton were not as pronounced across the ABF as in the vertical direction. In general, the copepod community was dominated by calanoid copepods. The dominance of calanoids in the area of the ABF was also observed by several other authors (Timonin 1997, Verheye et al. 2001, Loick et al. 2005). The common calanoid copepods along this transect were *Calanoides carinatus*, *Metridia lucens*, *Pleuromamma* spp. and *Eucalanus* spp. *C. carinatus* was the dominant copepod across the ABF, which agrees with the findings of Loick et al. (2005). The distribution patterns of these four species were similar in 2007 and 2008. All of these species occurred in higher numbers north of the ABF in depths of more than

200 m. This is in accordance with the general distribution of these species as it has been described in the previous section on vertical changes and by several authors (Timonin 1990, Auel et al. 2005, Hansen et al. 2005, Loick et al. 2005, Auel & Verheye 2007). Individuals of *C. carinatus* that were observed in these depths were most likely in diapause (Timonin 1997, Loick et al. 2005, Auel & Verheye 2007). Remarkable high abundance of *C. carinatus* was observed at the surface in areas south of the ABF in 2008. This can be related to general high abundances of herbivorous zooplankton south of the ABF due to rich availability of phytoplankton. It can be assumed that these observations correlate with the lifecycle of *C. carinatus* and different distribution patterns are based on its ontogenetic migrations in relation to upwelling phases in the Benguela region (Timonin 1997, Loick et al. 2005, Auel & Verheye 2007). The occurrence of *C. carinatus* in the surface layer also contributed to the observed increase in calanoid body size south of the ABF in 2008. Obvious changes in cyclopoid distribution across the ABF could not be recorded and is in agreement with results of Verheye et al. (2001).

Other crustaceans, such as copepod nauplii and decapod larvae were predominantly present in the south compared to the north in both years of study. Euphausiids in particular mainly occurred in 2007 south of the ABF and contributed to the increase in body size of total mesozooplankton south of the ABF. Verheye et al. (2001) observed that euphausiids were predominantly present within the area of the ABF and less present south of it.

Differences in the distribution of size spectra of calanoid copepods and total mesozooplankton across the ABF were not consistent in both years of study and the observed results did rather indicate trends than significant changes. In 2007, mesozooplankton in general showed increasing body sizes towards regions south of the ABF. The drastic increase in average body size resulted from bigger euphausiids that appeared in larger numbers in this area. In 2008, a trend towards larger organisms in the cool Benguela region could particularly be observed for calanoid copepods. These observed trends reflect general patterns in size distribution of marine animals, where larger sized organisms are dominantly found in region of higher productivity (Piontkovski et al. 2003, Isla et al. 2004, Martin et al. 2006). Decreasing mean sizes of zooplankton organisms from cold water regions towards subtropical Atlantic gyres were also confirmed in other studies (Martin et al. 2006). Mean size in the gyres was 0.18-0.41 mm (ECD) which is similar to mean body sizes of calanoid copepods observed north of the ABF in 2008. In regions with cooler water, zooplankton generally had a larger mean size of 0.34-0.6 mm (Martin et al. 2006), which can also be seen at stations south of the ABF in this study.

The present results show, that changes across the Angola-Benguela Front are different between the two years of study and highly depend on the prevailing conditions in each year. There are evident changes of parameters that characterise the zooplankton community north

and south of the ABF, but since the observed patterns are not consistent in both years of study, the proposed hypotheses have to be rejected.

Trophic-interactions in the northern Benguela upwelling region

Food webs in coastal upwelling regions often consist of only three trophic levels and represent efficient energy pathways (Fenchel 1988, Cushing 1989). Larger diatoms that often dominate in upwelling areas (Barlow et al. 2001), support rather short food chains, because most zooplankton and fish are able to feed directly on them (Lalli & Parsons 2002). High spatial and temporal fluctuations in the Benguela upwelling system lead to a high variability in phytoplankton abundance that herbivorous zooplankton has to adapt to (Jarre-Teichmann et al. 1998, Peterson 1998). Based on stable nitrogen isotopic signatures ($\delta^{15}N$) of different organisms, a conceptual model of the pelagic food web of the northern Benguela upwelling region is developed (Fig. 4.1) and trophic relations among organisms are discussed.

The trophic model shows that the majority of taxa exhibit a broad range of $\delta^{15}N$ ratios. Furthermore, $\delta^{15}N$ ratios of many organisms are in the same range and thus seem to share similar positions. Consumers are usually enriched in ^{15}N by 3.4‰±1.1 compared to their prey (Minagawa & Wada 1984, Peterson & Fry 1987, Michener & Schell 1994). If an enrichment factor for ^{15}N of +3.4‰±1.1 per trophic level is applied to the existing $\delta^{15}N$ ratios, trophic relations among organisms can be demonstrated. The mean trophic enrichment factor for $\delta^{15}N$ is a robust and commonly applied value (Vander Zanden & Rasmussen 2001, Post 2002) and based upon this relation, a conceptual food web can be developed. Even though the trophic model does not show distinct trophic levels, it can be hypothesised that displayed $\delta^{15}N$ ratios reflect three different positions that can be discussed in relation to each other.

Organisms that seem to occupy a position at the base of the suggested pelagic food web are the pteropod *Cymbulia* sp., the tunicate *Pyrosoma* sp., the anchovy *Engraulis capensis* and the calanoid copepod *Calanoides carinatus*. *Cymbulia* sp. and *Pyrosoma* sp. are typical filter feeders (Alldredge & Madin 1982), which is reflected in their low $\delta^{15}N$ ratios. *Calanoides carinatus* is one of the major herbivorous copepods in the Benguela upwelling region (Timonin 1990, Peterson 1998). *C. carinatus* is generally a typical species related to coastal upwelling (Peterson 1998) and has adjusted its lifecycle to the seasonal and sporadic diatom blooms (Auel et al. 2005, Verheye et al. 2005). It displayed one of the lowest $\delta^{15}N$ ratios (7.2‰, 7.6‰) of all analysed species, which supports its key role as important primary consumer and prey for higher consumers such as anchovy and sardine (Loick et al. 2005, Verheye et al. 2005, Auel & Verheye 2007, Lebourges-Dhaussy et al. 2009). The anchovy *Engraulis capensis* is a small and

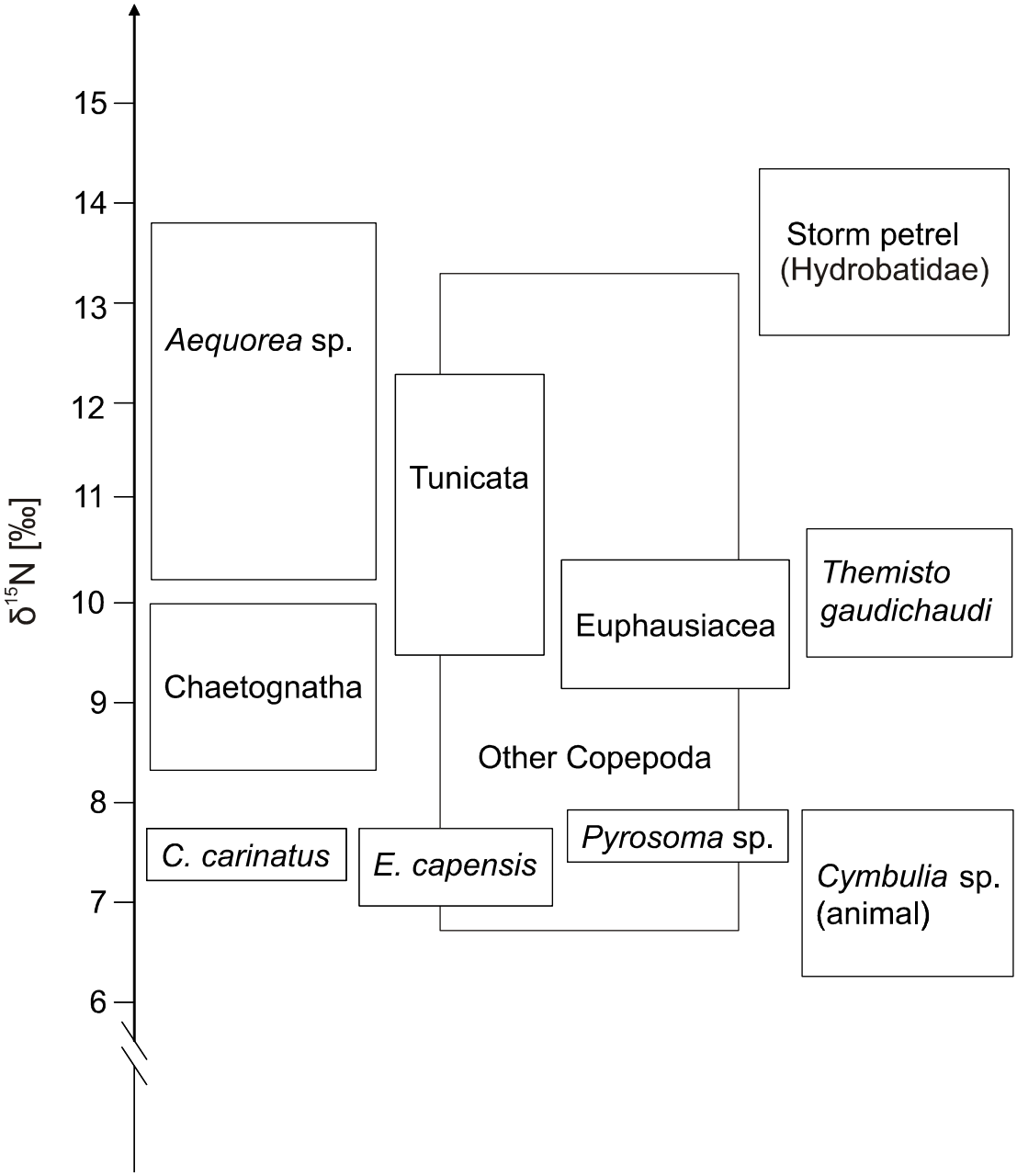

Fig. 4.1. A trophic model of the northern Benguela upwelling system based on stable nitrogen isotope signatures ($\delta^{15}N$).

abundant pelagic species in the Benguela region and of great commercial interest for the Namibian fisheries (Payne et al. 2001). *E. capensis* is a size-selective omnivorous species that alters feeding modes according to availability and size of food items (Gibbons et al. 1992, Lebourges-Dhaussy et al. 2009). Phytoplankton, calanoid copepods, e.g. *Calanoides carinatus*, other crustaceans and chaetognaths larger than 1 mm belong to its diet (Gibbons et al. 1992, Lebourges-Dhaussy et al. 2009). The low $\delta^{15}N$ ratios of 7.0-7.6‰ suggest that *E. capensis* most likely preyed on phytoplankton. This is a characteristic example of a short pathway within a food web and the anchovy therefore represents an important mid-trophic link between primary producers and higher levels in the Benguela region (Cury et al. 2000). Several top predators,

such as Cape cormorants and storm petrels, larger fish and marine mammals rely on anchovy populations as important food source (Crawford 1987, Crawford et al. 1992, Sekiguchi et al. 1992).

Mid-trophic positions in the suggested food web are occupied by chaetognaths, tunicates, euphausiids, the amphipod *Themisto gaudichaudi* and by the majority of analysed copepods. Other tunicates displayed clearly enriched $\delta^{15}N$ ratios compared to *Pyrosoma* sp. and individual signatures of analysed specimens showed great variations. This can possibly be related to their broad food spectrum, which includes small flagellates, ciliates, and other microzooplankton besides phytoplantkon (Alldredge & Madin 1982). Furthermore, tunicates are well adapted to oligotrophic waters and are able to feed on particles that are too small for other organisms (Acuña 2001). Euphausiids displayed also slightly enriched $\delta^{15}N$ ratios (8.9‰-10.3‰) compared to exclusively herbivorous organisms. This suggests that euphausiids in the Benguela region display a rather omnivorous feeding behaviour. Isotopic signatures of lighter individuals were higher compared to those of the heaviest animal. It can be assumed, that individuals with lesser weight are also of smaller body size and consume smaller food particles such as microzooplankton. This is in contradiction to results of Schmidt et al. (2004), who found that juvenile stages in the Southern Ocean generally expressed lower $\delta^{15}N$ ratios than adult animals. Nevertheless, it is widespread, that species alter their feeding behaviour during ontogenetic development (Rodríguez 1994) and may thus display different $\delta^{15}N$ ratios.

The main proportion of copepods displayed $\delta^{15}N$ ratios between 8‰ and 12‰, which cover a wide range, but mainly indicate that they occupy intermediate trophic positions within the Benguela food web. Studies on stable nitrogen isotope signatures of copepods in the Benguela region are still scarce. Nevertheless, the results indicate that the majority of copepods in the Benguela region express an omnivorous or carnivorous feeding behaviour since they are on average enriched in ^{15}N by 3.4‰±1.1 compared to primary consumers like *Calanoides carinatus.* Therefore, the majority can be assigned to the position of secondary consumers. Although one individual of *Gaetanus* sp. expressed a remarkable low isotopic ratio, only *Calanoides carinatus* displayed a distinct association to a position at the bottom of the food web and is therefore presented separately. *Euchaeta marina*, which is known to be carnivorous, expressed also very low $\delta^{15}N$ ratios. It may be assumed that copepods in the Benguela region feed on a variety of food items according to their availability. The diets of omnivorous copepods may consist of other crustaceans and phytoplankton, but also of detritus and microzooplankton such as ciliates and dinoflagellates (Batten et al. 2001, Bode & Alvarez-Ossorio 2004). According to Batten et al. (2001) the food spectrum of copepods is difficult to specify and relies very much on the prevailing biological conditions. Even though microzooplankton poses a minor proportion of the diet of omnivorous copepods, it should not be underestimated as an important

component (Batten et al. 2001, Calbet 2001). A copepod that exhibited very high $\delta^{15}N$ ratios was *Gaussia* sp. Its isotopic signature suggests a carnivorous diet which can be related to its rather large body size and predominant occurrence in deeper water layers.

Chaetognaths are a typically carnivorous group in the Benguela food web and primarily feed on copepods (Gibbons et al. 1992). They expressed an average $\delta^{15}N$ of 9.1‰±0.75. If an enrichment factor for ^{15}N of +3.4‰±1.1 is applied, and according to their known feeding behaviour, chaetognaths may possibly feed on the herbivorous copepod *Calanoides carinatus*.

The pelagic amphipod *Themisto gaudichaudi* is an obligate carnivorous species (Gibbons et al. 1992, Pakhomov & Perissinotto 1996). The diet of this species in the Southern Ocean consists of euphausids, copepods and pteropods ranging from 1-4 mm in size but might also contain polychaets or chaetognaths. Adult individuals of *T. gaudichaudi* are on average smaller in the area of the Benguela system (Auel & Ekau 2009) and therefore the size range may not apply to specimens of this study. Nevertheless, individuals of *Themisto* spp. in the Benguela system are known to feed on copepods, chaetognaths and fish larvae (Gibbons et al. 1992). According to its $\delta^{15}N$ ratio, it can be assumed that *T. gaudichaudi* most likely preyed on herbivorous organisms such as *Calanoides carinatus*. *T. gaudichaudi* itself, is an important food source for higher trophic level consumers such as fish, seabirds and marine mammals (Pakhomov & Perissinotto 1996).

Organisms that exhibited highest $\delta^{15}N$ ratios were the hydromedusae *Aequorea* sp. and the storm petrel of the family Hydrobatidae. According to their isotopic signatures of 12.5‰±1.59 and 13.5‰±0.73, respectively, both taxa reflect a carnivorous diet. *Aequorea* sp. is a common hydromedusae in this region and has a very diverse prey spectrum consisting of copepods as well as euphausiids and other gelatinous zooplankton (Gibbons et al. 1992). In the southern Ocean, the diet of the Wilson's storm petrel, which is also abundant off the Namibian coast, is predominantly composed of crustaceans such as euphausiids and copepods, but also fish (Croxall & North 1988, Croxall et al. 1988). The amphipod *Themisto gaudichaudi* was the dominant prey species among the crustaceans (Croxall et al. 1988) and may also pose an important prey species for storm petrels in the Benguela region. Besides crustaceans, the main proportion of the seabird's diet in the southern Benguela system is fish such as anchovy, sardine and horse mackerel (Duffy et al. 1987). The application of the common enrichment factor for ^{15}N along the food chain thus renders both species a trophic position at the top of the Benguela food web.

The trophic model suggested here, shows that there is evidence of energy transfer along traditional short food chains, but predator-prey relationships between organisms may also be more complex. It can be assumed, that the copepod *Calanoides carinatus* takes in an important

position in the food web of the Benguela upwelling system. Stable isotope signatures suggest, that omnivory is a wide spread feeding mode among organisms in the Benguela region and preferred diet may be predominantly determined by available food and suitable size of prey. A more generalised feeding behaviour decreases the dependence on a certain prey organisms and minimises negative effects of changes in the community structure of lower trophic levels (Crawford 1987, Cury et al. 2000). Moreover, discussed results show that there exists a positive correlation between body size and trophic position of an organism, since higher level consumers are often bigger than their prey organisms (Sheldon et al. 1972, Arim et al. 2007, Jennings et al. 2008). Trophic relationship-estimations based on $\delta^{15}N$ data and of zooplankton size classes only present a small fraction of the possible trophic-interactions among marine organisms in the Benguela upwelling systems. Stable nitrogen isotope concentrations may undergo seasonal variations in producers as well as in consumers, depending on fluctuations in nutrients and other environmental parameters (Bode & Alvarez-Ossorio 2004). Since the Benguela upwelling region is a highly variable ecosystem with seasonal differences in environmental parameters and food availability (Branch et al. 1987), stable isotope signatures of organisms are likely to display these fluctuations. Therefore, further information on $\delta^{15}N$ values of other zooplankton and fish species in different upwelling seasons, would add to a more detailed picture of the complex trophic structure of the Benguela coastal upwelling ecosystem.

5 Conclusion and Outlook

The distribution of biomass and abundance of zooplankton in the northern Benguela region are closely related to the season and the intensity of coastal upwelling (Timonin 1991, Timonin et al. 1992) and therefore to the availability of food. Differences were evident in coastal versus pelagic regions and across the Angola-Benguela Front. In general, abundance and biomass are rather low in austral fall when upwelling is at its minimum in the northern Benguela system and respectively higher during active upwelling season in winter and spring (Timonin et al. 1992). This difference is also reflected in the presence and distribution of certain species that are closely related to the upwelling cycle and the seasonally changing abundance of phytoplankton as primary food source.

One of the most important factors in determining the distribution of marine species in the northern Benguela upwelling region is the amount of dissolved oxygen in the water column (Loick et al. 2005, Auel & Verheye 2007). Concentrations below 1 ml l^{-1} are not tolerable for many organisms and oxygen minimum layers that almost permanently occur in the northern Benguela region, therefore influence and restrict the distribution of zooplankton species.

An enhanced intrusion of oxygen depleted water from the Angola Basin into the Benguela Current region in the future could be caused by increasing water temperatures and a reduction in upwelling activity. Consequences for the northern Benguela region could be an expansion of the OML, which might pose a survival problem for many species, including fish that are not adapted to increasingly hypoxic environments (Shannon & O'Toole 2003).

The distribution and size spectra of zooplankton determine also the structure of the food web and characterise trophic relations between species. The analysis of the size spectrum of zooplankton organisms as well as their isotopic composition, thus give insight into possible predator-prey relationships within a community (Rodríguez 1994).

Additionally, the food web structure might be altered by changing distributions and abundances of key species among copepods or small pelagic fish such as anchovy or sardine. It is suggested, that the increase in areas with hypoxic character in the northern Benguela region has contributed to the declining fish stocks off Namibia (Ekau & Verheye 2005, Auel & Verheye 2007).

Further studies on stable isotope signatures of a wide variety of organisms will fill gaps and allow a complete estimation of the food web structure in the Benguela region. In order to determine definite trophic levels with in a food web, it is obligatory to gain stable isotope information on phytoplankton as baseline of the food web. Through improved knowledge of

lower or intermediate trophic level dynamics, consequences for higher trophic levels may more easily be predictable. Moreover, other biochemical methods such as lipid or enzyme analyses could add further information on trophic issues. Another concern that may gain importance in the next years is the effect of increasing water temperatures on trophic positions of organisms and the entire food web structure.

The use of ZooImage as a method for automatic analysis of zooplankton samples proved to be a good choice for this study in terms of automatic size-measurements of zooplankton organisms. Once the rather time-consuming step of the creation of the training set was accomplished, much time could be saved and the analysis of a larger series of samples was possible. ZooImage provides a broad spectrum of applications that were not entirely exploited during this study. It is most likely that in the future more features will be added to extend the use of the software which makes ZooImage very adjustable to individual demands. Since it is especially designed for the analysis of larger series of zooplankton samples, it will probably find a broad interest since studies of long time series are still rather scarce. Nevertheless, human taxonomic knowledge and manual classification will presumably not be replaceable by automatic methods (Bell and Hopcroft 2008). Automated image analysis of plankton samples is only advantageous towards manual classification if a real time reduction can be accomplished and accuracy is still precise enough to detect trends in biological parameters such as abundance and biomass distributions and species composition (Bell and Hopcroft 2008).

6 References

Acuña JL (2001) Notes and comments. Pelagic tunicates: why gelatinous? The American Naturalist 158: 100-107

Albaina A, Irigoien X (2004) Relationships between frontal structures and zooplankton communities along a cross-shelf transect in the Bay of Biscay (1995 to 2003). Marine Ecology Progress Series 284: 65-75

Alcaraz M, Saiz E, Calbet A, Trepat I, Broglio E (2003) Estimating zooplankton biomass through image analysis. Marine Biology 143: 307-315

Alldredge AL, Madin LP (1982) Pelagic tunicates: unique herbivores in the marine plankton. BioScience 32: 655-663

Arashkevich EG, Drits AV, Timonin AG (1996) Diapause in the life cycle of *Calanoides carinatus* (Krøyer), (Copepoda, Calanoida). Hydrobiologia 320: 197-208

Arim M, Marquet PA, Jaksic FM (2007) On the relationship between productivity and food chain length at different ecological levels. American Naturalist 169: 62-72

Auel H, Ekau W (2009) Distribution and respiration of the high-latitude pelagic amphipod *Themisto gaudichaudi* in the Benguela Current in relation to upwelling intensity. Progress in Oceanography In Press

Auel H, Hagen W, Ekau W, Verheye HM (2005) Metabolic adaptations and reduced respiration of the copepod *Calanoides carinatus* during diapause at depth in the Angola-Benguela Front and northern Benguela upwelling regions. African Journal of Marine Science 27: 653-657

Auel H, Verheye HM (2007) Hypoxia tolerance in the copepod *Calanoides carinatus* and the effect of an intermediate oxygen minimum layer on copepod vertical distribution in the northern Benguela Current upwelling system and the Angola-Benguela Front. Journal of Experimental Marine Biology and Ecology 352: 234-243

Barlow RG, Aiken J, Sessions HE, Lavender S, Mantel J (2001) Phytoplankton pigment, absorption and ocean colour characteristics in the southern Benguela ecosystem. South African Journal of Science 97: 230-238

Batten SD, Fileman ES, Halvorsen E (2001) The contribution of microzooplankton to the diet of mesozooplankton in an upwelling filament off the north west coast of Spain. Progress in Oceanography 51: 385-398

Beaulieu SE, Mullin MM, Tang VT, Pyne SM, King AL, Twining BS (1999) Using an optical plankton counter to determine the size distributions of preserved zooplankton samples. Journal of Plankton Research 21: 1939-1956

Bell JL, Hopcroft RR (2008) Assessment of ZooImage as a tool for the classification of zooplankton. Journal of Plankton Research 30: 1351-1367

Benfield MC, Grosjean P, Culverhouse P, Irigoien X, Sieracki ME, Lopez-Urrutia A, Dam HG, Hu Q, Davis CS, Hansen A, Pilskaln CH, Riseman E, Schultz H, Utgoff PE, Gorsky G (2007) RAPID: research on automated plankton identificaiton Oceanography 20: 12-26

Bode A, Alvarez-Ossorio MT (2004) Taxonomic versus trophic structure of mesozooplankton: a seasonal study of species succession and stable carbon and nitrogen isotopes in a coastal upwelling ecosystem. Int. Counc. Explor. Sea Journal of Marine Science 61: 563-571

Bode A, Alvarez-Ossorio MT, Gonzalez N (1998) Estimations of mesozooplankton biomass in a coastal upwelling area off NW Spain. Journal of Plankton Research 20: 1005-1014

Boyer DC, Hampton I (2001) An Overview of the living marine resources of Namibia. In: Payne AIL, Pillar SC, Crawford RJM (eds) A decade of Namibian fisheries science. South African Journal of Marine Science 23: 5-35

Branch GM, Barkai A, Hockey PAR, Hutchings L (1987) Biological interactions - Causes or effects of variability in the Benguela ecosystem. South African Journal of Marine Science 5: 425-445

Calbet A (2001) Mesozooplankton grazing effect on primary production: A global comparative analysis in marine ecosystems. Limnology and Oceanography 46: 1824-1830

Copenhagen WJ (1953) The periodic mortality of fish in the Walvis region. Pretoria: Division of fisheries, Investigational Report No. 14.

Crawford RJM (1987) Food and population variability in five regions supporting large stocks of anchovy, sardine and horse mackerel. In: Payne AIL, Gulland JA, Brink KH (eds) The Benguela and comparable ecosystems. South African Journal of Marine Science 5: 735-757

Crawford RJM, Underhill LG, Raubenheimer CM, Dyer BM, Martin J (1992) Top predators in the Benguela ecosystem - Implications of their trophic position. South African Journal of Marine Science 12: 675-687

Croxall JP, North AW (1988) Fish prey of Wilson storm petrel *Oceanites Oceanicus* at South Georgia. British Antarctic Survey Bulletin: 37-42

Croxall JP, North AW, Prince PA (1988) Fish prey of the wandering albatross *Diomedea exulans* at South Georgia. Polar Biology 9: 9-16

Culverhouse PF, Williams R, Reguera B, Herry V, Gonzalez-Gil S (2003) Do experts make mistakes? A comparison of human and machine identification of dinoflagellates. Marine Ecology Progress Series 247: 17-25

Cury P, Bakun A, Crawford RJM, Jarre A, Quinones RA, Shannon LJ, Verheye HM (2000) Small pelagics in upwelling systems: patterns of interaction and structural changes in "wasp-waist" ecosystems. Int. Counc. Explor. Sea Journal of Marine Science 57: 603-618

Cushing DH (1989) A difference in structure between ecosystems in strongly stratified waters and in those that are only weakly stratified. Journal of Plankton Research 11: 1-13

Cutler DR, Edwards TC, Beard KH, Cutler A, Hess KT (2007) Random forests for classification in ecology. Ecology 88: 2783-2792

DeNiro MJ, Epstein S (1978) Influence of diet on distribution of carbon isotopes in animals. Geochimica et Cosmochimica Acta 42: 495-506

Dortch Q, Packard TT (1989) Differences in biomass structure between oligotrophic and eutrophic marine ecosystems. Deep-Sea Research I 36: 223-240

Duffy DC, Siegfried WR, Jackson S (1987) Seabirds as consumers in the southern Benguela region. South African Journal of Marine Science 5: 771-790

Duncombe Rae CM (2005) A demonstration of the hydrographic partition of the Benguela upwelling ecosystem at 26°40'S. African Journal of Marine Science 27: 617-628

Efron B, Gong G (1983) A leisurely look at the bootstrap, the jackknife, and cross-validation. American Statistician 37: 36-48

Ekau W, Verheye HM (2005) Influence of oceanographic fronts and low oxygen on the distribution of ichthyoplankton in the Benguela and southern Angola currents. African Journal of Marine Science 27: 629-639

Escribano R, Schneider W (2007) The structure and functioning of the coastal upwelling system off central/southern Chile - Preface. Progress in Oceanography 75: 343-347

Fenchel T (1988) Marine plankton food chains. Annual Review of Ecology and Systematics 19: 19-38

Fernandes JA, Irigoien X, Boyra G, Lozano JA, Inza I (2009) Optimizing the number of classes in automated zooplankton classification. Journal of Plankton Research 31: 19-29

Fock H (2000) Analysis of community structure. In: Harris RP, Wiebe PH, Lenz J, Skjoldal HR, Huntley M (eds) Int. Counc. Explor. Sea Zooplankton Methodology Manual. Academic Press, London, pp 154-174

Foote KG (2000) Optical Methods. In: Harris RP, Wiebe PH, Lenz J, Skjoldal HR, Huntley M (eds) Int. Counc. Explor. Sea Zooplankton Methodology Manual. Academic Press, London, pp 259-291

Gallienne CP, Robins DB (2001) Is *Oithona* the most important copepod in the world's oceans? Journal of Plankton Research 23: 1421-1432

Gibbons MJ, Stuart V, Verheye HM (1992) Trophic ecology of carnivorous zooplankton in the Benguela. South African Journal of Marine Science 12: 421-437

Grosjean P, Denis K (2007) ZooImage User's Manual. http://www.sciviews.org/Zoo/PhytoImage

Grosjean P, Picheral M, Warembourg C, Gorsky G (2004) Enumeration, measurement, and identification of net zooplankton samples using the ZOOSCAN digital imaging system. Int. Counc. Explor. Sea Journal of Marine Science 61: 518-525

Hansen FC, Cloete RR, Verheye HM (2005) Seasonal and spatial variability of dominant copepods along a transect off Walvis Bay (23°S), Namibia. African Journal of Marine Science 27: 55-63

Hardman-Mountford NJ, Richardson AJ, Agenbag JJ, Hagen E, Nykjaer L, Shillington FA, Villacastin C (2003) Ocean climate of the South East Atlantic observed from satellite data and wind models. Progress in Oceanography 59: 181-221

Hobson KA, Fisk A, Karnovsky N, Holst M, Gagnon JM, Fortier M (2002) A stable isotope ($\delta^{13}C$, $\delta^{15}N$) model for the North Water food web: implications for evaluating trophodynamics and the flow of energy and contaminants. Deep-Sea Research II 49: 5131-5150

Hobson KA, Welch HE (1992) Determination of trophic relationships within a high Arctic marine food web using $\delta^{13}C$ and $\delta^{15}N$ analysis. Marine Ecology-Progress Series 84: 9-18

Hocutt CH, Verheye HM (2001) BENEFIT marine science in the Benguela Current region during 1999: Introduction. South African Journal of Science 97: 195-198

Hodum PJ, Hobson KA (2000) Trophic relationships among Antarctic fulmarine petrels: insights into dietary overlap and chick provisioning strategies inferred from stable-isotope ($\delta^{15}N$ and $\delta^{13}C$) analyses. Marine Ecology-Progress Series 198: 273-281

Hu Q, Davis C (2006) Accurate automatic quantification of taxa-specific plankton abundance using dual classification with correction. Marine Ecology-Progress Series 306: 51-61

Isla JA, Llope M, Anadon R (2004) Size-fractionated mesozooplankton biomass, metabolism and grazing along a 50°N-30°S transect of the Atlantic Ocean. Journal of Plankton Research 26: 1301-1313

Jarre-Teichmann A, Shannon LJ, Moloney CL, Wickens PA (1998) Comparing trophic flows in the southern Benguela to those in other upwelling ecosystems. South African Journal of Marine Science 19: 391-414

Jennings S, Barnes C, Sweeting CJ, Polunin NVC (2008) Application of nitrogen stable isotope analysis in size-based marine food web and macroecological research. Rapid Communications in Mass Spectrometry 22: 1673-1680

John HC, Mohrholz V, Lutjeharms JRE, Weeks S, Cloete R, Kreiner A, Neto DD (2004) Oceanographic and faunistic structures across an Angola Current intrusion into northern Namibian waters. Journal of Marine Systems 46: 1-22

Kohavi R (1995) A study of cross-validation and bootstrap for accuracy estimation and model selection. Proceedings at the Fourteenth International Joint Conference on Artificial Intelligence 2: 1137-1143

Lalli CM, Parsons TR (2002) Biological oceanography an introduction. Butterworth-Heinemann, Oxford

Largier J, Boyd AJ (2001) Drifter observations of surface water transport in the Benguela Current during winter 1999. South African Journal of Science 97: 223-229

Lass HU, Schmidt M, Mohrholz V, Nausch G (2000) Hydrographic and current measurements in the area of the Angola–Benguela Front. Journal Of Physical Oceanography 30: 2589-2609

Lebourges-Dhaussy A, Coetzee J, Hutchings L, Roudaut G, Nieuwenhuys C (2009) Zooplankton spatial distribution along the South African coast studied by multifrequency acoustics, and its relationships with environmental parameters and anchovy distribution. Int. Counc. Explor. Sea Journal of Marine Science 66: 1055-1062

Lenz J (2000) Introduction In: Harris RP, Wiebe PH, Lenz J, Skjoldal HR, Huntley M (eds) Int. Counc. Explor. Sea Zooplankton Methodology Manual, Academic Press, London, pp 1-32

Loick N, Ekau W, Verheye HM (2005) Water-body preferences of dominant calanoid copepod species in the Angola-Benguela frontal zone. African Journal of Marine Science 27: 597-608

Manriquez K, Escribano R, Hidalgo P (2009) The influence of coastal upwelling on the mesozooplankton community structure in the coastal zone off Central/Southern Chile as assessed by automated image analysis. Journal of Plankton Research 31: 1075-1088

Martin ES, Harris RP, Irigoien X (2006) Latitudinal variation in plankton size spectra in the Atlantic Ocean. Deep-Sea Research II 53: 1560-1572

Mauchline J (1992) Restriction of body size spectra within species of deep-sea plankton. Marine Ecology Progress Series 90: 1-8

Meeuwis JM, Lutjeharms JRE (1990) Surface thermal-characteristics of the Angola-Benguela Front. South African Journal of Marine Science 9: 261-279

Michener RH, Schell DM (1994) Stable isotope ratios as tracers in marine aquatic food webs. In: Lajtha K, Michener RH (eds) Stable isotopes in ecology and enviromental science. Blackwell Scientific Publications, Oxford, pp 138-158

Minagawa M, Wada E (1984) Stepwise enrichment of ^{15}N along food chains - further evidence and the relation between $\delta^{15}N$ and animal age. Geochimica Et Cosmochimica Acta 48: 1135-1140

Mintenbeck K, Brey T, Jacob U, Knust R, Struck U (2008) How to account for the lipid effect on carbon stable-isotope ratio ($\delta^{13}C$): sample treatment effects and model bias. Journal of Fish Biology 72: 815-830

Mitchell-Innes BA, Silulwane NF, Lucas M (2001) Variability of chlorophyll profiles on the west coast of southern Africa in June/July 1999. South African Journal of Science 97: 246-250

Mohrholz V, Schmidt M, Lutjeharms JRE (2001) The hydrography and dynamics of the Angola-Benguela Frontal Zone and environment in April 1999. South African Journal of Science 97: 199-208

Mouton DP, Boyd AJ, Bartholomae CH (2001) Near-surface currents and hydrology off northern Namibia in July 1999. South African Journal of Science 97: 209-212

Nelson G, Hutchings L (1983) The Benguela Upwelling Area. Progress in Oceanography 12: 333-356

Nogueira E, Gonzalez-Nuevo G, Bode A, Varela M, Moran XAG, Valdes L (2004) Comparison of biomass and size spectra derived from optical plankton counter data and net samples: application to the assessment of mesoplankton distribution along the Northwest and North Iberian Shelf. Int. Counc. Explor. Sea Journal of Marine Science 61: 508-517

Olivar MP, Barangé M (1990) Zooplankton of the northern Benguela region in a quiescent upwelling period. Journal of Plankton Research 12: 1023-1044

Paffenhöfer GA (1993) On the ecology of marine cyclopoid copepods (Crustacea, Copepoda). Journal of Plankton Research 15: 37-55

Pakhomov EA, Perissinotto R (1996) Trophodynamics of the hyperiid amphipod *Themisto gaudichaudi* in the South Georgia region during late austral summer. Marine Ecology Progress Series 134: 91-100

Payne AIL, Pillar SC, Crawford RJM, (eds.) (2001) A decade of Namibian fisheries science. South African Journal of Marine Science 23: 1-4

Petchey OL, McPhearson PT, Casey TM, Morin PJ (1999) Environmental warming alters food-web structure and ecosystem function. Nature 402: 69-72

Peterson BJ, Fry B (1987) Stable isotopes in ecosystem studies. Annual Review of Ecology and Systematics 18: 293-320

Peterson W (1998) Life cycle strategies of copepods in coastal upwelling zones. Journal of Marine Systems 15: 313-326

Piontkovski SA, Landry MR, Finenko ZZ, Kovalev AV, Williams R, Gallienne CP, Mishonov AV, Skryabin VA, Tokarev YN, Nikolsky VN (2003) Plankton communities of the South Atlantic anticyclonic gyre. Oceanologica Acta 26: 255-268

Post DM (2002) Using stable isotopes to estimate trophic position: Models, methods, and assumptions. Ecology 83: 703-718

Postel L, da Silva AJ, Mohrholz V, Lass HU (2007) Zooplankton biomass variability off Angola and Namibia investigated by a lowered ADCP and net sampling. Journal of Marine Systems 68: 143-166

Quillfeldt P, McGill RAR, Furness RW (2005) Diet and foraging areas of Southern Ocean seabirds and their prey inferred from stable isotopes: review and case study of Wilson's storm petrel. Marine Ecology Progress Series 295: 295-304

Richardson AJ, Verheye HM (1999) Growth rates of copepods in the southern Benguela upwelling system: The interplay between body size and food. Limnology and Oceanography 44: 382-392

Richardson AJ, Verheye HM, Herbert V, Rogers C, Arendse LM (2001) Egg production, somatic growth and productivity of copepods in the Benguela Current system and Angola-Benguela Front. South African Journal of Science 97: 251-257

Rodríguez J (1994) Some comments on the size-based structural analysis of the pelagic ecosystem. In: Rodríguez J, Li WKW (eds) The size structure and metabolism of the pelagic ecosystem. Scientia Marina. 58 (1-2): 1-10

Rolke M, Lenz J (1984) Size structure analysis of zooplankton samples by means of an automated image analyzing system. Journal of Plankton Research 6: 637-645

Sakko AL (1998) The influence of the Benguela upwelling system on Namibia's marine biodiversity. Biodiversity and Conservation 7: 419-433

Schaffer C (1993) Selecting a classification method by cross-validation. Machine Learning 13: 135-143

Schmidt K, McClelland JW, Mente E, Montoya JP, Atkinson A, Voss M (2004) Trophic-level interpretation based on $\delta^{15}N$ values: implications of tissue-specific fractionation and amino acid composition. Marine Ecology Progress Series 266: 43-58

Sekiguchi K, Klages NTW, Best PB (1992) Comparative analysis of the diets of smaller odontocete cetaceans along the coast of Southern Africa. South African Journal of Marine Science 12: 843-861

Shannon LV, Agenbag JJ, Buys MEL (1987) Large-scale and mesoscale features of the Angola-Benguela Front. South African Journal of Marine Science 5: 11-34

Shannon LV, Nelson G (1996) The Benguela: large scale features and processes and system variability. In: Wefer G, Berger W H, Siedler G and Webb, D J (eds) The South Atlantic: present and past circulation. Berlin, Springer, pp 163-210

Shannon LV, O'Toole MJ (2003) Sustainability of the Benguela: *ex africa semper aliquid novi.* In: Hempel G, Sherman K (eds) Large marine ecosystems of the world: trends in exploitation, protection and research. Elsevier Verlag, Amsterdam, pp 227-253

Sheldon RW, Prakash A, Sutcliff WH (1972) The size distribution of particles in the ocean. Limnology and Oceanography 17: 327-340

Smyntek PM, Teece MA, Schulz KL, Thackeray SJ (2007) A standard protocol for stable isotope analysis of zooplankton in aquatic food web research using mass balance correction models. Limnology and Oceanography 52: 2135-2146

Stone M (1974) Cross-validatory choice and assessment of statistical predictions. Journal of the Royal Statistical Society Series B-Statistical Methodology 36: 111-147

Timonin AG (1990) Composition and zooplankton distribution in the Benguela upwelling area of Namibia. Okeanologiya 30: 651-655

Timonin AG (1991) Correlation between distribution of zooplankton and hydrologic conditions in the Benguela upwelling zone. Okeanologiya 31: 191-195

Timonin AG (1997) Diel vertical migration of *Calanoides carinatus* and *Metridia lucens* (Copepoda: Calanoida) in the northern Benguela upwelling area. Okeanologiya 37: 782-787

Timonin AG, Arashkevich EG, Drits AV, Semenova TN (1992) Zooplankton dynamics in the northern Benguela ecosystem, with special reference to the copepod *Calanoides carinatus*. South African Journal of Marine Science 12: 545-560

Turner JT (2004) The importance of small planktonic copepods and their roles in pelagic marine food webs. Zoological Studies 43: 255-266

Vander Zanden MJ, Rasmussen JB (1999) Primary consumer $\delta^{13}C$ and $\delta^{15}N$ and the trophic position of aquatic consumers. Ecology 80: 1395-1404

Vander Zanden MJ, Rasmussen JB (2001) Variation in $\delta^{15}N$ and $\delta^{13}C$ trophic fractionation: Implications for aquatic food web studies. Limnology and Oceanography 46: 2061-2066

Verheye HM, Field JG (1992) Vertical distribution and diel vertical migration of *Calanoides carinatus* (Krøyer, 1849) developmental stages in the southern Benguela upwelling region. Journal of Experimental Marine Biology and Ecology 158: 123-140

Verheye HM, Hagen W, Auel H, Ekau W, Loick N, Rheenen I, Wencke P, Jones S (2005) Life strategies, energetics and growth characteristics of *Calanoides carinatus* (Copepoda) in the Angola-Benguela frontal region. African Journal of Marine Science 27: 641-651

Verheye HM, Hutchings L, Peterson WT (1991) Life-history and population maintenance strategies of *Calanoides carinatus (*Copepoda, Calanoida) in the southern Benguela ecosystem. South African Journal of Marine Science 11: 179-191

Verheye HM, Rogers C, Maritz B, Hashoongo V, Arendse LM, Gianakouras D, Giddey CJ, Herbert V, Jones S, Kemp AD, Ruby C (2001) Variability of zooplankton in the region of

the Angola-Benguela Front during winter 1999. South African Journal of Science 97: 257-258

Viitasalo M, Koski M, Pellikka K, Johansson S (1995) Seasonal and long-term variations in the body size of planktonic copepods in the northern Baltic Sea. Marine Biology 123: 241-250

Von Bodungen B, John HC, Lutjeharms JRE, Mohrholz V, Veitch J (2008) Hydrographic and biological patterns across the Angola-Benguela Frontal Zone under undisturbed conditions. Journal of Marine Systems 74: 189-215

Warembourg C, Grosjean P, Picheral M, Ibanez F, Gorsky G (2005) Le ZOOSCAN: un système d'imagerie numérique rapide pour la mesure et la classification automatique du zooplankton. Journal de recherche océanographique

Wasmund N, Lass HU, Nausch G (2005) Distribution of nutrients, chlorophyll and phytoplankton primary production in relation to hydrographic structures bordering the Benguela-Angolan frontal region. African Journal of Marine Science 27: 177-190

Appendix

Tab. A1. Mesozooplankton abundance along the meridional transect T-3 in 2007.

Dr Fridtjof Nansen cruise
Transect T-3

Station 33	**0-30 m**	**30-60 m**	**60-100 m**	**100-140 m**	**140-200 m**
Calanoida	1715.2	1194.7	249.6	137.6	130.1
Cyclopoida	776.5	537.6	163.2	138.4	106.7
Harpacticoida	0.0	0.0	0.0	0.8	2.1
Crustacea other	68.3	98.1	25.6	16.0	7.5
Pteropoda	0.0	0.0	0.0	0.0	0.0
Chaetognatha	76.8	17.1	8.0	2.4	5.3
Appendicularia	392.5	162.1	12.8	9.6	4.3
Thaliacea	34.1	0.0	0.0	1.6	1.1
Total Abundance	3114.7	2013.9	462.4	307.2	257.1

Station 29	**0-30 m**	**30-60 m**	**60-100 m**	**100-140 m**	**140-200 m**	**200-300 m**	**300-400 m**	**400-500 m**	**500-600 m**
Calanoida	460.8	341.3	57.2	29.2	56.0	33.0	60.2	43.5	68.5
Cyclopoida	405.3	546.1	50.4	20.4	47.5	34.2	54.7	32.3	47.4
Harpacticoida	4.3	25.6	0.0	0.8	2.1	0.6	0.0	0.3	1.3
Crustacea other	25.6	42.7	11.6	2.0	7.5	1.9	3.2	1.3	5.1
Pteropoda	8.5	0.0	2.0	0.0	0.0	0.6	0.0	0.0	0.0
Chaetognatha	29.9	46.9	8.4	4.0	7.5	3.2	1.0	0.3	0.0
Appendicularia	72.5	76.8	0.4	2.4	9.1	0.0	0.0	0.0	1.3
Thaliacea	224.5	17.1	2.4	0.0	3.5	0.6	0.0	0.0	4.5
Total Abundance	1254.4	1105.1	132.4	60.0	133.3	74.2	119.4	77.8	128.6

Station 38	**0-30 m**	**30-60 m**	**60-100 m**	**100-140 m**	**140-200 m**
Calanoida	955.7	708.3	100.0	40.0	58.7
Cyclopoida	802.1	1416.5	139.2	78.4	96.5
Harpacticoida	0.0	17.1	3.2	2.4	3.7
Crustacea other	93.9	51.2	16.8	8.0	9.1
Pteropoda	0.0	0.0	1.6	0.8	0.0
Chaetognatha	34.1	17.1	6.4	5.6	1.6
Appendicularia	110.9	17.1	4.8	0.8	3.2
Thaliacea	128.0	153.6	5.6	3.2	3.2
Total Abundance	2133.3	2414.9	281.6	139.2	177.6

Station 53	**0-30 m**	**30-60 m**	**60-100 m**	**100-140 m**	**140-200 m**
Calanoida	17.6	43.7	55.2	63.2	136.5
Cyclopoida	0.8	5.9	11.2	16.0	53.3
Harpacticoida	0.0	0.0	0.8	1.6	2.1
Crustacea other	2.7	4.9	4.6	3.2	4.3
Pteropoda	0.0	0.0	0.0	1.6	0.0
Chaetognatha	1.9	11.2	15.2	20.0	6.4
Appendicularia	0.0	0.0	0.0	0.0	0.0
Thaliacea	0.0	1.1	0.0	0.0	0.0
Total Abundance	25.1	66.7	88.8	108.8	201.6

Tab. A2. Mesozooplankton abundance along the meridional transect T-3 in 2008. n. d. signifies no data.

Maria S. Merian cruise **Transect T-3**					
Station 244	**0-20 m**	**20-40 m**	**40-80 m**	**80-200 m**	**200-600 m**
Calanoida	2816.0	3891.2	428.8	76.8	250.9
Cyclopoida	716.8	793.6	396.8	162.1	414.7
Harpacticoida	0.0	0.0	0.0	4.3	10.2
Crustacea other	51.2	51.2	12.8	10.7	0.0
Pteropoda	153.6	25.6	0.0	0.0	0.0
Chaetognatha	102.4	51.2	0.0	2.1	0.1
Appendicularia	1075.2	588.8	44.8	0.0	0.0
Thaliacea	0.0	0.0	0.0	0.0	5.1
Total Abundance	4915.2	5401.6	883.2	256.0	681.0
Station 242	**0-50 m**	**50-200 m**	**200-400 m**	**400-600 m**	
Calanoida	1402.9	148.5	174.1	153.6	
Cyclopoida	768.0	145.1	291.8	163.8	
Harpacticoida	10.2	1.7	0.0	0.0	
Crustacea other	102.4	13.7	5.1	12.8	
Pteropoda	10.2	1.7	0.0	0.0	
Chaetognatha	10.2	1.7	0.1	0.0	
Appendicularia	235.5	0.0	0.0	0.0	
Thaliacea	0.0	0.0	0.1	0.0	
Total Abundance	2549.8	312.3	471.0	330.2	
Station 231	**0-10 m**	**10-25 m**	**25-50 m**	**50-100 m**	**100-155 m**
Calanoida	2611.2	n. d.	n. d.	2181.1	493.4
Cyclopoida	819.2	n. d.	n. d.	1146.9	530.6
Harpacticoida	0	n. d.	n. d.	0.0	0.0
Crustacea other	716.8	n. d.	n. d.	184.3	55.9
Pteropoda	51.2	n. d.	n. d.	20.5	0.0
Chaetognatha	0	n. d.	n. d.	20.5	9.3
Appendicularia	716.8	n. d.	n. d.	20.5	9.3
Thaliacea	51.2	n. d.	n. d.	0.0	0.0
Total Abundance	4966.4	n. d.	n. d.	3573.8	1098.5
Station 231	**0-25 m**	**25-40 m**	**40-70 m**	**70-150 m**	**150-220 m**
Calanoida	2949.1	n. d.	n. d.	320	263.3
Cyclopoida	2457.6	n. d.	n. d.	524.8	468.1
Harpacticoida	0.0	n. d.	n. d.	12.8	0.0
Crustacea other	81.9	n. d.	n. d.	153.6	21.9
Pteropoda	81.9	n. d.	n. d.	0	0.0
Chaetognatha	0.0	n. d.	n. d.	0	0.0
Appendicularia	819.2	n. d.	n. d.	12.8	0.0
Thaliacea	81.9	n. d.	n. d.	0	0.0
Total Abundance	6389.8	n. d.	n. d.	1024	753.4

Tab. A3. Mesozooplankton abundance along the cross-shelf transect T-7 in 2008. n. d. signifies no data.

Maria S. Merian cruise
Transect T-7

Station 106	**0-30 m**	**30-60 m**
Calanoida	1979.7	n. d.
Cyclopoida	5461.3	n. d.
Harpacticoida	102.4	n. d.
Crustacea other	375.5	n. d.
Pteropoda	307.2	n. d.
Chaetognatha	0.0	n. d.
Appendicularia	273.1	n. d.
Thaliacea	0.0	n. d.
Total Abundance	8499.2	n. d.

Station 107	**0-30 m**	**30-60 m**	**60-100 m**	**100-120 m**
Calanoida	162.1	29.9	121.6	204.8
Cyclopoida	563.2	55.5	787.2	2201.6
Harpacticoida	136.5	12.8	345.6	153.6
Crustacea other	12.8	0.0	7.2	27.4
Pteropoda	0.3	0.1	57.6	25.6
Chaetognatha	21.3	12.8	19.2	25.6
Appendicularia	8.5	0.0	0.0	0.0
Thaliacea	0.0	0.0	0.0	0.0
Total Abundance	904.5	110.9	1337.6	2636.8

Station 108	**0-20 m**	**20-50 m**	**50-140 m**	**140-170 m**	**170-230 m**
Calanoida	2713.6	597.3	25.6	34.1	324.3
Cyclopoida	4403.2	981.3	253.2	157.9	836.3
Harpacticoida	153.6	145.1	19.9	46.9	51.2
Crustacea other	0.0	0.0	0.0	4.3	25.7
Pteropoda	0.0	0.1	0.0	0.0	0.0
Chaetognatha	0.0	0.0	0.0	0.0	0.0
Appendicularia	0.0	0.0	0.0	0.0	0.0
Thaliacea	0.0	0.0	0.0	0.0	0.0
Total Abundance	7270.4	1723.7	298.7	243.2	1237.3

Station 109	**0-30 m**	**30-200 m**	**200-300 m**	**300-500 m**	**500-950 m**
Calanoida	921.6	27.9	53.8	151.0	21.3
Cyclopoida	887.5	61.7	281.6	149.8	50.1
Harpacticoida	0.0	9.0	84.5	11.5	0.3
Crustacea other	102.7	6.1	7.7	12.8	0.9
Pteropoda	2.5	0.2	0.0	0.0	0.0
Chaetognatha	17.1	4.5	10.2	2.6	0.0
Appendicularia	34.1	0.0	0.0	0.0	0.6
Thaliacea	0.0	0.0	0.0	6.4	0.0
Total Abundance	1962.7	109.2	440.3	337.9	73.1

Station 110	**0-30 m**	**30-100 m**	**100-200 m**	**200-600 m**	**600-1000 m**
Calanoida	1160.5	89.6	21.8	39.0	6.4
Cyclopoida	102.4	53.0	28.5	48.3	11.8
Harpacticoida	0.0	3.7	0.3	1.6	0.2
Crustacea other	34.1	1.8	4.8	1.0	0.5
Pteropoda	0.0	0.0	0.0	0.0	0.3
Chaetognatha	0.0	0.0	0.0	0.6	0.2
Appendicularia	341.3	0.0	0.0	0.0	0.0
Thaliacea	256.0	0.0	0.0	0.0	0.0
Total Abundance	1894.4	148.1	55.4	90.6	19.4

Tab. A4. Mean body size and standard deviation (SD) of Calanoida, Cyclopoida and total zooplankton indicated as mm (ECD) along the meridional transect T-3 in 2007.

Dr Fridtjof Nansen cruise Transect T-3	mean	SD	mean	SD	mean	SD	mean	SD	mean	SD	mean	SD	mean	SD	mean	SD	mean	SD
Station 33	**0-30 m**		**30-60 m**		**60-100 m**		**100-140 m**		**140-200 m**									
Calanoida	0.58	0.29	0.53	0.22	0.57	0.21	0.57	0.33	0.60	0.29								
Cyclopoida	0.48	0.11	0.44	0.09	0.41	0.10	0.39	0.09	0.46	0.13								
total Zooplankton	0.66	0.62	0.52	0.22	0.60	0.63	0.53	0.54	0.55	0.24								
Station 29	**0-30 m**		**30-60 m**		**60-100 m**		**100-140 m**		**140-200 m**		**200-300 m**		**300-400 m**		**400-500 m**		**500-600 m**	
Calanoida	0.74	0.38	0.69	0.35	0.71	0.37	0.78	0.37	0.72	0.42	0.66	0.31	0.90	0.43	1.19	0.44	1.10	0.35
Cyclopoida	0.57	0.11	0.48	0.13	0.45	0.15	0.47	0.12	0.43	0.11	0.50	0.12	0.48	0.12	0.52	0.12	0.52	0.12
total Zooplankton	0.84	0.51	0.66	0.38	0.71	0.64	0.77	0.84	0.69	0.47	0.71	0.59	0.74	0.55	0.92	0.58	0.91	0.44
Station 38	**0-30 m**		**30-60 m**		**60-100 m**		**100-140 m**		**140-200 m**									
Calanoida	0.64	0.25	0.67	0.42	0.65	0.34	0.58	0.16	0.56	0.27								
Cyclopoida	0.46	0.11	0.46	0.11	0.43	0.11	0.45	0.14	0.44	0.11								
total Zooplankton	0.65	0.42	0.61	0.41	0.59	0.46	0.59	0.56	0.56	0.41								
Station 53	**0-30 m**		**30-60 m**		**60-100 m**		**100-140 m**		**140-200 m**									
Calanoida	0.68	0.45	0.73	0.49	1.14	0.51	0.94	0.36	0.96	0.36								
Cyclopoida	n. d.	n. d.	0.50	0.12	0.42	0.07	0.40	0.07	0.47	0.14								
total Zooplankton	1.35	1.24	1.22	1.23	1.16	0.92	0.98	0.71	0.84	0.41								

Tab. A5. Mean body size and standard deviation (SD) of Calanoida, Cyclopoida and total zooplankton indicated as mm (ECD) along the meridional transect T-3 in 2008. n. d. signifies no data.

Maria S. Merian cruise **Transect T-3**										
	mean	**SD**	**mean**	**SD**	**mean**	**SD**	**mean**	**SD**	**mean**	**SD**
Station 244	**0-20 m**		**20-40 m**		**40-80 m**		**80-200 m**		**200-600 m**	
Calanoida	0.47	0.14	0.41	0.11	0.47	0.21	0.54	0.29	0.75	0.34
Cyclopoida	0.43	0.13	0.33	0.08	0.36	0.09	0.33	0.07	0.35	0.08
total Zooplankton	0.56	0.39	0.42	0.18	0.41	0.17	0.39	0.18	0.52	0.32
Station 242	**0-50 m**		**50-200 m**		**200-400 m**		**400-600 m**			
Calanoida	0.54	0.34	0.48	0.18	1.15	0.38	0.98	0.49		
Cyclopoida	0.36	0.08	0.35	0.05	0.38	0.10	0.44	0.10		
total Zooplankton	0.49	0.32	0.42	0.16	0.68	0.45	0.69	0.44		
Station 231	**0-10 m**		**10-25 m**		**25-50 m**		**50-100 m**		**100-155 m**	
Calanoida	0.67	0.36	n.d.		n.d.		0.58	0.38	0.56	0.31
Cyclopoida	0.36	0.08	n.d.		n.d.		0.33	0.06	0.40	0.11
total Zooplankton	0.58	0.33	n.d.		n.d.		0.52	0.35	0.48	0.26
Station 230	**0-25 m**		**25-40 m**		**40-70 m**		**70-150 m**		**150-220 m**	
Calanoida	0.60	0.24	n.d.		n.d.		0.62	0.47	0.73	0.27
Cyclopoida	0.37	0.07	n.d.		n.d.		0.38	0.08	0.33	0.08
total Zooplankton	0.57	0.31	n.d.		n.d.		0.44	0.28	0.48	0.26

Tab. A6. Mean body size and standard deviation (SD) of Calanoida, Cyclopoida and total zooplankton indicated as mm (ECD) along the cross-shelf transect T-7 in 2008.

Maria S. Merian cruise **Transect T-7**										
	mean	**SD**	**mean**	**SD**	**mean**	**SD**	**mean**	**SD**	**mean**	**SD**
Station 106	**0-30 m**									
Calanoida	0.53	0.19								
Cyclopoida	0.33	0.04								
total Zooplankton	0.39	0.14								
Station 107	**0-30 m**		**30-60 m**		**60-100 m**		**100-120 m**			
Calanoida	0.49	0.23	0.55	0.38	0.55	0.42	0.36	0.12		
Cyclopoida	0.32	0.06	0.33	0.09	0.33	0.04	0.31	0.03		
total Zooplankton	0.42	0.32	0.74	0.90	0.39	0.18	0.37	0.33		
Station 108	**0-20 m**		**20-50 m**		**50-140 m**		**140-170 m**		**170-230 m**	
Calanoida	0.56	0.29	0.49	0.16	0.40	0.11	0.72	0.43	0.60	0.24
Cyclopoida	0.31	0.06	0.33	0.06	0.31	0.03	0.32	0.06	0.37	0.06
total Zooplankton	0.39	0.21	0.40	0.15	0.34	0.08	0.43	0.22	0.44	0.17
Station 109	**0-30 m**		**30-200 m**		**200-300 m**		**300-500 m**		**500-950 m**	
Calanoida	0.60	0.35	0.95	0.47	0.74	0.42	1.08	0.63	1.13	0.61
Cyclopoida	0.40	0.12	0.36	0.09	0.37	0.11	0.45	0.12	0.43	0.09
total Zooplankton	0.52	0.29	0.64	0.66	0.51	0.35	0.79	0.62	0.64	0.46
Station 110	**0-30 m**		**30-100 m**		**100-200 m**		**200-600 m**		**600-1000 m**	
Calanoida	0.43	0.13	0.60	0.29	0.90	0.69	0.85	0.28	1.55	0.92
Cyclopoida	0.55	0.22	0.39	0.11	0.38	0.13	0.41	0.13	0.39	0.08
total Zooplankton	0.46	0.14	0.55	0.31	0.55	0.49	0.63	0.34	0.76	0.74

Tab. A7. Mesoplankton biomass indicated as biovolume along transect T-3 in 2007 and 2008 and along transect T-7 in 2008.

Dr Fridtjof Nansen cruise Transect T-3			Maria S. Merian cruise Transect T-3			Maria S. Merian cruise Transect T-7		
Station	Depth Interval [m]	Biovolume [ml/m3]	Station	Depth Interval [m]	Biovolume [ml/m3]	Station	Depth Interval [m]	Biovolume [ml/m3]
33	0-30	2.9	**244**	0-20	1.9	**106**	0-30	1.4
	30-60	1.13		20-40	1.5		30-60	4.7
	60-100	0.55		40-80	0.5			
	100-140	0.23		80-200	0.21	**107**	0-30	0.52
	140-200	0.27		200-600	0.31		30-60	0.6
							60-100	0.5
29	0-30	3.07	**242**	0-50	0.92		100-120	1.3
	30-60	1.67		50-200	0.13			
	60-100	0.3		200-400	0.25	**108**	0-20	1.4
	100-140	0.1		400-600	0.18		20-50	1.2
	140-200	0.5					50-140	0.18
	200-300	0.28	**231**	0-10	7.8		140-170	0.35
	300-400	0.22		10-25	6.8		170-230	1.3
	400-500	0.16		25-50	8.8			
	500-600	0.24		50-100	0.7	**109**	0-30	5.07
				100-155	0.6		30-200	0.42
38	0-30	2.53					200-300	0.48
	30-60	2.07	**230**	0-25	2.56		300-500	0.72
	60-100	0.33		25-40	5.3		500-950	0.17
	100-140	0.2		40-70	14			
	140-200	0.33		70-150	0.5	**110**	0-30	1.73
				150-220	0.4		30-100	1.26
53	0-30	0.53					100-200	0.18
	30-60	1					200-600	0.13
	60-100	0.75					600-1000	0.12
	100-140	0.27						
	140-200	0.53						

Tab. A8. Stable carbon and nitrogen isotope signatures of zooplantkon and non-zooplanton organisms. x signifies no available data.

Species	n	Stage	Dry mass [mg]	Isotopic signature [‰] $^{13}C/^{12}C$	Isotopic signature [‰] $^{15}N/^{14}N$	Content [%] C	Content [%] N	C/N ratio
Storm petrel (Hydrobatidae)	1		1.37	-17.5	14.2	45.92	15.38	3.0
Storm petrel (Hydrobatidae)	1		1.57	-17.6	14.0	43.96	14.41	3.1
Storm petrel (Hydrobatidae)	1		3.50	-17.2	12.7	43.6	18.5	2.4
Storm petrel (Hydrobatidae)	1		4.41	-16.8	13.0	47.2	15.6	3.0
Aequorea sp.	part		4.10	-17.5	10.2	22.1	5.2	4.3
Aequorea sp.	part		4.36	-17.7	13.3	1.5	0.5	3.0
Aequorea sp.	part		4.61	-16.4	12.6	1.8	0.6	3.0
Aequorea sp.	part		6.01	-17.8	13.9	1.4	0.5	2.8
Aequorea sp.	part		2.92	-19.7	13.4	50.5	8.5	5.9
Aequorea sp.	part		5.20	-18.1	10.4	45.7	9.5	4.8
Cyclothone sp.	part		2.92	-19.7	13.4	50.5	8.5	5.9
Cyclothone sp.	part		5.20	-18.1	10.4	45.7	9.5	4.8
Engraulis capensis	1		4.86	-16.0	7.0	61.8	10.9	5.7
Engraulis capensis	1		6.24	-16.4	7.6	61.17	10.12	6.0
Chaetognatha	2		4.42	-18.2	8.4	42.6	8.9	4.8
Chaetognatha	1		4.54	-17.5	9.5	38.0	8.6	4.4
Chaetognatha	1		5.45	-18.6	8.6	48.5	11.3	4.3
Chaetognatha	1		5.94	-18.4	10.0	46.3	8.3	5.6
Chaetognatha	2		8.64	-17.6	**x**	38.14	9.98	3.8
Chaetognatha	1		8.80	-19.1	**x**	43.31	11.64	3.7
Chaetognatha	2		10.21	-17.7	**x**	40.51	9.20	4.4
Mysidacea	part		4.40	-17.7	11.0	55.3	10.0	5.5
Euphausiacea	2		2.62	-18.0	9.6	41.8	10.9	3.8
Euphausiacea	3		3.54	-18.1	10.3	43.5	11.2	3.9
Euphausiacea	1		5.84	-18.4	8.9	47.4	12.2	3.9
Euphausiacea	1		8.39	-18.1	**x**	44.06	11.28	3.9
Themisto gaudichaudi	1		1.96	-17.2	9.4	24.4	6.2	3.9
Themisto gaudichaudi	1		2.97	-17.9	10.5	29.0	7.4	3.9
Gaussia sp.	1	male?	2.78	-19.1	13.2	39.3	9.5	4.1
Gaussia sp.	1	C5	3.43	-20.1	13.2	47.4	9.5	5.0
Gaussia sp.	1	female	7.33	-20.3	12.1	55.74	9.96	5.6
Lucicutia sp.	1	female	1.27	-21.9	11.9	60.83	6.36	9.6
Pleuromamma sp.	2	female	0.97	-18.5	11.6	40.40	10.27	3.9
Pseudochirella sp.	1		2.31	-20.1	11.0	40.9	10.4	3.9
Scaphocalanus sp.	1		0.77	-20.3	10.0	41.5	6.8	6.1
Megacalanus pileatus	1	C5	2.29	-18.6	10.8	41.4	10.2	4.1
Megacalanus pileatus	2	C4	2.65	-18.9	9.7	45.3	9.7	4.7
Megacalanus pileatus	1	male	7.71	-20.6	**x**	55.32	10.50	5.3
Megacalanus pileatus	1	C5-male	8.03	-26.4	**x**	55.89	10.33	5.4
Gaetanus pileatus	1	female	1.56	-18.3	9.4	41.89	10.77	3.9
Gaetanus pileatus	1		1.66	-18.1	9.1	39.9	9.4	4.2
Gaetanus sp.	2	C5	1.40	-19.5	9.7	35.2	8.9	4.0
Gaetanus sp.	1		1.41	-17.4	6.6	44.3	9.4	4.7

to be continued on the next page

Species	n	Stage	Dry mass [mg]	Isotopic signature [‰] $^{13}C/^{12}C$	Isotopic signature [‰] $^{15}N/^{14}N$	Content [%] C	Content [%] N	C/N ratio
Paraeuchaeta hansenii	1	female	4.63	-19.1	9.3	59.2	8.7	6.8
Paraeuchaeta gracilis	2	female	3.03	-19.3	8.2	52.2	9.3	5.6
Paraeuchaeta gracilis	2	female	3.10	-20.0	9.6	58.6	7.3	8.0
Paraeuchaeta gracilis	2	female	3.14	-19.0	8.8	58.2	8.4	6.9
Paraeuchaeta gracilis	3	female	3.73	-19.5	9.5	51.6	8.9	5.8
Paraeuchaeta gracilis	3	female	4.37	-18.2	8.3	50.7	10.7	4.7
Euchirella sp.	1	female	1.09	-18.9	8.1	41.82	11.56	3.6
Euchaeta marina	3	female+C5	0.83	-20.4	8.2	44.3	10.9	4.1
Euchaeta marina	3	female	0.83	-20.8	8.5	45.24	11.80	3.8
Calanoides carinatus	15	C5	2.41	-19.8	7.2	62.9	6.3	10.0
Calanoides carinatus	15	C5	2.53	-19.8	7.6	62.3	6.3	9.9
Tunicata	part		2.23	-22.3	9.6	2.00	0.40	5.0
Tunicata	part		3.72	-22.4	11.6	1.1	0.2	5.5
Tunicata	part		2.67	-22.1	10.0	1.7	0.3	5.7
Tunicata	part		2.47	-24.2	12.1	0.9	0.3	3.0
Pyrosoma sp.	part		3.55	-20.4	7.9	13.1	2.8	4.7
Pyrosoma sp.	part		3.57	-20.8	7.8	10.6	2.4	4.4
Cymbulia sp. (animal)	part		1.00	-18.8	7.9	15.06	4.38	3.4
Cymbulia sp. (animal)	part		1.72	-18.8	6.2	15.60	4.60	3.4
Cymbulia sp. (animal)	part		2.27	-19.5	7.9	14.20	4.10	3.5
Cymbulia sp. (animal)	part		2.31	-18.4	7.6	16.7	4.9	3.4
Cymbulia sp. (pseudoconch)	part		3.18	-21.0	8.5	3.2	0.6	5.3
Cymbulia sp. (pseudoconch)	part		4.52	-20.1	6.1	2.7	0.5	5.4

Danksagung

Ich danke PD Dr. Holger Auel für die Möglichkeit meine Diplomarbeit in der Marinen Zoologie an der Universität Bremen durchzuführen und für die Übernahme des Erstgutachters. Ich bedanke mich für die wissenschaftliche Leitung, für viele hilfreiche Diskussionen und die konstruktive Kritik.

Herrn Prof. Dr. Gerhard von der Emde möchte ich für die Übernahme des Koreferats und für die Unterstützung aus Bonn danken.

Ich bedanke mich sehr bei allen Mitarbeitern der Arbeitsgruppe Marine Zoologie an der Uni Bremen für die freundliche Aufnahme in ihre Arbeitsgruppe und für die schöne Zeit. Ganz besonders möchte ich mich bei Anna, Britta und Silke bedanken, die mit mir bei allen Fragen und Problemen eine Lösung gefunden haben und für die freundschaftliche Unterstützung und lustigen Stunden während der gesamten Zeit.

Prof. Dr. Wilhelm Hagen, Dr. Werner Ekau und Dr. Hans Verheye danke ich für die Bereitstellung von Literatur.

Bei meinen Freunden aus Bonn möchte ich mich bedanken, ganz besonders bei Marie, Marit, Jana, Freda, Sabine, Désirée und Jule für die tolle Studienzeit und die vielen schönen Erlebnisse in Bonn und auf den Exkursionen.

Ich bedanke mich bei meiner Mitbewohnerin Caro, für die vielen lustigen Abende in unserer WG, die guten Gespräche und die gemeinsamen Kaffeepausen.

Ich bedanke mich sehr bei Dennis für unsere schöne gemeinsame Zeit in Bonn und für die emotionale Unterstützung, aber auch für die geduldige Lösung aller technischen Probleme.

Ganz besonders möchte ich mich bei meinen Eltern Brigitte und Hajo und bei meiner Schwester Christine bedanken, dafür dass sie mich von Anfang an in aller Hinsicht unterstützt haben und für die aufmunternden Worte in anstrengenden Zeiten.

Erklärung

Hiermit erkläre ich, dass ich die vorliegende Arbeit selbständig verfasst und keine anderen als die angegebenen Quellen verwendet habe.
Die aus anderen Werken entnommenen Abbildungen und Zitate sind als solche unter Angabe der Quelle gekennzeichnet.

Bonn, den 2. November 2009

_____

Lena Teuber